İSTANBUL TECHNICAL UNIVERSITY ★ INSTITUTE OF SCIENCE AND TECHNOLOGY

QUANTUM MECHANICAL and EXPERIMENTAL INVESTIGATION of THE ELECTROCHEMICAL PROPERTIES of N-SUBSTITUTED PYRROLE DERIVATIVES

M.Sc. Thesis by

Fatma BAYATA

Department: Polymer Science and Technology

Programme: Polymer Science and Technology

JANUARY 2007

İSTANBUL TECHNICAL UNIVERSITY ★ INSTITUTE OF SCIENCE AND TECHNOLOGY

QUANTUM MECHANICAL and EXPERIMENTAL INVESTIGATION of THE ELECTROCHEMICAL PROPERTIES of N-SUBSTITUTED PYRROLE DERIVATIVES

M.Sc. Thesis by

Fatma BAYATA

(515041031)

Date of submission: 25 December 2006

Date of defence examination: 29 January 2007

Supervisors (Chairmen): **Prof. Dr. A. Sezai SARAÇ**

Assist. Prof. Dr. Nurcan TÜZÜN

Members of the Examining Committee: **Prof. Dr. Mine YURTSEVER**

Prof. Dr. M. Ferhat YARDIM

Assoc. Prof. Dr. Safiye Sağ ERDEM (M.Ü.)

JANUARY 2007

İSTANBUL TEKNİK ÜNİVERSİTESİ ★ FEN BİLİMLERİ ENSTİTÜSÜ

N-SÜBSTİTÜYE PİROL TÜREVLERİNİN ELEKTROKİMYASAL ÖZELLİKLERİNİN KUANTUM MEKANİKSEL ve DENEYSEL İNCELENMESİ

YÜKSEK LİSANS TEZİ

Fatma BAYATA

(515041031)

Tezin Enstitüye Verildiği Tarih: 25 Aralık 2006

Tezin Savunulduğu Tarih: 29 Ocak 2007

Tez Danışmanları: Prof. Dr. A. Sezai SARAÇ

Y. Doç. Dr. Nurcan TÜZÜN

Diğer Jüri Üyeleri: Prof. Dr. Mine YURTSEVER

Prof. Dr. M. Ferhat YARDIM

Doç. Dr. Safiye Sağ ERDEM (M.Ü.)

OCAK 2007

ACKNOWLEDGEMENTS

I wish to express my appreciation to both Assist. Prof. Dr. Nurcan Tüzün and Prof. Dr. Sezai Saraç, my supervisors, whose academic expertise, consistent direction and encouragement provided me with the inspiration to undertake and expand upon the research of this study. Also, I am grateful to them for trusting in me, giving me opportunity to approach the thoughts that I just dream of.

I am deeply indebted to my family, who give their ever-present love and devotion, for all the guidance and support.

December, 2006 **Fatma BAYATA**

CONTENTS

ABBREVIATIONS

AM1	**:** Austin Model 1
AO	**:** Atomic Orbital
B3LYP	**:** Becke Style Three Parameter Functional in Combination with the Lee-Yang Parr Correlation Functional
CFME	**:** Carbon Fiber Modified Electrode
CNDO	**:** Complete Neglect of Differential Overlap
CV	**:** Cyclic Voltametry
DFT	**:** Density Functional Theory
E	**:** Energy
EA	**:** Electron Affinities
HF	**:** Hartree-Fock
HOMO	**:** Highest Occupied Molecular Orbital
IP	**:** Ionization Potential
LDA	**:** Local Density Approximation
LUMO	**:** Lowest Unoccupied Molecular Orbital
LYP	**:** Lee-Yang-Parr Correlation Functional
MNDO	**:** Modified Neglect of Diatomic Overlap
MO	**:** Molecular Orbital
NBO	**:** The Natural Bond Orbital Method
NDDO	**:** Neglect of Differential Diatomic Overlap
PM3	**:** Parametic Method Number 3
SOMO	**:** Singly Occupied Molecular Orbital

LIST OF TABLES

Page No.

LIST OF FIGURES

Page No.

SYMBOLS

E	**:** Energy of the System
E_a	**:** Oxidation Potential
E_c	**:** Reduction Potential
E_{onset}	**:** Onset Potential
$E_{½}$	**:** Half Peak Potential
ΔE	**:** Difference of Anodic and Catodic Potential
E_T	**:** Kinetic Energy
E_V	**:** Potential Energy
E_J	**:** Coulomb Energy
E_{XC}	**:** Exchange-correlation Energy
f(r)	**:** Fukui Function
$f^+(r)$	**:** Fukui Reactivity Index for a Nucleophilic Attack
$f^-(r)$	**:** Fukui Reactivity Index for an Electrophilic Attack
$f^0(r)$	**:** Fukui Reactivity Index for a Radical Attack
H	**:** Hamiltonian Operator
Ia	**:** Anodic Current
I_c	**:** Catodic Current
I_p	**:** Peak Current
1- (|Ia/Ic|)	**:** A Measure of Deviation from Reversibility
1/n	**:** Inverse Chain Length
K_x, K_H	**:** The Acidity Constants for the Substituted Benzoic Acid and Benzoic Acid
N	**:** Number of Electrons
s	**:** Local Softness
T [ρ]	**:** Kinetic Energy of Interacting Electrons
T_s [ρ]	**:** Kinetic Energy of Non-interacting Electrons
v(r)	**:** Potential Imposed by the Nuclei at Position r
V_{ee} [ρ]	**:** Interelectronic Interactions
μ	**:** Chemical Potential
$v_{xc}(r)$	**:** Exchange-correlation Potential
$v_{eff}(r)$	**:** External effective Potential
ρ(r)	**:** Electron Density Function
σ	**:** Electronic Substituent Parameter (Hammett Parameter)
Ψ	**:** Wavefunction

SUMMARY

In this study, correlations were built up between the calculated and the experimentally found properties of a set of pyrrole monomers. With this purpose, a number of N-substituted monomers, have been optimized with the DFT B3LYP/6-31+G* method which produced considerable information on the 3-dimensional structures, charge distributions, spin density distributions and molecular orbital energies. Besides, exprimental electrochemical data were produced on a set of monomers by enforcing them to electropolymerize exactly at the same conditions. Then these experimental data were correlated with the calculated data.

In calculations most stable geometries for monomers are found. The dimer and oligomer geometries of M1 up to n=7 have been obtained. The HOMO-LUMO energy differences, HOMO and LUMO energies were decreased as the number of monomer units increased, thus conjugation increased. The polymer properties were obtained from oligomer calculations by plotting the results, against inverse chain length and extrapolating to infinity. With this method, band gap and ionization potential values could be obtained. Spin density calculations in cation radicals of all studied N-pyrrole derivatives were performed to provide information on the site of propagation of polymerization. The spin density calculation results suggest that β preference may be slightly enhanced with monomers of high β spin density. The relationship between hammett parameters and theoretically calculated values were sought in N-pyrrole derivatives. This revealed that electronic property of substitution is effective on HOMO energy level of the monomer. The main attention was concentrated on the effect of substituent on monomer properties. The effect of substituents on calculated HOMO- LUMO difference, LUMO and HOMO energy values and the experimentally found properties from cyclic voltammetry was discussed.

The effect of the nature of substituent on electrochemical properties could be understood by calculations. The correlations demonstrated that the calculated molecular orbital energies would be correlated succesfully to experimental data such as Ia/Ic, Ea, Ec. These correlations may in turn guide in designing of new monomers. Having results that are in accordance with literature, DFT methodology with B3LYP/6-31+G* basis set can be concluded to be a reliable method to treat systems of this kind.

N-SÜBSTİTÜYE PİROL TÜREVLERİNİN ELEKTROKİMYASAL ÖZELLİKLERİNİN KUANTUM MEKANİKSEL ve DENEYSEL İNCELENMESİ

ÖZET

Bu çalışmada, çeşitli pirol N-sübstitüye türevlerinin hesaplamalı ve elektrokimyasal yöntemlerle bulunan özellikleri arasında oluşturulabilecek korelasyonlar incelenmiştir. Bu amaçla N-sübstitüye pirol monomerleri YFT (Yoğunluk Fonksiyonel Teorisi) B3LYP/6-31+G* metoduyla optimize edilerek, buradan 3 boyutlu yapısı, yük dağılımı, spin yoğunluğu, moleküler orbital enerjileri gibi birçok bilgi üretilmiştir. Bütün monomerler aynı şartlar altında elektrokimyasal yöntemlerle polimerleştirilmeye çalışılmıştır. Elde edilen sayısal değerlerle, CV datalarından bulunan deneysel oksidasyon potansiyelleri, redüksiyon potansiyelleri, iletkenlik değerleri kıyaslanarak aralarındaki korelasyonlar bulunmuştur.

Hesaplamalı yöntemlerle, monomerlerin en kararlı geometrileri bulunmuştur. Fenilpirol monomeri ile heptafenilpirole kadar gidilerek polimerin 3 boyutlu yapısına ait bilgi edinilmiştir. Oligomer hesaplamalarından faydalanılarak ise polimerin iyonizasyon potansiyeli, bant aralığı gibi özellikleri hakkında bilgi elde edilmiştir. Elektrokimyasal polimerleşme esnasında oluşan radikalik merkezin lokasyonu belirlenerek, polimerleşmenin monomerin hangi atomu üzerinden ilerleyebileceği hakkında çeşitli hesaplamalar yapılmıştır. Bu hesaplamaların sonucunda ise, incelenen monomerlerin büyük çoğunluğunda, polimerleşmenin α karbonu üzerinden ilerleme ihtimalinin β karbonunkinden daha fazla olduğu tespit edilmiştir. Bazı N-sübstitüye pirol türevlerinin hammett parametreleri ile hesaplamalı yöntemlerle elde edilen sayısal değerleri arasındaki ilişki incelenmiştir. Elde edilen korelasyonlara göre, sübstitüyenin elektronik özelliğinin, monomerlerin HOMO enerji seviyesi üzerinde daha çok etkili olduğu tespit edilmiştir.

Ayrıca bu çalışmada, monomer üzerinde sübstitüye etkisi ayrıntılı olarak incelenmiştir. Hesaplamalı yöntemlerle elde edilen HOMO, SOMO, HOMO-SOMO değerleri ile deneysel elde edilen Ea, Ec, Ea-Ec, $E_{1/2}$, Ia, Ic, Ia/Ic değerler arasında korelasyonlar oluşturulmuştur. Böylece pirol N-sübstitüye türevlerinin elektronik özellikleri ile elektrokimyasal davranışları arasında bir ilişki aranarak, sübstitüyenin bu ilişkiye etkisi incelenmiştir. Elde edilen korelasyonlar ve sübstitüyenin monomerin elektrokimyasal davranışlarını nasıl etkilediğinin bilinmesi istenilen ürünün sentezlenmesinde yol gösterici olabilecektir. Ayrıca, elde edilen sonuçların literatür ile uyumlu olması, bu tür sistemler için B3LYP/6-31+G* baz setli YFT (Yoğunluk Fonksiyonel Teorisi) metodunun güvenilir bir metot olduğu sonucuna varılmıştır.

1 INTRODUCTION

1.1 Conductive Polymers

The field of conducting polymers has attracted the interest of many academic and industrial researchers after the first report of electrical conductivity in a conjugated polymer (polyacetylene) in 1977 by Shirakawa [1].

Conducting polymers have the potential of combining the high conductivity of pure metals with the processibility, corrosion resistance and low density of polymers and are beginning to find applications in the fields of anti-static anti-corrosion coatings, sensors batteries, supercapacitors, light emitting diyotes, electrochromic devices and transparent electrode materials [2, 3]. Thus, during the last years many researches have been carried out aimed at investigating the molecular and electronic structure of these conducting polymer and their derivatives [3].

Conducting polymers can be prepared via chemical or electrochemical polymerization. The second way is generally preferred because it provides a better control of film thickness and cleaner polymers when compared to chemical oxidation. Films of electronically conducting polymers are generally obtained onto a support electrode surface by anodic oxidation (electropolymerization) of the corresponding monomer in the presence of an electrolyte solution. Electrical conductivity is achieved in the film of conducting polymer by oxidation (p-doping) or reduction (n-doping), followed respectively by the insertion of anodic or cationic species. Due to the double bond alternation in the conjugated polymer backbone, the charged species formed upon doping are able to move along the carbon chain (delocalization) allowing electron transport and thus giving an electronically conductive material.

The major difficulty to the rapid development of conductive polymers is the lack of understanding of how electrical current passes through them. All conductive polymers have two things in common:

1- They contain extended π-conjugated systems-single and double bonds alternating along the polymer chains,

2- They can be exposed to doping.

A basic research goal in this field is to understand the relationship between the chemical structure of the repeating unit of the polymer and its electrical properties. Such an understanding would enable the electronic and mechanical properties of these materials to be tailored at the molecular level.

Simple band theory fails to explain conductivity in polymers. The electrical properties of any material are determined by its electronic structure. The theory that most reasonably explains the electronic structure of materials is band theory. In the solid state, the atomic orbitals of each atom overlap with the same orbitals of their neighbouring atoms in all directions to produce molecular orbitals similar to those in small molecules. When this many orbitals are spaced together in a given range of energies, they form what look like continuous energy bands.

The energy spacing between the highest occupied and the lowest unoccupied bands is called the band gap. The highest occupied band is called the valance band, and the lowest unoccupied band is the conduction band (Figure 1.1).

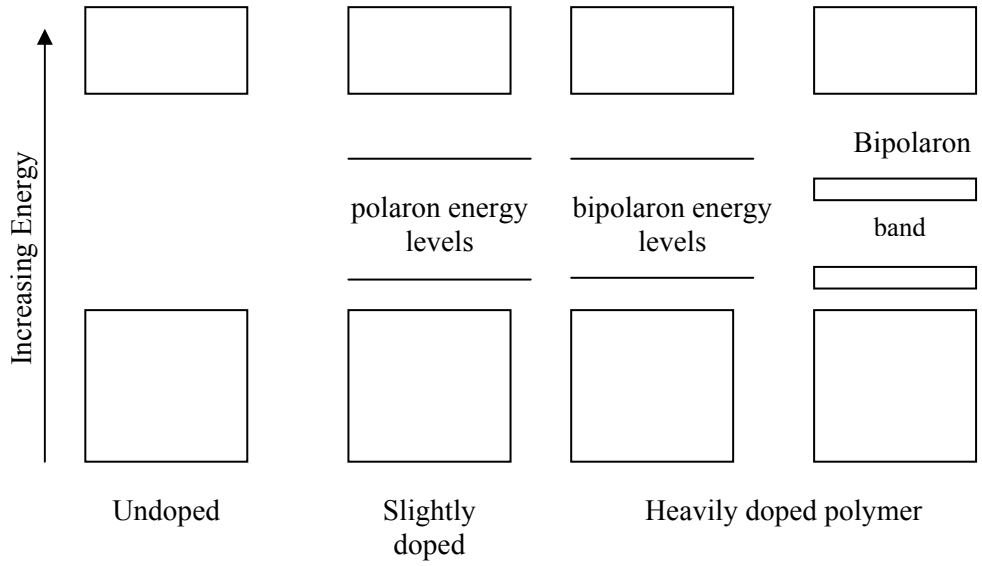

Figure 1.1 The energy spacing between the highest occupied and lowest unoccupied band [4]

The electrical properties of conventional materials depend on how the bands are filled. When the bands are filled or empty, no conduction occurs. If the band gap is

narrow, at room temperature thermal excitation of electrons from the valance band to the conduction band gives rise to conductivity. This is what happens in classical semiconductors. When the band gap is too wide, thermal excitation at room temperature is insufficient to excite electrons across the gap and become an insulator. The partially occupied band, a partially filled conduction band, a partially empty valance band, or a zero band gap make metals highly conductive. (Figure 1.2).

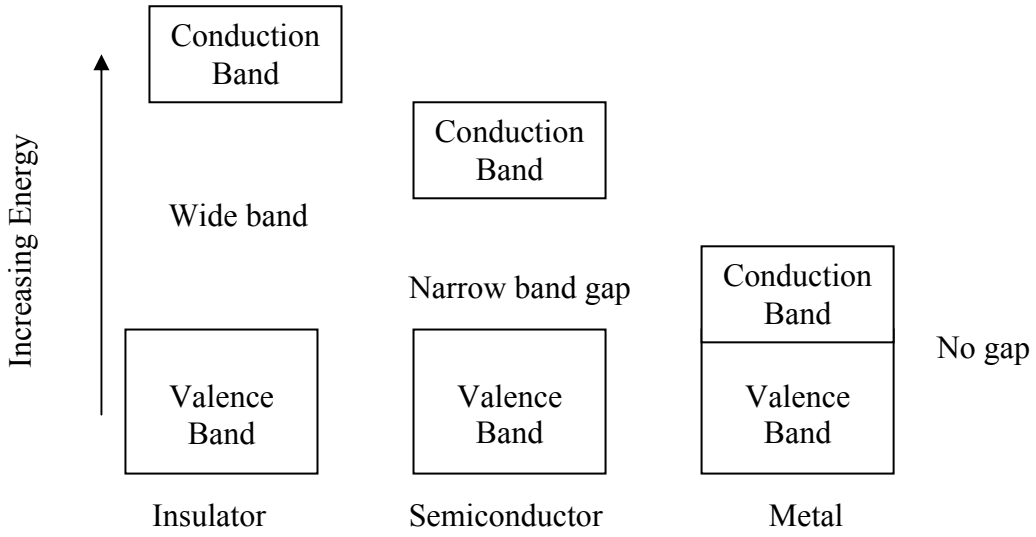

Figure 1.2 A partially filled conduction band, a partially empty valance band, or a zero band gap [4].

When an electron is removed from the top of the valance band of a conjugated polymer, such as polyacetylene or polypyrrole, a vacancy (hole or radical cation) is created that does not delocalize completely, as would be expected from classical band theory. Only partial delocalization occurs, extending over several monomeric units and causing them to deform structurally. The energy level associated with this radical cation represents a destabilised bonding orbital and thus has a higher energy than the energies in the valance band. In other words, its energy is in the band gap. This rise in energy is similar to the rise in energy that takes place after an electron is removed from a filled bonding orbital [5].

In the polymer, the pyrrole units, which will be given as an example, have positive charges, which are balanced by a variety of so-called dopant anions. Anions are expelled from the polymer film (undoping) when a negative potential is applied to the films, thus reducing it to the neutral state. Conversely, when positive potential is applied to oxidize the neutral film (doping), anions are taken up [5].

During the doping-undoping process, the volume of the film changes as much as 50%, depending on the specific volume of the doped anion. Also, dramatic color changes occur because the visible spectra of the doped and undoped film are very different [4].

It has been found that about a dozen different polymers and polymer derivatives undergo this transition when doped with a weak oxidation agent or reducing agent. They are all various conjugated polymers. This early work has led to an understanding of the mechanisms of charge storage and charge transfer in these system. All have a highly conjugated electronic state. This also causes the main problems with the use of these systems, that of processibility and stability. Most early conjugated polymers were unstable in air and were not capable of being processed. The most recent research in this has been the development of highly conducting polymers with good stability and acceptable processing attributes [5].

The polymer may store charge in two ways. In an oxidation process it could either lose an electron from one of the bands or it could localize the charge over a small section of the chain. Localizing the charge causes a local distortion due to a change in geometry, which costs the polymer some energy. However, the generation of this local geometry decreases the ionization energy of the polymer chain and increases its electron affinity making it more able to accommodate the newly formed charges. This method increases the energy of the polymer less than it would if the charge was delocalized and, hence, takes place in preference of charge delocalization. This is consistent with an increase in disorder detected after doping by Raman spectroscopy. A similar scenario occurs for a reductive process [5].

The oxidative doping of polypyrrole proceeds in the following way. An electron is removed from the p-system of the backbone producing a free radical and a spinless positive charge. The radical and cation are coupled to each other via local resonance of the charge and the radical. In this case, a sequence of quinoid-like rings is used. The distortion produced by this is of higher energy than the remaining portion of the chain. The creation and separation of these defects costs a considerable amount of energy. This limits the number of quinoid-like rings that can link these two bound species together. In the case of polypyrrole it is believed that the lattice distortion extends over four pyrrole rings. This combination of a charge site and a radical is called a polaron. This could be either a radical cation or radical anion. This creates a

new localized electronic states in the gap, with the lower energy states being occupied by a single unpaired electrons. The polaron state of polypyrrole are symmetrically located about 0.5 eV from the band edges [5].

Upon further oxidation the free radical of the polaron is removed, creating a new spinless defect called a bipolaron. This is of lower energy than the creation of two distinct polarons. At higher doping levels it becomes possible that two polarons combine to form a bipolaron. Thus at higher doping levels the polarons are replaced with bipolarons. The bipolarons are located symmetrically with a band gap of 0.75 eV for polypyrrole. This eventually, with continued doping, forms into a continuous bipolaron bands. Their band gaps also increase as newly formed bipolarons are made at the expense of the band edges. For a very heavily doped polymer it is conceivable that the upper and the lower bipolaron bands will merge with the conduction and the valence bands respectively to produce partially filled bands and metallic like conductivity [5].

A polaron and bipolaron in polypyrrole are shown below:

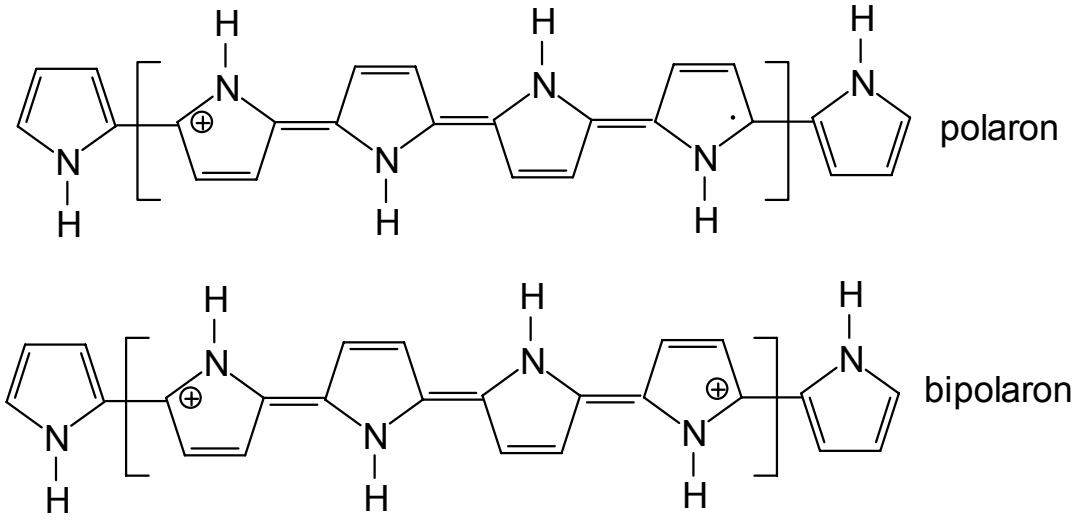

Figure 1.3 Polaron and bipolaron for polypyrrole chain [4].

1.2 Pyrrole Derivatives

Synthesis and investigation of new conjugated polymers are essential to improve the electronic and optielectronic properties of these materials and in turn for improvement of the performance of the devices [6].

Polypyrroles are certainly one of the most, widely studied organic conducting polymers due to the ease of synthesis, good redox properties, stability in the oxidized form, ability to give high electrical conductivies and useful electrical and optical properties [2, 4]. As a result of its good intrinsic properties, polypyrrole has proven promising for several applications, including batteries, supercapacitors, electrochemical (bio)sensors, conductive textiles and fabrics, mechanical actuators, electromagnetic interference (EMI) shielding, anti-static coatings and drug delivery systems [2]. Also because of its conductive properties polypyrrole has been shown to work as a protective layer against photocorrosion for photoelectrodes and its polymer coatings on electrode surface and change the catalytic activity of the electrodes [7].

Electronically conducting polymers are an extremely promising category of materials. In practice, most electronically conductive polymers are not easily processable in their pure form. Although high-capacity polypyrrole capacitors and rechargeable polyaniline batteries are in commercial production, it is generally thought that the potential of conducting polymers has not really been tapped. The conformation and packing of these polymers in the amorphous glassy state are poorly understood, despite the fact that such characteristics dictate their most important physical and mechanical properties. The processing of currently known conducting polymers is difficult and there is a strong incentive to increase their processability through blending with other polymers or by chemical functionalisation. Developing an ability to predict the structure and structure property relations of conducting polymers in the bulk will assist the design of new structures that combine processability with favourable electronic properties [8].

Besides, it was observed that many of these polymers have interesting and specific properties although there is one nearly universal and overriding disadvantage with respect to technological applications: linear unsubstituted compounds are intractable and infusible [9]. A crucial step in the continuing effort to develop more processable conjugated polymers has been the addition of solubilizing substituents on the monomer. However, the introduction of substituents to confer solubility and enhance process ability can produce dramatic changes in the structure and electronic properties [9].

Also, the conjugated polymers composed of 5–membered heteroatomic rings present challenging problems in terms of their structural analysis and electronic

properties[10]. Among these systems, the conducting polymer of polypyrrole is still considered to be an important material for future technological applications. However, an exact determination of its structure is still not possible due to extremely low solubility and crystallinity [10].

In summary, for electrochemically prepared conjugated polymers, it is usually very difficult to get accurate information on the structure; hence theoretical calculations may be resorted [11].

Computer simulation techniques are clearly now able to provide valuable insight into the structure and properties of polymers at the atomic level [8]. In addition to this, quantum mechanical calculations on small oligomers have been extensively used to predict the substitution effects [9]. Future developments are likely to include the extension of electronic-structure techniques to larger and more complex systems [8].

Substituents are widely used to modify the properties of conducting polymers [12]. In designing new monomers, it is important to have a clear understanding of the effect of substituents on energy levels. In an investigation, the electronic effects of various substituents in different positions of heterocyclic dimers are theoretically examined and correlations are established which allow to understand and predict substituent effects on bandgaps [13]. These values are calculated by employing the density functional theory (DFT) and analyzed with the natural bond orbital method (NBO). For bridged dimers, HOMO-LUMO gaps correlate with л -electron densities in the carbon backbone and energy gap reductions correlate with the strength of л - л* interactions from the backbone to the bridging group. Substituent effects are strongest on dipyrrole derivatives. According to this argument, dipyrrole derivatives have an even smaller energy gap than the other dimers [13]. Also for dipyrrole derivatives, substantial energy gap reductions result from stronger LUMO energy compared to HOMO energy lowerings [13].

In a different study regarding the substitution effect, $C=C(CN)_2$, C=O, and C=S substitutions were examined on dipyrrole, difuran, dicyclopentadiene, and diborole[14]. Electronic structures were analyzed with respect to their suitability as building blocks for conducting polymers with the natural bond orbital (NBO) method. All bridging groups investigated decrease HOMO-LUMO gaps compared to the unsubstituted parent dimers. Substitution affects HOMO and LUMO energies.

The energy gap reductions can be correlated with the strengths of the donor-acceptor interactions between the backbones and the bridging groups. Compared to unsubstituted dimers, the strongest substituent effects are found with pyrroles. Energy gap reduction is caused by a stronger decrease of LUMO energies compared to HOMO energies. By electron withdrawal, the dicyanomethylene group thus lowers the energy of the LUMO with respect to the HOMO. Also a correlation is investigated between the stabilization energies associated with the donor-acceptor interactions from the carbon π-system to the bridging groups and the energy gap reductions compared to those for the parent dimers [14].

According to a recent investigation, since the electron-withdrawing substituent deduced the π electron overlap in the carbazole ring, the IP and EA values increased while decreasing the orbital energies of HOMO and LUMO [15]. The orbital energy of LUMO decreased much more than that of HOMO decreasing in CN-substituted carbazole derivatives. Thus, the band gap decreased in these carbazole derivatives. It has also been reported that electron donating-substituents display the opposite trend [15].

To study substituent effects on energy levels and energy gaps systematically, CH_3-, OH-, NH_2-, CN-, and CCH_3-substituted bithiophenes were also examined with density functional theory and NBO analysis in a recent study [13]. Total charges and л-electron densities were analyzed separately to examine σ- and π-effects. NBO orbital energies were employed to investigate the effect of alternating donor-acceptor substitution. Furthermore, no correlation was found between total charges in the carbon backbone and energy gaps [13]. Substituents in 3- and 4-positions shift HOMO and LUMO levels in parallel and hardly influence HOMO-LUMO gaps. In shifting of the levels, the л -donating and л -accepting abilities are most important; electronegativity mainly influences the σ -orbitals and is less crucial in determining energy gaps. As mentioned previously, alternating donor-acceptor substitution leads to HOMO and LUMO energies that are average between those of the parent systems and has little effect on energy gaps [12].

Alternating donor-acceptor groups do not reduce energy gaps and lead to systems with average HOMO and LUMO levels compared to the parent molecules. To decrease energy gaps, л -electron density needs to be withdrawn from the л -backbone. The substituents have to be placed in positions where HOMOs have nodes

to prevent parallel shifting of HOMO and LUMO levels [13]. In addition to this, it was stated in another study, for successful designing of low band gap polymers with donor-acceptor moieties, symmetry considerations seem to be crucial [12]. If substituents can be placed in a position where the HOMO and LUMO are affected differently, then one of the levels can be shifted with respect to the other and band gaps decrease [12].

Another interesting study is concerned with N-substituted nitropyrroles. The previous DFT investigation of the molecular geometries and energies of various substituted nitrobenzenes show good agreement with the experimental results [16]. Hence, the DFT method (at B3LYP/6-311G** level) can be applied to the studies of the molecular geometries and the internal rotational barriers of the nitro group for various N-substituted 2-and 3-nitropyrrole molecules, that has CH_3, OH, NH_2, and NO_2 groups as N-substituents. The structural parameters of pyrrole and N-methylpyrrole molecules obtained by B3LYP/6-311G** calculation also approach the experimental data. The energy barrier and the associated one-dimensional potential of molecule convey information regarding intramolecular interaction and molecular electronic structure. The potential for internal rotation of the nitro group in nitroaromatic compounds is a measure of the strength of π-conjugated stabilization relative to the steric effects of the neighboring substituents. The calculated NO_2 internal rotational barriers of all title molecules of nitropyrrole derivatives depend on the resonance, inductive, conjugate, hydrogen bond, and steric effects between the substituted group and the pyrrole ring [16].

The calculations of the vibrational properties of oligopyrroles were extended to even longer oligopyrroles, for n =5–10 by applying the semi-empirical PM3 and AM1 methods [8]. Because of the insolubility of polypyrrole, vibrational spectroscopic techniques have been widely used for its characterisation. The vibrational values in the literature for the conducting polypyrrole were very close to the modelled ones. The trends in the computed harmonic force fields, vibrational frequencies and intensities are monitored as a function of the chain length. The data are analysed in conjunction with the trends in computed equilibrium geometries. The theoretical vibrational spectra of the *n*PPy series converge nicely with each other at increasing chain length, at least as far as the frequencies are concerned. Also this information is required for the explicit treatment of very long oligomers [8].

In a different study, the singlet excited electronic states of two medium size molecules, furan and pyrrole, were studied using time-dependent density functional theory [17]. The vertical excitation energies, optimized geometries of the excited states, harmonic vibration frequencies, and excitation energies are all in good agreement with both experimental and recent ab initio results. The dipole moments of many excited states show a large variation with the basis set and functional; this is due to the fact that the states have an extremely large polarisability [17].

Formal oxidation potentials, $E°$, and lifetimes of the electrogenerated cation radicals have been measured at low or high scan rate cyclic voltammetry for several substituted pyrrolethiophene-pyrrole oligomers and terthiophenes [18,19]. As expected, substitution by a methyl group induces a lowering of the oxidation potentials except when the methyl is introduced on the β'-positions of the mixed oligomers which impedes the cation radical to achieve a planar configuration as confirmed by molecular modeling. A very good agreement is found between the variations of the experimental $E°$ and of the differences of energies ΔEn (energy of neutral oligomers - energy of cation radical) calculated by ab initio methods. Polymer properties can be obtained from oligomer calculations by plotting the results, against inverse chain length and extrapolating to infinity [18, 19]. For oligopyrroles, the reactivity of oligomers decrease upon increasing the ring number. Furthermore, the spin density calculation in the cation radicals indicate that the dimerization on the β or β' does not play a major role, suggesting that the α-α coupling is the major process even in the substituted compound and that branched coupling are negligible [18].

Besides, in an investigation, ab-initio calculations of a large number of isomeric structure of pyrrole oligomers were presented [20]. The purpose is to determine thermodynamical probabilities of linking α and β carbons in oligomers. The geometrical structures, energetics and charge localization of oligomers of pyrrole up to pentamers were studied by ab-initio quantum mechanical calculations. Detailed ab-initio calculations of a number of pyrrole oligomers are carried out in order to find out relative stability of structures bonded through α and β carbons. Energetics of dimers, trimers and tetramers with all possible linkage types and several pentamers were obtained from fully optimized geometries. The energy differences between types of structures suggest that a great deal of branching is probable. It is shown that

relative energies of 65 oligomers can be fairly reproduced by a simple partitioning in terms of monomer types [20].

In a very recent study, theoretical methods were used to analyze the conformational and electronic effects produced by hydroxyalkyl substitution on the N-position of the pyrrole ring [9]. Thus, the molecular geometry, torsional potential, ionization potential and π- π^* transition energy calculations based on the density functional theory (DFT) were used to ascertain the structural properties of 2,2-bipyrroles N-substituted with hydroxymethyl and hydroxypropyl in a neutral state. Furthermore, the band gap of the hydroxymethylpyrrole was predicted to be smaller than that of 2,2-bipyrrole when a planar anti conformation is considered. After this, the properties of pyrrole and *N*-hydroxyalkylpyrrole-containing oligomers formed by *n* repeating units, where *n* ranges from 1 to 5, have been examined by Hartree-Fock (HF) and DFT calculations. The loss of planarity produced by the *N*-substitution was detected in the *N*-substituted derivatives. Results are explained as a combined actuation of electron donation effects induced by the hydroxyl groups, repulsive steric interactions generated by the *N*-substitution and attractive specific interactions associated to the hydroxyl groups [9].

Related to *N*-hydroxyalkylpyrroles, in another study, ab initio quantum chemical calculations have been used to analyze the structural and electronic effects induced by the N-hydroxymethylation of polypyrrole in both undoped and p-doped states [21]. For this purpose, molecular chains formed by n rings of N-hydroxymethylpyrrole and pyrrole (n-MeOHPy and n-Py, respectively) have been calculated in both the neutral and positively charged states. The variations of band gap and IP with inverse chain length (1/n) were calculated for structures [21].

Polymer data are obtained from oligomer calculations by plotting the results against inverse chain length and extrapolating to infinity. This approach is well established for band gaps and IPs. In a study, band gaps (*E*g), ionization potentials (IPs), electron affinities (EAs), vs inverse chain lengths for thiophene, pyrrole, thiazole, and thiophene-thiazole oligomers were plotted by making use of DFT theory [19]. Furthermore, experimental λ_{max} and calculated HOMO-LUMO gaps versus inverse chain length plotted for pyrrole through heptapyrrole. Theoretical and experimental data show that monomers do not lie on straight lines going through the other points

for the larger oligomers. The correlation coefficients are excellent if the short-chain oligomers (up to about nine carbon atoms) are excluded [19].

Furthermore, in the study of Salzner et al., geometries of monomers through hexamers of a number of monomers including pyrrole were optimized employing density functional theory with a slightly modified B3P86 hybrid functional [22]. Bandgaps and bandwidths were obtained by extrapolating the appropriate energy levels of trimers through hexamers to infinity against inverse chain lengths. Bandgaps increase with increasing π -donor strengths of the heteroatom. Vertical ionization potentials (IPs) and electron affinities (EAs) were estimated from extrapolated - HOMO and LUMO energies, respectively. Vertical excitation energies (λ_{max}) were calculated from extrapolated HOMO-LUMO gaps and compared to the corresponding λ_{max} in the observed absorption spectra of oligomers. According to results PPy has the lowest IP and the lowest EA of all polymers studied here. This agrees nicely with experimental observation that PPy can be p- but not n-doped although PPy has the smallest HOMO bandwidth of all systems studied in the mentioned reserach [22].

In a comparative study, the electronic structures and conduction properties of neutral heterocyclic polymers polypyrrole, polythiophene and polyfuran were reported [23]. The general features of the energy band structures of all the three heterocyclic polymers are found to be similar. The calculated trend in the values of the gap is in excellent agreement with experiment. The results predicted polpyrrole to be the strongest and polyfuran to be the weakest candiate for forming materials through oxidative doping [23].

Also the structure and energetics of the pyrrole dimer are investigated by the extent of hydrogen bonding character between the N–H hydrogen of one monomer and the π-system of the other monomer is examined [24].

There are also some investigations on the electrochemical polymerization of pyrrole [10, 25]. The mechanism was studied using accurate density functional theory (DFT) calculations. The primary emphasis was on the structures and stability of intermediates generated during various mechanism. Structures of the radical cations, which play role in reactions, were optimized to elucidate radical-radical and radical-

neutral pathways. The competing probabilities of reactions between various size oligomers were discussed in terms of their thermodynamical stability [10, 25].

The aforementioned literature findings have proven the success and the efficiency of calculations in reproducing and producing the electrochemical properties of conducting or potentially conducting polymers. These studies have shown that it is possible to use quantum mechanical calculations in order to see the effect of substitution on electrochemical properties of monomers, which in turn affects the physical and bulk properties of the so formed product. The main objective of this study is to build up a correlation between the calculated and the experimentally found properties of a set of pyrrol monomers. With this purpose, a number of N-substituted monomers, shown in Figure 1.4., have been optimized with the DFT B3LYP/6-31+G* method which produced considerable information. These are 3-dimensional structures, charge distributions, spin density distributions and molecular orbital energies. This study aims to find the best correlations between the calculated and the experimental data. This will allow one to deduce some information on electrochemical properties of the monomer prior to experiments within the framework of this study. The main attention will be concentrated on the effect of substituent on monomer properties. The effect of substituents on calculated and the experimentally found properties from cyclic voltammetry will be discussed. To know how substitution affects electrochemical properties of monomer may guide the synthesis of the tailor made products of desired properties.

Location of radicalic centers may give information on the possibility of β-linkages which is a hard task to determine experimentally. Polymer properties will be deduced at the monomer level. Thus, one should account on how well an approximation this is. With this purpose, HOMO, LUMO energies and band gap calculation will be performed on oligomers up to 7 monomers. Besides molecular orbital energies, the 3-dimensional geometry of the parent monomer, **M1** will be discussed and related to known experimental data. This study will also allow us to account on the reliability of the theoretical methods used in this study.

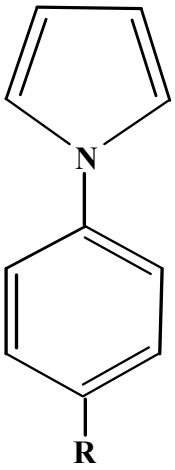

M1: R = H

M2: R = Cl

M3: R = CH_3

M4: R = OCH_3

M5: R =

M6: R = NO_2

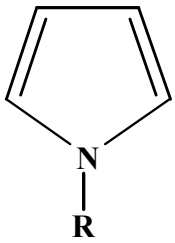

M7: R =

M8: R =

M9: R = CH_2CH_2CN

M10: R = $N(CH_3)_2$

M11: R = $CO_2C(CH_3)_3$

Figure 1.4 The optimized N-substituted pyrrole derivatives

2 THEORY

2.1 Calculation Methods

The electronic structure methods use the laws of quantum mechanics. The energy and other related properties of a molecule may be obtained by solving the Schrödinger Equation

$$\mathbf{H}\Psi = E\Psi \tag{2.1}$$

where, Ψ is the wavefunction describes the x, y and z spatial coordinates of the particles in the system, E is the energy of the sytem at that state and **H** is the Hamiltonian operator to derive the kinetic and potential energy of a sytem. Exact solutions are not computationally practical for large molecules. Approximations are introduced to electronic structure methods. The mostly encountered three major classes of electronic structure methods are:

- Semi-empirical methods, they use parameters derived from experimental data. Different semi-empirical methods are characterized by their different parameters.
- Ab initio methods, no experimental parameters are used.
- Density functional methods, the total energy of the system only depends on the electron density [26].

2.1.1 Semi-empirical Theory

The difficulty of performing ab-initio calculations on large molecules led to develop semi-empirical methods. In semi-empirical models, rather than solving all the integrals of the Schrödinger equation, parameters originating from experimental data are used. Semi-empirical models can be used to yield continuous energy surfaces. They are neither variational nor size consistent. More importantly, semi-empirical methods are inherently dependent on the choice of parameters. The parameterization is tested against a limited set of molecules to ensure its accuracy. This dependence on parameters can be minimized by using a large and varied training set of molecules to

establish parameters. Like numerical iteration, this process is a continuing one. Parameters are introduced in order to reproduce experimental equilibrium geometries, heats of formation, electric dipole moments and ionization potentials.

In solving Schrödinger equation, the number of off-diagonal one-electron integrals rapidly becomes very large and computationally burdensome. To handle this task, the approximation was made to set the overlap integrals to zero. With this assumption the secular determinant for the Hartree-Fock method reduces to

$$| \mathbf{F} - E | = 0 \qquad (2.1.1)$$

The Fock matrix, **F**, here is the sum of the usual one-electron and two-electron positions. The latter presents a particularly difficult hurdle since the number of integrals of the form

$$\iint \Psi_i (1)\, \Psi_j (2)\, (1/r_{12})\, \Psi_k (1)\, \Psi_l (2)\, \delta\tau (1)\, \delta\tau (2) \qquad (2.1.2)$$

are encountered where r_{12} is the distance between the particles. The overlap assumption sets these integrals to zero except in the case where i=j and k=l. The assumption led to the designation of CNDO, complete neglect of differential overlap. An additional assumption was that the off-diagonal resonance integral H_{ij} could be made proportional to the overlap integral i.e., although the overlap matrix disappears, values are still assigned to certain S_{ij} to allow evaluation of the H_{ij} and for later computation of charge distribution. A somewhat later upgrade in the parameterization was forthcoming under the tittle CNDO/2. Although the CNDO methods did not introduce electron-electron repulsions, they do not handle the question of the interactions between electrons with parallel and anti-parallel spins, especially when the electrons are on the same atom. NDDO (Neglect of Differential Diatomic Overlap) model is another semi-empirical model. This theory neglects differential overlap between atomic orbitals on different atoms. The first practical NDDO method was introduced by Dewar and Thiel in 1977, called “modified neglect of diatomic overlap” (MNDO). This model was parameterized on experimental molecular geometries, heats of formation, dipole moments and ionization potentials. The MNDO model is a very successful model, but it has also some limitations in reproducing hydrogen bonding successfully.

In this study, the semi-empirical PM3 model which is the third parameterization of the original MNDO model is used. This is a NDDO method which utilizes more adjustable parameters for the core-core repulsion term. In PM3, all quantities that enter the Fock matrix and the total energy expressions have been treated as pure parameters. To accomplish this task of optimizing parameters an automatic procedure was introduced, allowing a parameter search over many elements simultaneously. This model employs minimal basis of Slater type orbitals. For hydrogen 1s, for first row elements 2s, 2p and for second row elements 3s and 3p orbitals are used.

Each atom is characterized through 13-16 parameters that are present in AM1 and additionally five parameters that define the one-center, two-electron integrals. In PM3, the parameters were optimized using an automatic optimization routine that used a large set of reference molecular data. It is the most precisely parameterized semi-empirical model but again it has some limitations. Lone-pair repulsions are not always well represented in these methods and care must be taken [26].

2.1.2 Ab-initio Methods

In ab initio method, the Hamiltonian and the wavefunction (Ψ) have been defined, the effective electronic energy can be found by use of the variational method. In the variational method, the best wavefunction is found by minimizing the effective electronic energy with respect to parameters in the wavefunctions.

Common levels of ab initio theory include Hartree-Fock. Hartree-Fock replaces the many electron problem by a one electron problem [26].

2.1.3 Density Functional Theory

Density Functional Theory (DFT) is an approach to the electronic structure of atoms and molecules based upon a theory presented by Hohenberg and Kohn in 1964 which states that all the ground-state properties of a system are functions of the charge density. The DFT methods achieve significantly greater accuracy than Hartree-Fock theory at only a modest increase in cost. Although both methods account for the instantaneous interactions of pairs of electrons with opposite spin, DFT methods include the effects of electron correlation (electrons in a molecular system react to one another's motion and attempt to keep out of another's way) while Hartree-Fock

calculations see this effect in an average sense (each electron sees and reacts to an averaged electron density).

Density functional methods partition the electronic energy into several terms and compute them separately.

$$E = E_T + E_V + E_J + E_{XC} \tag{2.1.3.1}$$

E_T is the kinetic energy term, E_V is the potential energy of the nuclear-electron attraction and nuclear-nuclear repulsion term, E_J is the electron-electron repulsion term (also called Coulomb energy), E_{XC} is the exchange-correlation term that includes the remaining part of the electron-electron interactions.

All the terms except the nuclear-nuclear repulsion, are functions of electron density, $\rho(r)$. E_{XC} can be divided into exchange and correlation functionals. E_{XC} accounts for the exchange energy arising from the antisymmetry of the quantum mechanical wavefunction and the dynamic correlation in the motions of the individual electrons.

In 1964, Hohenberg-Kohn provided the proof (DFT based methods ultimately derive from quantum mechanics research from the 1920's especially the Thomas-Fermi-Dirac model and may be regarded as an approximation to the exact theory) that DFT is in fact an exact theory for describing the electronic behavior of matter. The variational principle determines the ground state energy and electron density in terms of the electron density. Further, the ground state electron density $\rho(r)$ determines the external potential, $v(r)$ and variationally determines the ground state properties of the system of interest.

The electronic energy can be expressed as a functional of the electron density:

$$E[\rho] = \int v(r)\rho(r)dr + T[\rho] + V_{ee}[\rho] \tag{2.1.3.2}$$

where $T[\rho]$ is the kinetic energy of interacting electrons and $V_{ee}[\rho]$ is the interelectronic interactions.

The electronic energy may be written in the form of Kohn-Sham approach.

$$E[\rho] = \int v(r)\rho(r)dr + T_s[\rho] + J[\rho] + E_{xc}[\rho] \tag{2.1.3.3}$$

This is based upon an orbital density description that removes the necessity of knowing the exact form of $T[\rho]$. Kohn-Sham proposed focusing on the kinetic energy of non-interacting system of electrons $T_s[\rho]$, as a functional of a set of single particle orbitals that give exact density.

$$T_s[\rho] = \sum_{i=1}^{N} \langle \Psi_i | -\frac{1}{2}\nabla^2 | \Psi_i \rangle \tag{2.1.3.4}$$

$J[\rho]$ represents the electron-electron repulsion (Coulomb energy), and $E_{xc}[\rho]$ is the exchange-correlation energy functional with its functional derivative called the exchange-correlation potential, $v_{xc}(r)$.

$$E_{xc}[\rho] = T[\rho] - T_s[\rho] + V_{ee}[\rho] - J[\rho] \tag{2.1.3.5}$$

$$v_{xc}(r) = \frac{\partial E_{xc}[\rho]}{\partial \rho(r)} \tag{2.1.3.6}$$

$E_{xc}[\rho]$ is divided into two parts, namely an exchange functional, $E_x[\rho]$ and a correlation functional, $E_c[\rho]$.

$$E_{xc}[\rho] = E_x[\rho] + E_c[\rho] \tag{2.1.3.7}$$

$E_x[\rho]$ and $E_c[\rho]$ functionals can be both local or gradient-corrected functionals. Local or gradient-corrected functionals are called traditional functionals. Local functionals depend only on electron density ρ, while gradient-corrected fuctionals depend on both ρ and its gradient, $\Delta\rho$.

A system of non-interacting electrons moving in an external effective potential $v_{eff}(r)$ is shown as;

$$v_{eff}(r) = v(r) + \frac{\partial J[\rho]}{\partial \rho(r)} + \frac{\partial E_{xc}[\rho]}{\partial \rho(r)} = v(r) + \int \frac{\rho(r')}{|r - r'|} dr' + v_{xc}(r) \tag{2.1.3.8}$$

Now, an equation very similar to the Schrödinger Equation exists.

$$\left[-\frac{1}{2}\nabla^2 + v_{eff}(r)\right]\Psi_i = \varepsilon_i \Psi_i \qquad (2.1.3.9)$$

(2.1.3.3), (2.1.3.4), (2.1.3.5), (2.1.3.6), (2.1.3.7), (2.1.3.8) are Kohn-Sham Equations.

In order to evaluate the exchange-correlation functional some approximations are made. The first one is the local density approximation (LDA). It is based upon a model of uniform electron gas. In the uniform electron gas model, a large number of electrons uniformly spread out in a cube where there is a uniform distribution of the positive charge to make the system neutral. It assumes that the charge density varies slowly throughout the molecule so that a localized region of the molecule behaves like a uniform electron gas The energy expression is:

$$E[\rho] = T_s[\rho] + \int \rho(r)v(r)dr + J[\rho] + E_{xc}[\rho] + E_b \qquad (2.1.3.10)$$

where E_b is the electrostatic energy of the positive background. Since the positive charge density is the negative to the electron density the equation reduces to:

$$E[\rho] = T_s[\rho] + E_{xc}[\rho] = T_s[\rho] + E_x[\rho] + E_c[\rho] \qquad (2.1.3.11)$$

The exchange functional is given by:

$$E_x[\rho] = -C_x \int \rho(r)^{4/3} dr \qquad (2.1.3.12)$$

C_x=0.7386, this form was developed to reproduce the exchange energy of a uniform electron gas.

DFT methods are defined by pairing an exchange functional with a correlation functional and can be named as traditional or hybrid functionals. Hybrid functionals include the exact term in the exchange functional, whereas traditional functionals do not.

BLYP (Becke's gradient-corrected exchange functional with Lee-Yang-Parr's gradient-corrected correlation functional) method is a traditional functional whereas, B3LYP (Becke style three parameter functional in combination with the Lee-Yang-Parr correlation functional) method, the linear combination of LDA, B88, Exexact

and LYP functionals, is a hybrid functional:

$$E_{xc} = E_{xc}^{LDA} + a_0(E_x^{exact} - E_x^{LDA}) + a_x \Delta E_x^{B88} + a_c \Delta E_c^{non-local} \quad (2.1.3.13)$$

where ΔE_x^{B88} is the Becke's gradient correction, i.e. the second term at the right hand side of the equation (2.1.3.11) and the correction to the correlation ($\Delta E_c^{non-local}$) is provided by the Lee-Yang-Parr functional. But, LYP includes both local and non-local terms, then the correlation functional used is actually: $a_c E_c^{LYP} + (1 - a_c) E_c^{VWN}$ where E_c^{VWN} is the Vosko-Wilk-Nusair correlation energy. The parameters are specified by Becke by fitting the atomization energies, ionization potentials, proton affinities and first row atomic energies in the molecule set, a0=0.20, ax=0.72 and ac=0.81. Hybrid functionals have proven to be superior to the traditional functionals [26].

2.1.3.1 Basis Sets

The basis sets used in quantum mechanical calculations are composed of atomic functions. The molecular orbitals are expressed as linear combination of a pre-defined set of one-electron functions called basis functions. The most convenient way is to use atomic orbitals as basis functions. Among the types of the basis sets (minimal basis sets, split valence basis sets, polarized basis sets, high angular momentum basis sets) the most popular one is the split valence basis set which is developed by Pople and his group termed as K-MNG. 4-31G, 5-31G, 6-31G. In split valence basis sets, each inner shell is represented by a single basis function taken as a sum of K Gaussian functions and each valence orbital is split into two parts, an inner part described by M Gaussians and an outer part described by N Gaussians. Split valence basis sets allow orbitals to change size not the shape. Polarized basis sets remove this limitation by adding orbitals with angular momentum beyond the ground state configuration for each atom. In this study 6-31G*, also known as 6-31G(d) polarization basis set is used where d functions are added to heavy atoms [26].

2.1.3.2 Local Descriptors

Local softness (s) describes local perturbation in terms of electron density ($\rho(\mathbf{r})$) with respect to a global change in chemical potential, μ:

$$s(\mathbf{r}) = \delta\rho(\mathbf{r}) / \delta\mu \quad (2.1.3.2.1)$$

The Fukui function, f(**r**), is a space-dependent local function and "*it measures how sensitive a system's chemical potential is to an external perturbation at a particular point*" . It also gives information about a quantity related to the electron density of an atom or molecule in its frontier regions:

$$f(\mathbf{r}) = (\delta\mu / \delta v(\mathbf{r}))N = (\delta\rho(\mathbf{r})/ \delta N)v(_{\mathbf{r}}) \qquad (2.1.3.2.2)$$

These two local properties are related to each other through global softness, S:

$$s(\mathbf{r}) = f(\mathbf{r})\, S \qquad (2.1.3.2.3)$$

Since, however, $\delta\rho(\mathbf{r})/ \delta N$ is a discontinuous function of N, it will have one value from the right, one from the left and an average at some integral value of N:

$f+(\mathbf{r}) = [\delta\rho(\mathbf{r})/ \delta N] +$ (as N goes from N0 to N0 + δ) (2.1.3.2.4)

$f\text{-}(\mathbf{r}) = [\delta\rho(\mathbf{r})/ \delta N] -$ (as N goes from N0-δ to N0) (2.1.3.2.5)

$f0(\mathbf{r}) = 1/2\ [f+(\mathbf{r}) + f\text{-}(\mathbf{r})]\ 0$ (average) (2.1.3.2.6)

where $f+(\mathbf{r})$ is the reactivity index for a nucleophilic attack, $f\text{-}(\mathbf{r})$ for an electrophilic attack and $f\ 0(\mathbf{r})$ for a radical attack. Within the finite difference approximation, these relationships can be written as

$$f+(\mathbf{r}) = \delta\rho_N(\mathbf{r}) - \delta\rho_{N-1}(\mathbf{r}) \qquad (2.1.3.2.7)$$

$$f\text{-}(\mathbf{r}) = \delta\rho_{N+1}(\mathbf{r}) - \delta\rho_N(\mathbf{r}) \qquad (2.1.3.2.8)$$

$$f\ 0(\mathbf{r}) = ½\ [\delta\rho_{N+1}(\mathbf{r}) - \delta\rho_{N-1}(\mathbf{r})] \qquad (2.1.3.2.9)$$

A more convenient way of calculating the f(r) functions is to use the condensed Fukui functions obtained from the previous equations, when integrated over the k^{th} atomic region for the nucleophilic, electrophilic and radical attacks, respectively.

$$f^{+} = q_k(N+1) - q_k(N) \qquad (2.1.3.2.10)$$

$$f^{-} = q_k(N) - q_k(N-1) \qquad (2.1.3.2.11)$$

$$f^{0} = ½\ [q_k(N+1) - q_k(N-1)] \qquad (2.1.3.2.12)$$

Here q_k is the electronic population of atom k in the molecule under consideration. It is known that these descriptors are generally used to probe the regio-selective nature of a reaction [26].

2.2 Experimental Methods

2.2.1 Electropolymerization Process

Electrochemical polymerization is recognized as an effective technique for the synthesis of conducting polymers. It is widely used, because it is simple and can be used as a one step method [27].

The electropolymerization procedure offers the advantage of controlling the thickness, and functionality of such a 'reactive' coating through selective process parameters (i.e. current density and monomer concentration, etc.) and uniform coatings can be achieved [28].

During the process, the monomer is electrochemically oxidised at a polymerization potential giving rise to free radicals. These radicals are adsorbed onto the electrode surface and undergo subsequently a wide variety of reactions leading to the polymer network [29]. In Figure 2.1. electrochemical polymerizatıion mechanism of pyrrole is shown.

The growth of this polymer depends on its electrical character. If the polymer is electrically nonconducting, its growth is self-limited. Such films are very thin (10 - 100 nm). In contrast, the growth of conductive polymers is virtually unlimited.

The process is governed by the electrode potential and by the reaction time, which allows us to control the thickness of the resulting film [29]. In order to have uniform and reproducible results, the process parameters of electrochemical polymerization have to be optimized. The parameters:

1) type of electrolyte,

2) concentration ratio of monomer and electrolyte,

3) pH of the electrolyte and

4) current density will affect the conductivity and morphology of the synthesized polymer film [27].

There are mainly 3 types of electropolymerization techniques. These are:

1. Potentiodynamic by cyclic voltammetry
2. choronoamperometry (constant current)
3. choronopotentiometry (constant potential)

In this study, potentiodynamic by cyclic voltammetry technique is used in electropolymerization.

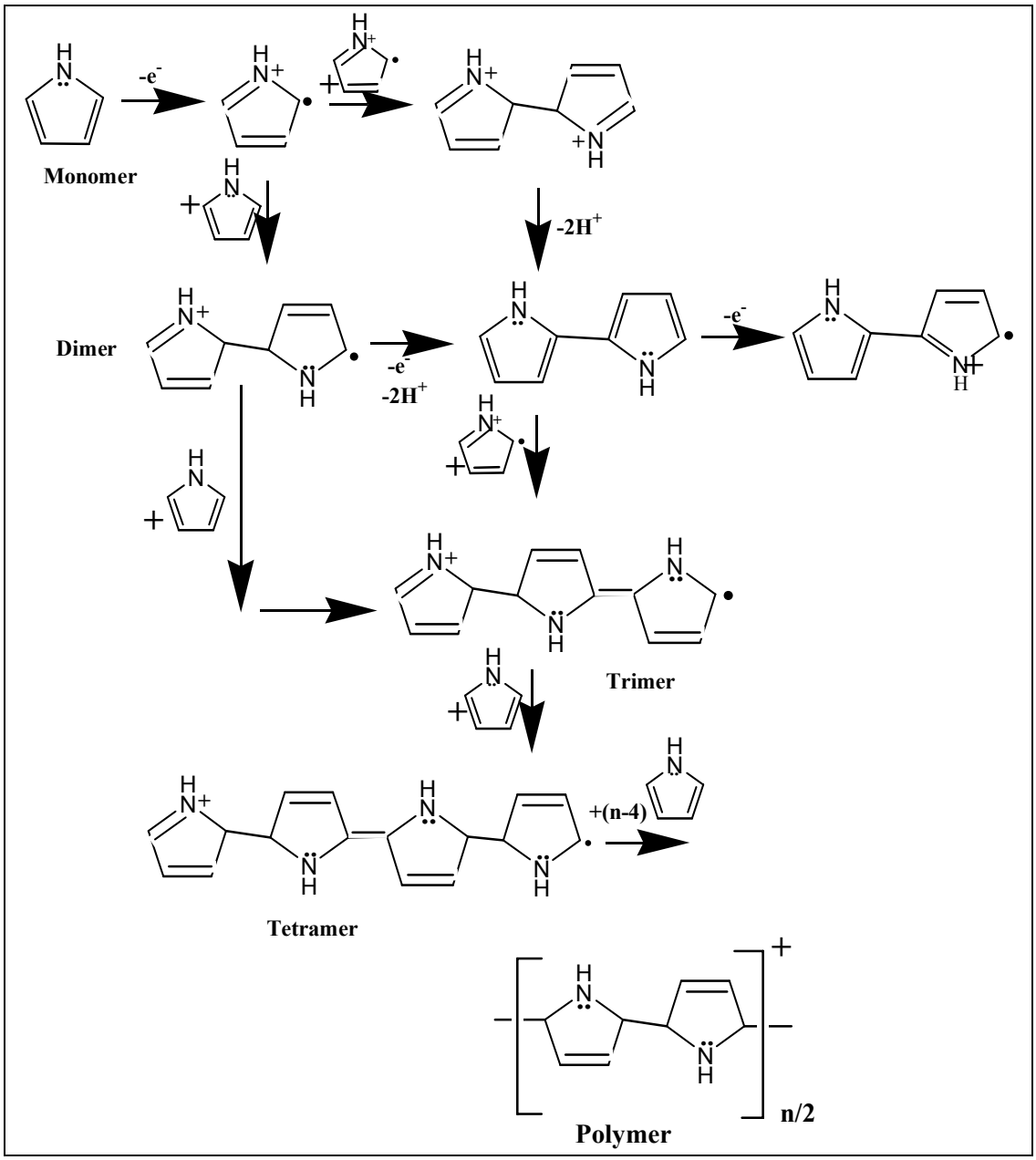

Figure 2.1 The electrochemical polymerization mechanism of pyrrole [30, 31]

2.2.2 Cyclic Voltametry (CV)

Electrochemistry deals with the transfer of electrons from one substance to another. This transfer creates a current, the magnitude of which can give us clues about our substances. Cyclic voltammetry is an important electrochemical technique used in electrochemistry. CV studies;

- The electroactivity of compounds, particularly biological molecules.
- Coupled chemical reactions: particularly to determine mechanisms and rates of oxidation/reduction reactions,
- Electrode surfaces.

Cyclic Voltammograms trace the transfer of electrons during an oxidation-reduction (redox) reaction. The reaction begins at a certain potential (voltage). As the potential changes, it controls the point at which the redox reaction will take place. Electrodes are placed in an electrolyte solution. The electrolyte contains analyte that will undergo the redox reaction [27].

At the negative electrode, the cathode, electrons are given off, and reduction takes place. At the positive electrode, the anode, the excess electrons are collected, and oxidation occurs. This giving-and-taking of electrons creates an electric current.

In CV, three types of electrodes are generally used. These are;

Working Electrode: The most important electrode in CV is the working electrode. Electrochemical reactions being studied occur at the working electrode and polymer coating is formed on it. Redox of the analyte takes place here. The working electrode can be made from a variety of materials including: platinum, gold, silver, glassy carbon, nickel and palladium.

Counter Electrode: is also known as the auxiliary electrode. Its purpose is to conduct electricity from the signal source into the solution, maintaining the correct current. It is usually inert conductor like platinum or graphite.

Reference Electrode: A reference electrode is used in measuring the working electrode potential. A reference electrode should have a constant electrochemical potential as long as no current flows through it. The potential that is cycled is the potential difference between the working electrode and the reference electrode. It is

usually made from silver/silver chloride (Ag/AgCl) or saturated calomel (SCE). This electrode's potential is known and constant.

In CV, the current in the cell is measured as a function of potential. The potential of an electrode in solution is linearly cycled from a starting potential to the final potential and back to the starting potential. This process, in turn, cycles the redox reaction. Multiple cycles can take place. During the CV process, first the system starts off with an initial potential at which no redox can take place.Then, at a critical potential during the forward scan, the electroactive species will begin to be reduced. After reversal of potential scan direction and depletion of the oxidized species the reverse reaction, oxidation, takes place. Then a plot of potential versus current is produced [27].

3 METHODOLOGY

3.1 Computational Methodology

In this study, quantum mechanical modeling methods, PM3 and DFT have been applied in the gas phase. In DFT methodology B3LYP/6-31+G* basis set have been utilized. This method is superior due to its ability to save computation time although it includes electron correlation in an average way. DFT methodology has proven to be successful in reproducing and predicting geometrical and electrochemical properties [3, 32, 33, 34, 35, 36]. In some of the studies, it is reported that the use of DFT functionals yielded estimates of energy band gaps which are in good agreement with experimental value in different polymeric systems [3]. In DFT calculations Gaussian 03 [37] and in semi-empirical PM3 calculations Spartan (Linux version) package programmes have been used. For all the monomers, these steps have been followed:

i. The conformational search for all monomers **M1**-**M11** have been done by optimizing all possible rotamers by fully optimizing the structures at the DFT B3LYP/6-31+G* level in the gas phase. The structures that are discussed throughout the manuscript are the global minima.

ii. Monomers with radical cation have been formed by optimizing the most stable neutral singlet structure obtained from the previous step.

iii. Charge distributions in the neutral and radicalic monomers have been carried out by NBO [38, 39, 40, 41, 42] and CHELP [43] calculations. Mulliken charges are also discussed in the text.

iv. The spin densities for some selected monomers have been discussed, which is expected to provide information on the site of propagation of polymerization.

v. The lowest unoccupied and the highest occupied molecular orbital energies of monomers have been estimated. Oxidation potentials, reduction potential, current values in oxidation and reduction have been measured from CV data of

these monomers. From these CV data, potential difference, half peak potential and current ratios have been calculated. Then these experimental data have been correlated with the calculated data.

vi. Fukui calculations on two representative monomers, **M3** and **M6**, have been performed in order to find the most available radicalic site.

vii. Hammett parameters of substituents of the phenylring belonging to **M2**, **M3**, **M4** and **M6** monomers have been correlated with the calculated HOMO, LUMO, HOMO-LUMO values.

viii. The effect of the number of monomer units on electrochemical properties have been investigated by optimizing structures with increasing the number of monomer units. A representative monomer, **M1** has been chosen for this purpose. The DFT calculations have been performed on **M1**, dimer and oligomers up to n, the number of monomer units, equals 7.

3.2 Experimental Methodology

3.2.1 Materials

All chemicals were used as received from Fluka and Aldrich Chemical without further purification. High strength carbon fibres [C 320 000 (CA)-Sigri Carbon, Meitingen, Germany, containing 320.000 single flaments in a roving] were used as working electrode. Dichloromethane were obtained from Merck. These were all the highest reagent grade chemicals and were used as obtained.

3.2.2 Instrumentation

The conventional three-electrode system was used for electrochemical oxidation. The working electrode was a carbon fiber electrode, the counter electrode was Pt wire and the pseudo reference electrode was Ag wire. The electrochemical measurements are carried out using Parstat 2263 potentiostat / galvanostat in three electrode with power suite programme.

3.2.3 Preparation of the CFMEs

Nearly 100 filaments of the CFME were used as working electrode All the electrodes were prepared by using 3cm of the CFME attached to a copper wire with another

copper wire. Only 1cm of the carbon fibres was dipped into the solution to keep the electrode area constant.

3.2.4 Electropolymerization and Characterization

The polymerization reactions were performed potentiodynamically via cyclic voltammetry in dicloromethane solution containing 0.1M Bu_4NPF_6 and 0.01M monomers. The polymerization was carried out at room temperature (25^0C). For electropolymerization reactions four different pyrrole derivatives were used at the same concentrations (0.01M); 1-(4-Methylphenyl)-1H-pyrrole **(M3)**, 1-(4-Methoxyphenyl)-1H-pyrrole **(M4)**, 1-(4-Chlorophenyl)-1H-pyrrole **(M2)** and 1-(2-Cyanoethyl)pyrrole **(M9).**

Monomers were dissolved in 5ml of 0.1M Bu_4NPF_6, which is used as a supporting electrolyte. Working electrode was carbon fiber, counter electrode was Pt wire and the referance electrode was Ag wire. Polymerizations were carried out at the same conditions.

4 RESULTS AND DISCUSSION

4.1 Experimental Results And Discussion

4.1.1 Cyclovoltametric results on CFMEs with Different Monomers

For electrochemical polymerization 1-(4-Methylphenyl)-1H-pyrrole **(M3)**, 1-(4-Methoxyphenyl)-1H-pyrrole **(M4)**, 1-(4-Chlorophenyl)-1H-phenylpyrrole **(M2)**, 1-(2-Cyanoethyl)pyrrole **(M9)** and 1-Phenyl-1H-pyrrole **(M1)** were used as monomers. The polymer growth and polymer film formation were carried out by using CV measurements and current vs. potential changes were plotted.

4.1.2 Electropolymerization

One of the first characteristics of a CV of a conducting polymer film is the rate (ν) dependence of the peak current (I_p) on the scan. According to well established electrochemical treatments, for a behaviour dominated by diffusion effects, I_p is proportional to $\nu^{1/2}$, whilst for a material localized on an electrode surface, such as a conducting polymer film, I_p is proportional to ν [28]. All coatings were performed by applying 50mV/scan rate. In monomer free solution, scan rates from 50 to 300 mv/s. The CVs obtained during polymer film growth on CFMEs are represented in figures below.

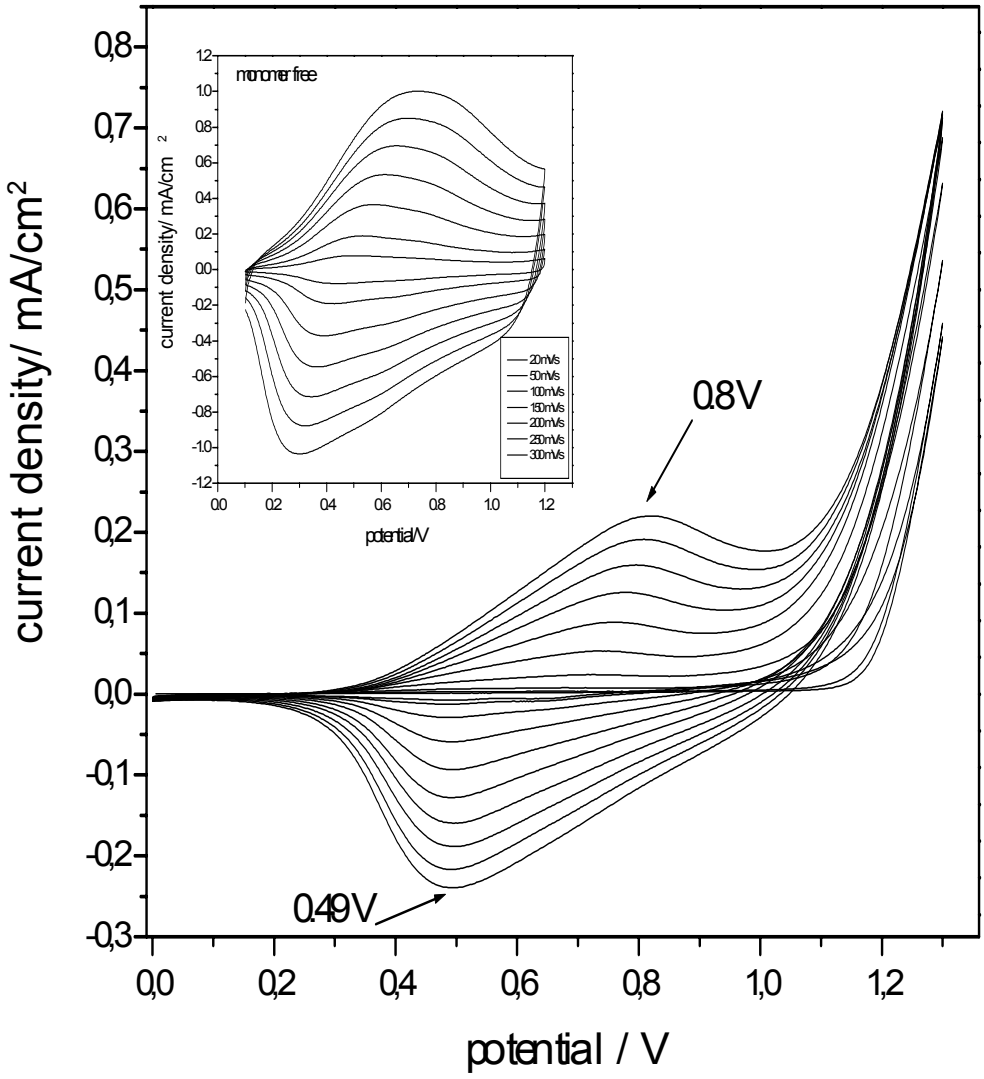

Figure 4.1 Cyclic voltammogram for potentiodynamic growth of 1-(4-Methylphenyl)-1H-pyrrole **(M3)** on CFME in 0.1M Bu_4NPF_6 containing dichloromethane (CH_2Cl_2) at 50 mv/s

Inset: Scan rate dependence of poly-1-(4-Methylphenyl)-1H-pyrrole (PMPPy) which was grafted with 50mv/s on CFME in 0.1M Bu_4NPF_6 containing CH_2Cl_2 in monomer free solution. (Scan rate = 50-300v/s)

As it is seen in Figure 4.1, the CFME coated with **M3** is reversible. In polymer growth, the oxidation potential and reduction potential are found as 0.8V and 0.49V, respectively. The onset value is observed in 0.407V. As illustrated in inset of Figure 4.1 in monomer free diagram the current is proportional to scan rate. Also the monomer free diagram has a rectangular like shape which means that it could be used as supercapasitors.

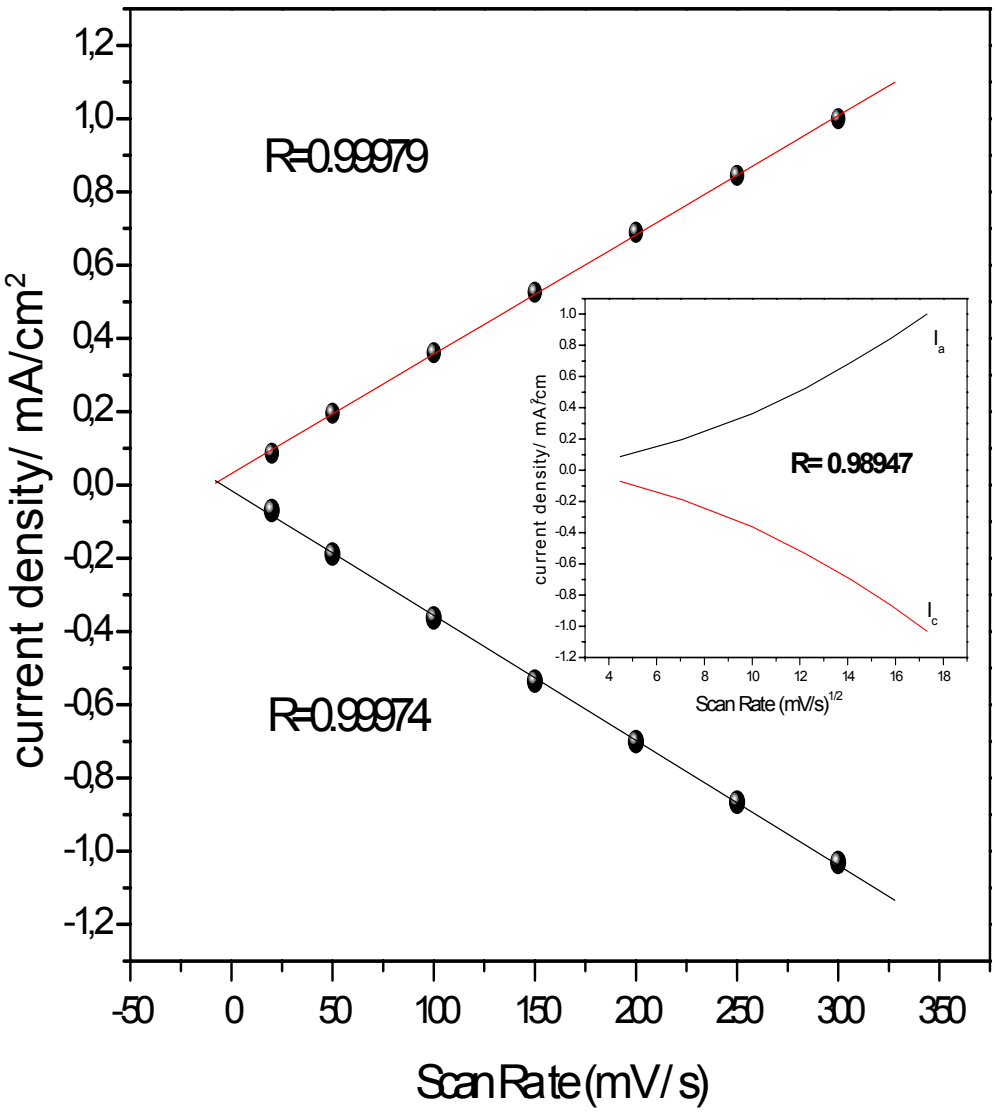

Figure 4.2 Scan rate effect on current in monomer free solution.

Inset: The effect of square root of scan rate on current in monomer free solution.

In Figure 4.2, the current density in monomer free is plotted against both scan rate and square root of scan rate. As it is seen, the regression coefficient value in the plot of current density vs scan rate is bigger. This means that thin film formation is observed in this molecule. Besides, the electron transfer is fast and this causes an increase in the rate of electropolymerization.

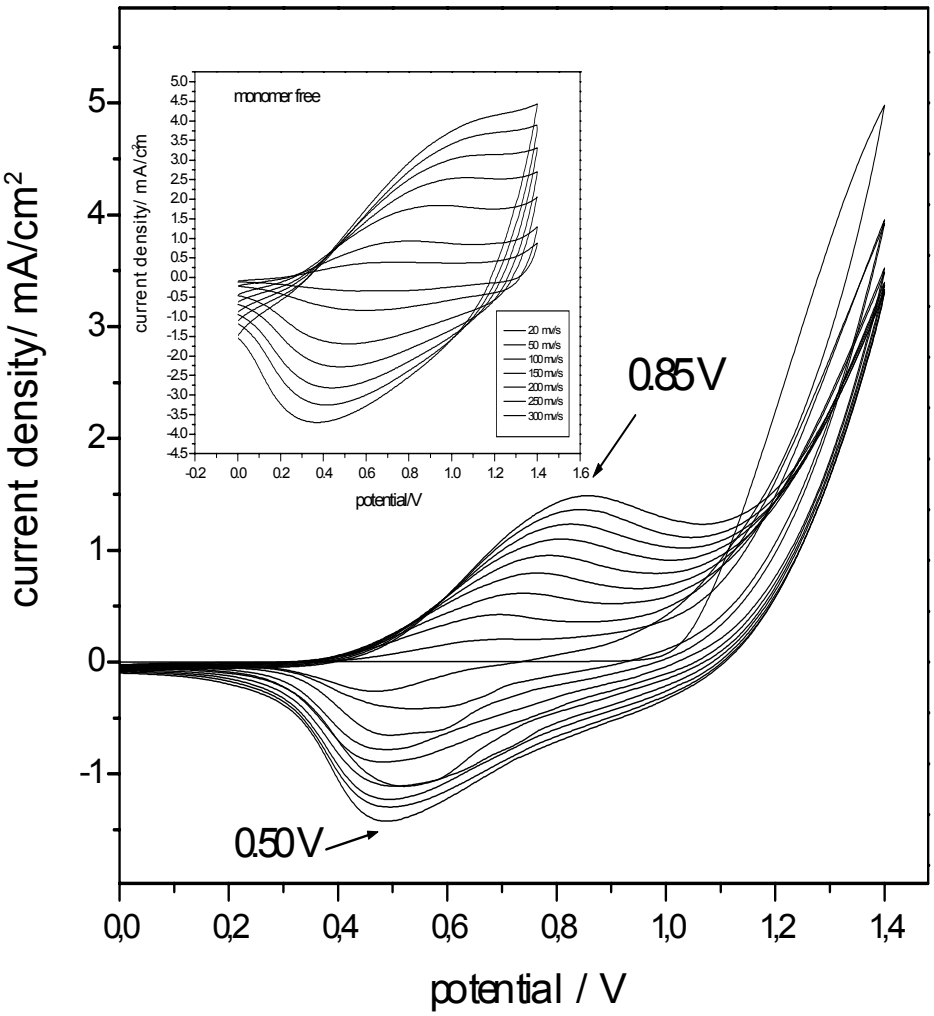

Figure 4.3 Cyclic voltammogram for potentiodynamic growth of 1-(4-Methoxyphenyl)-1H- pyrrole on CFME in 0.1M Bu_4NPF_6 containing CH_2Cl_2 at 50 mv/s

Inset: Scan rate dependence of poly-1-(4-Methoxyphenyl)-1H-pyrrole which was grafted with 50mv/s on CFME in 0.1M Bu_4NPF_6 containing CH_2Cl_2 in monomer free solution (Scan rate = 50-300mv/s)

As illustrated in Figure 4.3, the CFME coated with **M4** is reversible. In polymer growth, the oxidation potential and reduction potential are found as 0.85V and 0.50V, respectively. The onset value is observed in 0.407V. Also these values (E_c, E_a, E_{onset}) get closer to the values of **M2, M3.** As illustrated in inset of Figure 4.3 in monomer free diagram the current is proportional to scan rate. Besides the monomer free diagram has a rectangular like shape.

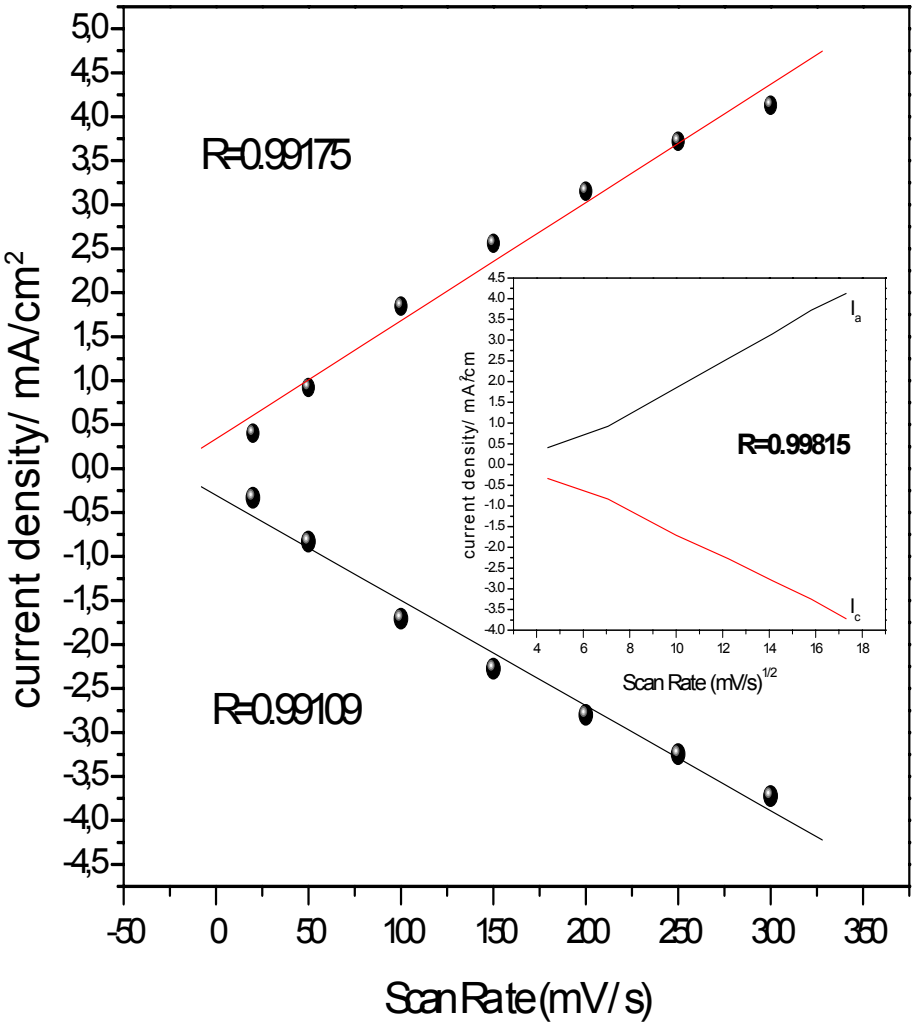

Figure 4.4 Scan rate effect on current in monomer free solution.

Inset: The effect of square root of scan rate on current in monomer free solution.

In Figure 4.4, the current density in monomer free is plotted against both scan rate and square root of scan rate. Different from **M1, M2, M3, M9,** only this monomer's regression coefficient value in the plot of current density vs scan rate is smaller. This result indicates that the reaction is diffusion controled. Additionally, this causes a decrease in the rate of electropolymerization.

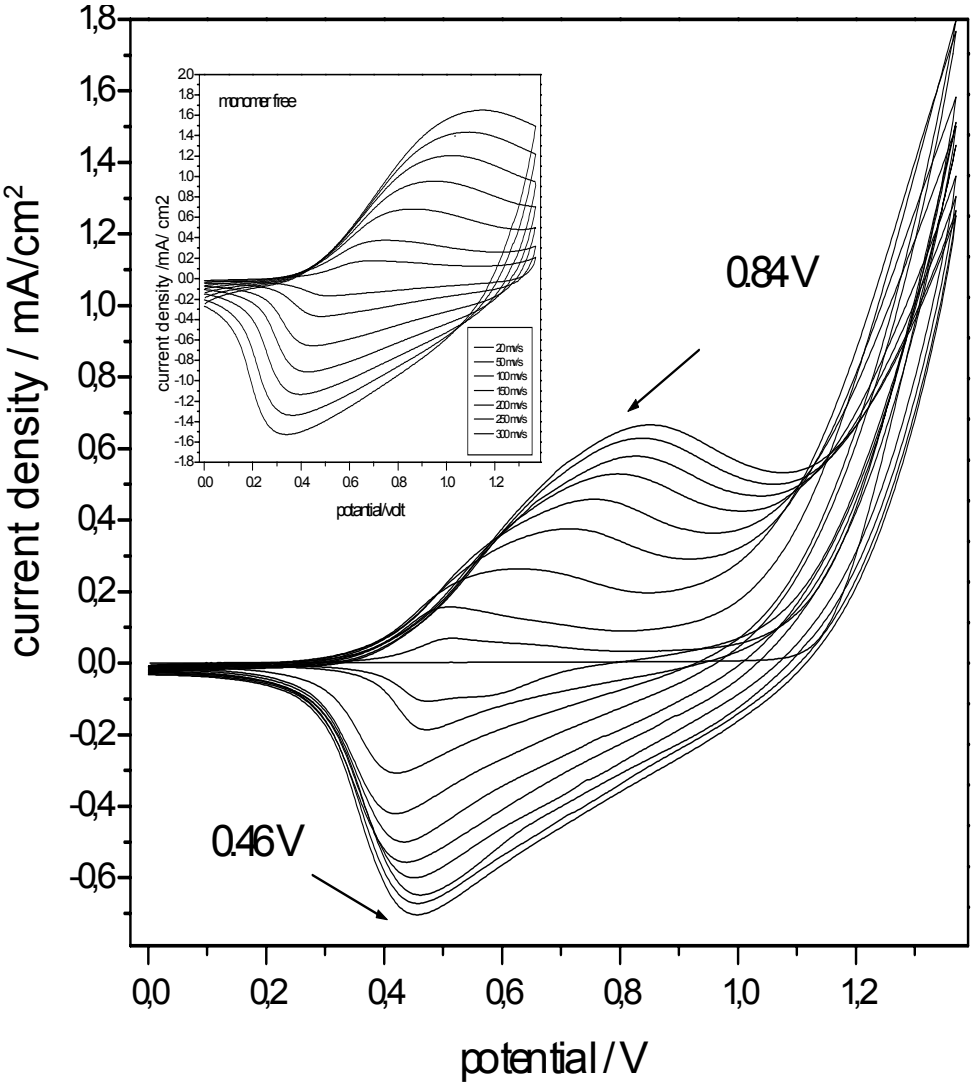

Figure 4.5 Cyclic voltammogram for potentiodynamic growth of 1-(4-Chlorophenyl)-1H-phenylpyrrole on CFME in 0.1M Bu_4NPF_6 containing CH_2Cl_2 at 50 mv/s

Inset: Scan rate dependence of poly-1-(4-Chlorophenyl)-1H-pyrrole which was grafted with 50mv/s on CFME in 0.1M Bu_4NPF_6 containing CH_2Cl_2 in monomer free solution. (Scan rate = 50-300mv/s)

As seen in Figure 4.5, the CFME coated with **M2** is the most reversible one among **M1, M3, M4, M9** monomers. In polymer growth, the oxidation potential and reduction potential are found as 0.84V and 0.46V, respectively. The onset value is observed in 0.391 V.

Furthermore, as illustrated in inset of Figure 4.5 in monomer free diagram the current is proportional to scan rate and the monomer free diagram has a rectangular like shape.

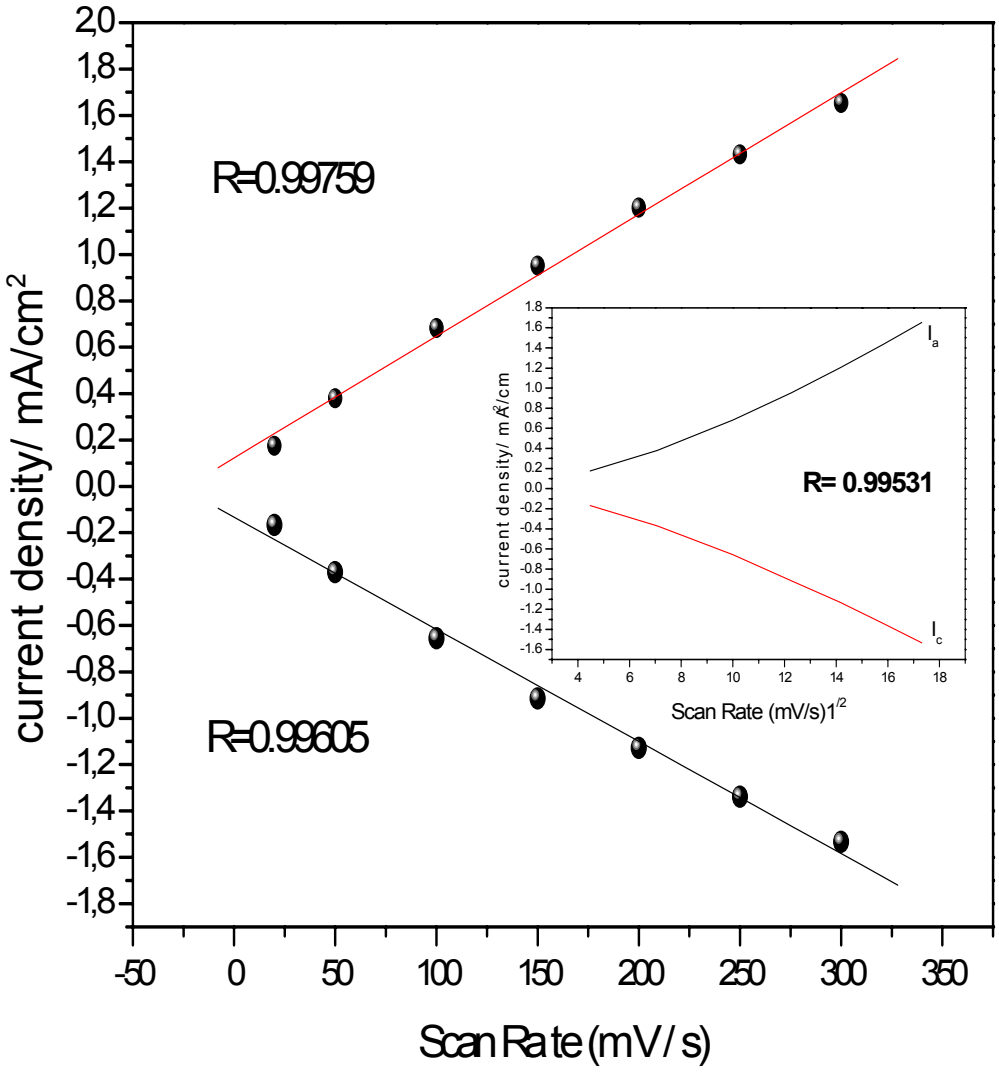

Figure 4.6 Scan rate effect on current in monomer free solution.

Inset: The effect of square root of scan rate on current in monomer free solution.

In Figure 4.6 the current density in monomer free is plotted against both scan rate and square root of scan rate. As it is seen, the regression coefficient value in the plot of current density vs scan rate is bigger. This means that thin film formation is observed in this molecule. Furthermore, electron transfer is fast and this causes an increase in the rate of electropolymerization.

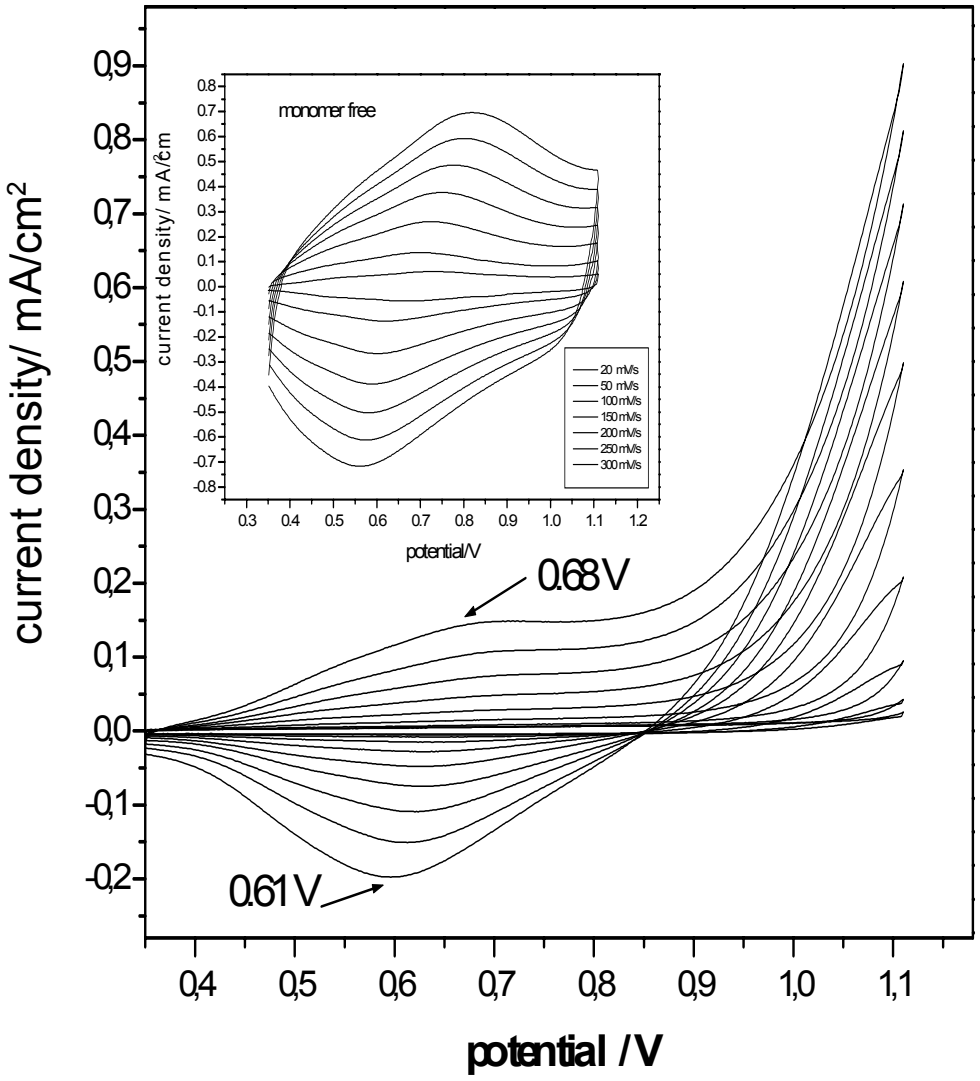

Figure 4.7 Cyclic voltammogram for potentiodynamic growth of 1-(2-Cyanoethyl)pyrrole on CFME in 0.1M Bu_4NPF_6 containing CH_2Cl_2 at 50 mv/s

Inset: Scan rate dependence of poly-1-(2-Cyanoethyl)pyrrole which was grafted with 50mv/s on CFME in 0.1M Bu_4NPF_6 containing CH_2Cl_2 in monomer free solution. (Scan rate = 50-300 mv/s)

As seen in Figure 4.7, the CFME coated with **M9** is reversible. In polymer growth, the oxidation potential and reduction potential are found as 0.68V and 0.61V, respectively. The oxidation potential value is lower according to **M1, M2, M3, M4.** The onset value is observed in 0.444 V. As illustrated in inset of Figure 4.7 in monomer free diagram the current is proportional to scan rate. Besides the monomer free diagram has a rectangular like shape.

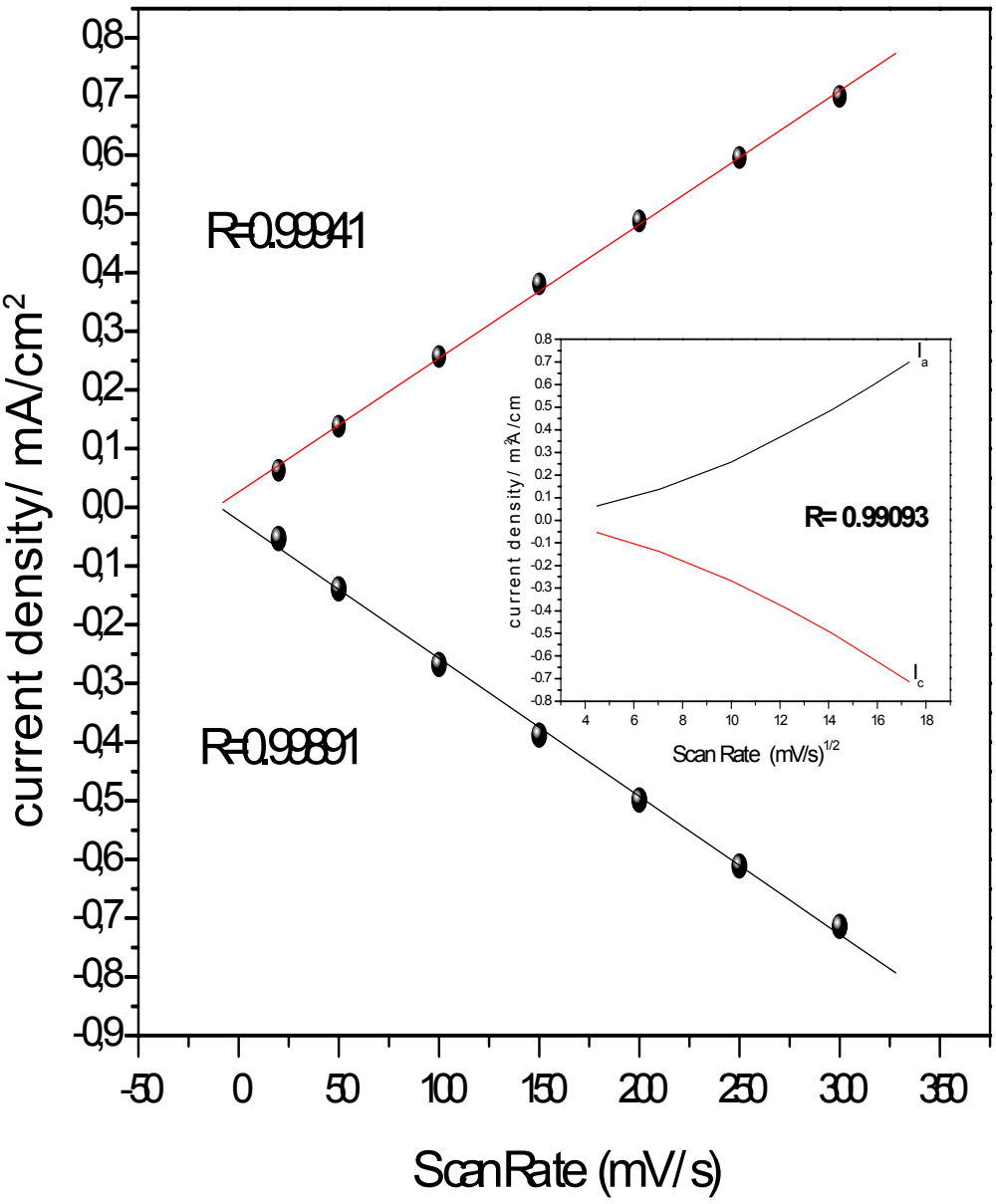

Figure 4.8 Scan rate effect on current in monomer free solution.

Inset: The effect of square root of scan rate on current in monomer free solution.

In Figure 4.8, the current density in monomer free is plotted against both scan rate and square root of scan rate. As it is seen, the regression coefficient value in the plot of current density vs scan rate is bigger. This result indicates that thin film formation is observed in this molecule. Besides, the electron transfer is fast and this causes an increase in the rate of electropolymerization.

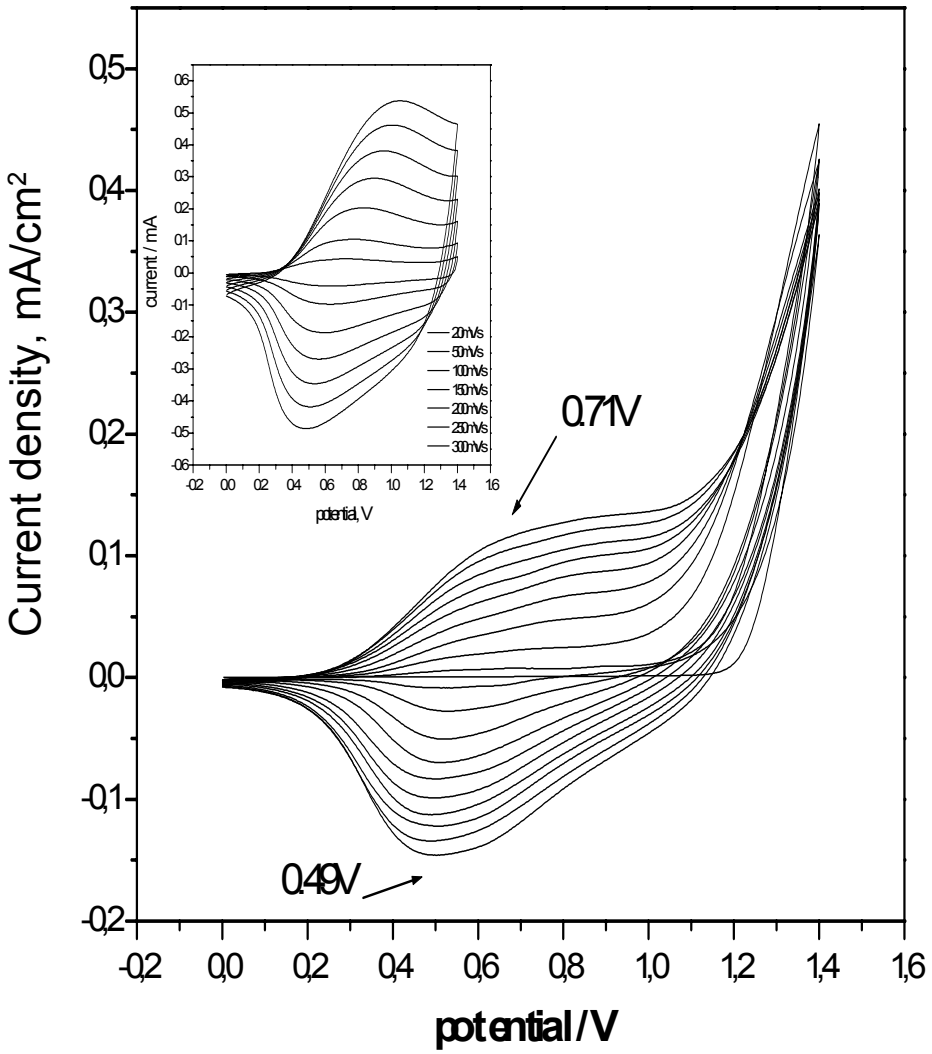

Figure 4.9 Cyclic voltammogram for potentiodynamic growth of 1-Phenyl-1H-pyrrole on CFME in 0.1M Bu_4NPF_6 containing CH_2Cl_2 at 50 mv/s

Inset: Scan rate dependence of poly-1-Phenyl-1H-pyrrole which was grafted with 50mv/s on CFME in 0.1M Bu_4NPF_6 containing CH_2Cl_2 in monomer free solution (Scan rate = 50-300mv/s)

As illustrated in Figure 4.9, the CFME coated with **M1** is reversible. In polymer growth, the oxidation potential and reduction potential are found as 0.71V and 0.49V, respectively. The onset value is observed in 0.340V. As illustrated in inset of Figure 4.9 in monomer free diagram the current is proportional to scan rate. Besides the monomer free diagram has a rectangular like shape.

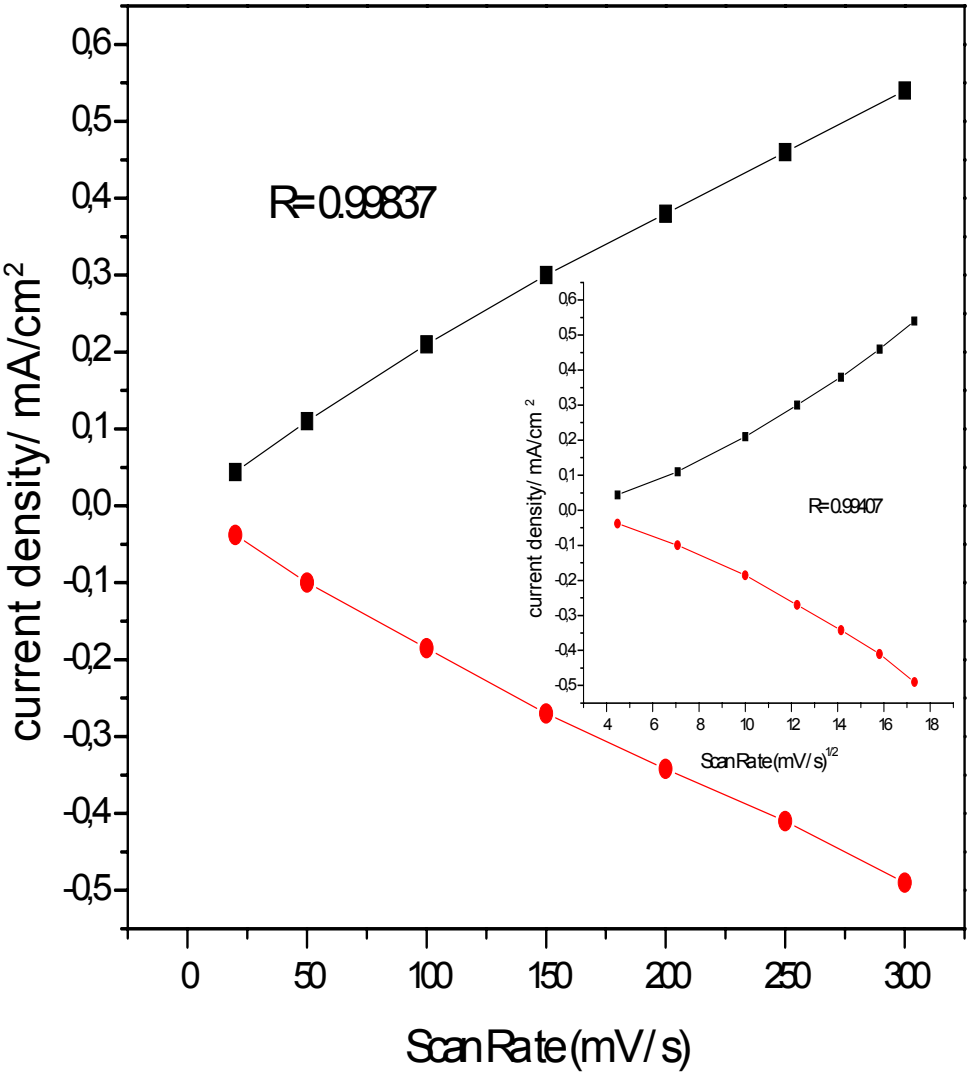

Figure 4.10 Scan rate effect on current in monomer free solution.

Inset: The effect of square root of scan rate on current in monomer free solution.

In Figure 4.10, the current density in monomer free is plotted against both scan rate and square root of scan rate. As it is seen, the regression coefficient value in the plot of current density vs scan rate is bigger. This result indicates that thin film formation is observed in this molecule. Besides, the electron transfer is fast and this causes an increase in the rate of electropolymerization.

As indicated in Table 4.1 different substitutions like 1-(4-Methylphenyl)-1H-pyrrole, 1-(4-Methoxyphenyl)-1H-pyrrole, 1-(4-Chlorophenyl)-1H-pyrrole, 1-(2-Cyanoethyl)pyrrole and 1-Phenyl-1H-pyrrole differentiate the E_{onset}, $E_{½}$ ($E_{1/2}=E_a+E_c/2$), ΔE ($\Delta E= E_a-E_c$) and I_a / I_c values. It can be easily seen that all the modified

electrodes are reversible because I_a / I_c ratios are nearly equal to 1, implying the degree of reversibility. It is shown that the most reversible one is coated with 1-(4-Chlorophenyl)-1H-pyrrole. Oxidation potentials, anodic and cathodic peak potentials of homopolymer coated electrodes were calculated as suggested in literature [29].

Table 4.1 Substitution effects on redox parameters of electrogrowth processes of pyrrole derivatives on carbon fiber micro electrodes.

Monomers	**E_{onset}(V)**	**E_a(V)**	**E_c(V)**	**$E_{½}$ (V)**	**ΔE (V)**	**I_a / I_c**
*Phenyl*pyrrole **(M1)**	0.340	0.713	0.498	0.606	0.215	0.841
*Methyphenyl*pyrrole **(M3)**	0.407	0.807	0.497	0.642	0.330	0.930
*Methoxyphenyl*pyrrole **(M4)**	0.447	0.850	0.505	0.678	0.345	1.062
*Chlorophenyl*pyrrole **(M2)**	0.391	0.842	0.467	0.655	0.375	0.953
*Ethylcyano*pyrrole **(M9)**	0.444	0.688	0.614	0.660	0.074	0.739

There is an another good property of these grafted CFMEs. According to literature, an ideal double layer capacitance behaviour of an electrode material is expressed in the form of a rectangular shape of the voltammetry characteristic in monomer free solution.

A good example of material giving capacitance properties are conducting polymers called also *synthetic metals.* They can be doped and dedoped rapidly to high charge density, hence, they can be applied as active materials for supercapacitors. Higher energy densities can be achieved because charging occurs through the volume of material [44].

As illustrated in all insets of Figures 4.1, 4.3, 4.5, 4.7, 4.9, monomer free diagrams have a rectangular like shape which are potentially candidates to be used as supercapasitors [44].

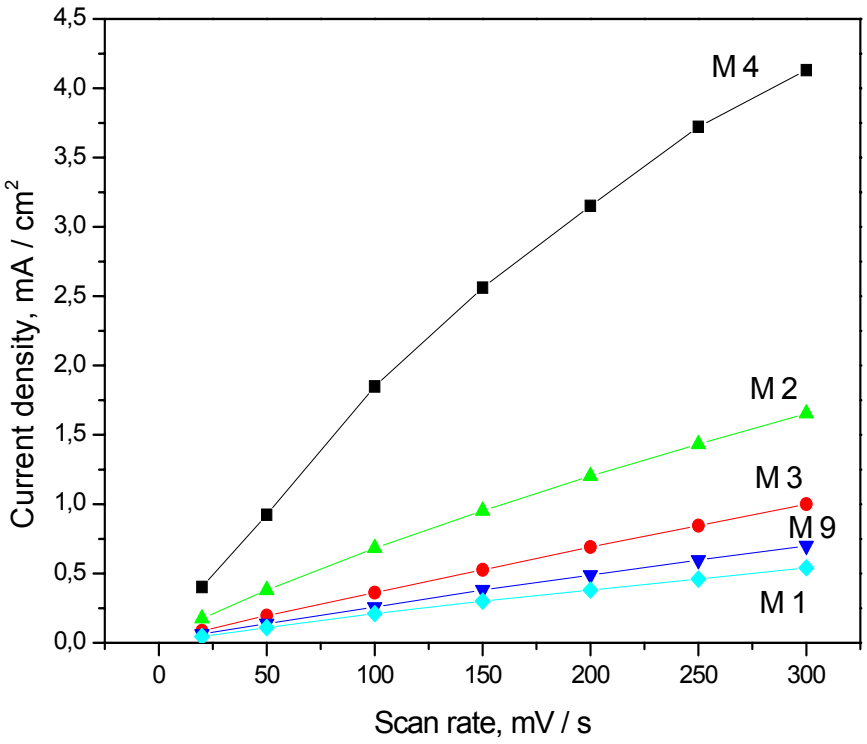

Figure 4.11 Plot of scan rate vs current density in monomer free

Figure 4.11 shows the relationship between scan rate and current density in monomer free for 5 monomers. It is seen that as the scan rate increases the current density increases. The significant increase in current density is observed in **M4** and the lowest increase in current density is observed in **M1**.

4.2 Theoretical Results And Discussion

4.2.1 The 3-Dimensional Geometry of Monomers

Throughout the discussion, the numbering scheme shown below will be used. (Figure 4.12)

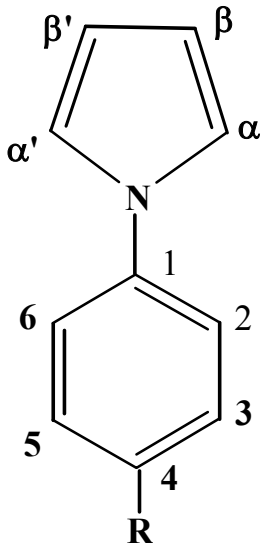

Figure 4.12 The numbering scheme of N-substituted pyrrole derivatives

M1 (1-(phenyl)-1H-pyrrole)

The most stable conformer of **M1**, its bond lengths and charges are shown in Figure 4.13 Phenyl pyrrole consists of two rings which are planar as expected. There is a slight delocalization on the pyrrole ring which would ideally like to extend this delocalization on the phenyl ring. However, the phenyl ring tilted 38.01˚ degrees out of the plane of pyrrole. As it is known conjugation throughout the molecule is a must of electrical conductivity. The molecule finds the optimal three-dimensional orientation where it adopts a nearly planar configuration and avoids steric repulsion between the H of α-C of pyrrole ring and the H of phenyl at ortho positon. Thus, this causes the phenyl ring to tilt out of the plane of pyrrole. N-C distances indicate that the lone-pair of N is delocalized towards the pyrrole ring. This causes a shortening of N-C_1 distance (1.385 Å) with respect to that of N-$(CH_3)_3$ (1.47 Å) proving the contribution of lone-pair to delocalization. The β-β' distance of 1.427 Å which is shorter than C-C distance of a typical cyclopentadiene, also shows the delocalization taking place on the pyrrole ring.

The N-C_1 bond distance of 1.418 Å indicates that the delocalization is active between the two planar rings although they do not exhibit a perfect co-planar geometry. These are also demonstrated by the NBO analysis of the compound. There is a delocalization of 21.95 kcal/mol from the lone-pair of N to bonding orbital of C_1-C_2. Delocalization from nitrogen's lone-pair to C_α-C_β bond of pyrrole ring are bigger.

This localization is as follows: lone-pair (1) N → C_α-C_β * 32.67 kcal/mol. This is the strongest donor-acceptor interaction that is observed in this molecule.

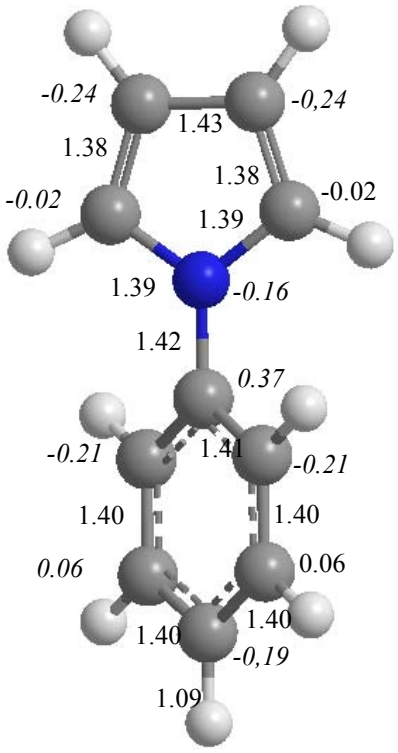

Figure 4.13 The bond length and ESP charges of the global minimum of 1-(phenyl)-1H-pyrrole **(M1)**

M2 and M3 (1-(4-Chlorophenyl)-1H-pyrrole and 1-(4-Methylphenyl)-1H-pyrrole)

Chlorine and methyl substitutions on phenyl ring do not make significant changes in the geometry of the parent **M1** monomer as shown in Figures 4.14 and 4.15 Bond lengths are also the same with **M1** monomer. The degree of coplanarity is also unaffected by Cl and CH_3 substitutions as C_α-N-C_1-C_2 dihedral angles for Cl and CH_3 substitutions are 38.0˚ and 39.2˚, respectively.

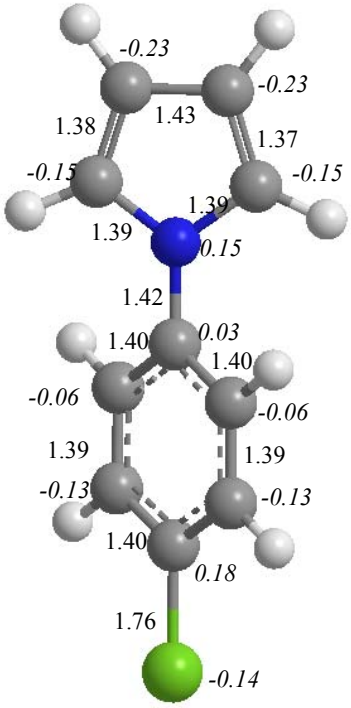

Figure 4.14 The bond length and ESP charges of the global minimum of 1-(4-Chlorophenyl)-1H-pyrrole **(M2)**

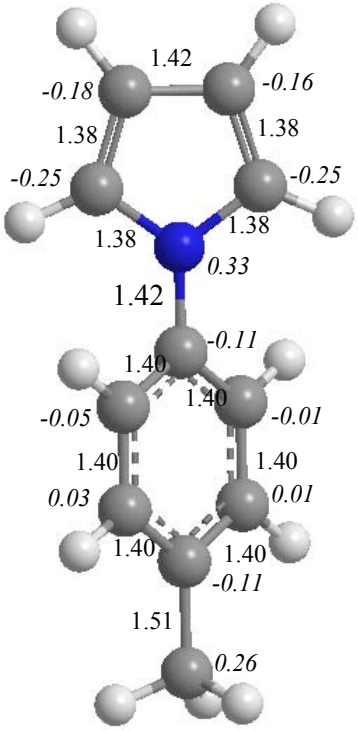

Figure 4.15 The bond length and ESP charges of the global minimum of 1-(4-Methylphenyl)-1H-pyrrole (**M3)**

M4 (1-(4-Methoxyphenyl)-1H-pyrrole)

The phenyl ring in **M4** is tilted slightly more from the plane of pyrrole with respect to **M1** (by almost 5˚) (Figure 4.16). This causes a very slight increase in N-C (phenyl) bond length (1.421 Å) as compared to that of **M1** monomer, since the phenyl rings and the pyrrole rings are less coplanar. -CH_3 group of methoxy is eclipsed with the phenyl ring. The symmetric bond length distribution seen in parent molecule is disturbed in **M4**. -OCH_3 group affects the phenyl ring by contributing to the delocalization on the phenyl ring. This contribution stemmed by the delocalization from the lone-pairs of oxygen to the phenyl ring causes O-C bond to shrink to 1.367 Å

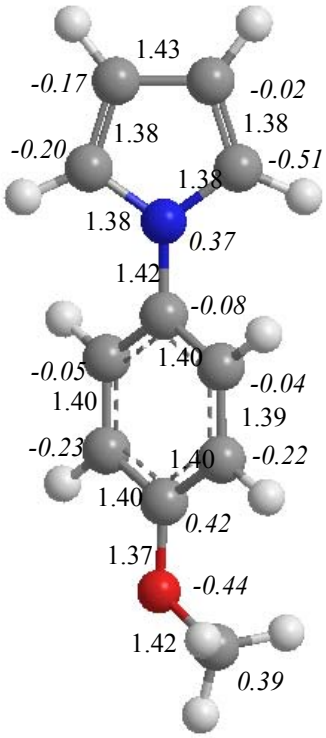

Figure 4.16 The bond length and ESP charges of the global minimum of 1-(4-Methoxyphenyl)-1H-pyrrole (**M4)**

M5 (1-(4-(1H-Pyrrol-1-YL)Phenyl)-1H-Pyrrole)

This monomer can be viewed as two planar pyrrole rings in which phenyl ring is sandwiched (Figure 4.17). The phenyl ring cannot be coplanar with the pyrrole ring due to H-H repulsions mentioned earlier, thus, it is tilted 38˚ out of the pyrrole's plane. The bond lengths of pyrrole rings are almost equal to that of **M1**'s. N-C_1 bonds are also unchanged in **M5** with respect to **M1**.

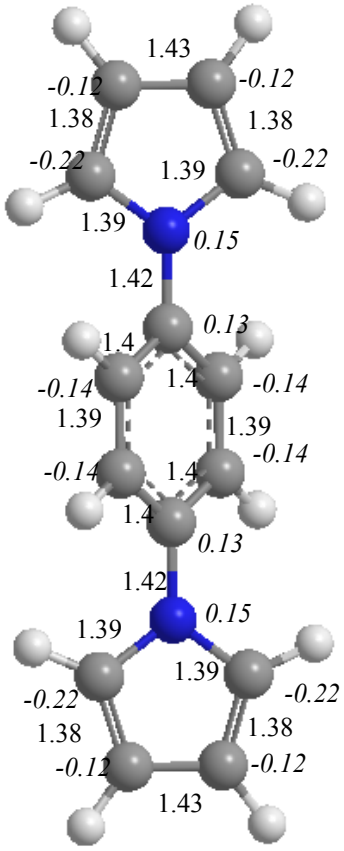

Figure 4.17 The bond length and ESP charges of the global minimum of 1-(4-(1H-Pyrrol-1-YL)Phenyl)-1H-Pyrrole **(M5)**

M6 (1-(4-Nitrophenyl)-1H-pyrrole)

The 3-dimensional geometry of the molecule exhibits the general trends observed so far (Figure 4.18). The C_{α}-N-C_1-C_2 dihedral is 31˚ in contrast to 38-42˚ observed in **M1**-**M5**. This causes a slighty more efficient delocalization between the pyrrole and the phenyl ring. This is reflected in the shorted N-C_1 bond length (1.407 Å), which is the shortest that is observed in **M1**-**M5**. –NO_2 group is perfectly coplanar with the phenyl ring.

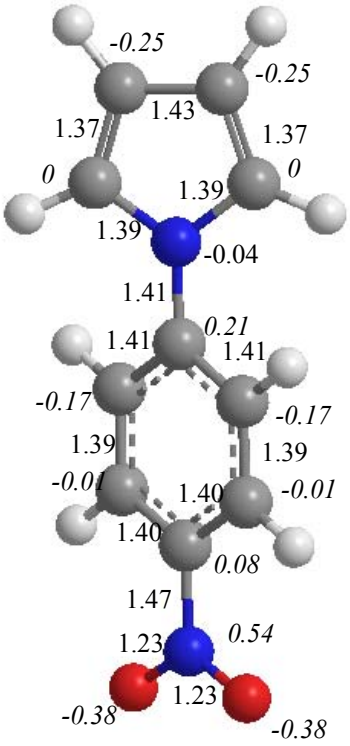

Figure 4.18 The bond length and ESP charges of the global minimum of 1-(4-Nitrophenyl)-1H-pyrrole **(M6)**

M7 and M8 (1-(p-Tolysulfonyl) pyrrole and 1-(Phenylsulfonyl) pyrrole)

There is a big distinction in the 3-dimensional geometry of **M7** from **M1**-**M6** monomers. Pyrrole ring has a planar structure as in other monomers discussed throughout but the phenyl ring is not on the same plane with pyrrole. The N-S- C_1-C_2 dihedral is 90.1˚ and the pyrrole ring and the phenyl ring are viewed as they are perpendicular to each other as expected. The shortened bond distances of N-C_α (1.392 Å) indicate that the lonepair of N is delocalized to the pyrrole ring, however, it is still slightly longer than N- C_α of **M1** (1.385 Å). Methyl substitution on phenyl ring did not change the geometry such that the bond lengths of **M8** are the same with **M7**.

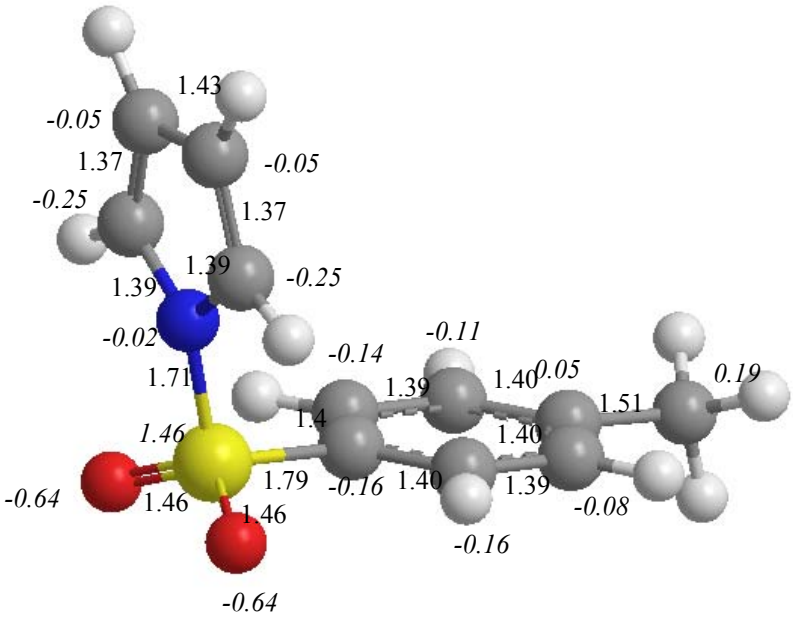

Figure 4.19 The bond length and ESP charges of the global minimum of 1-(p-Tolysulfonyl) pyrrole **(M7)**

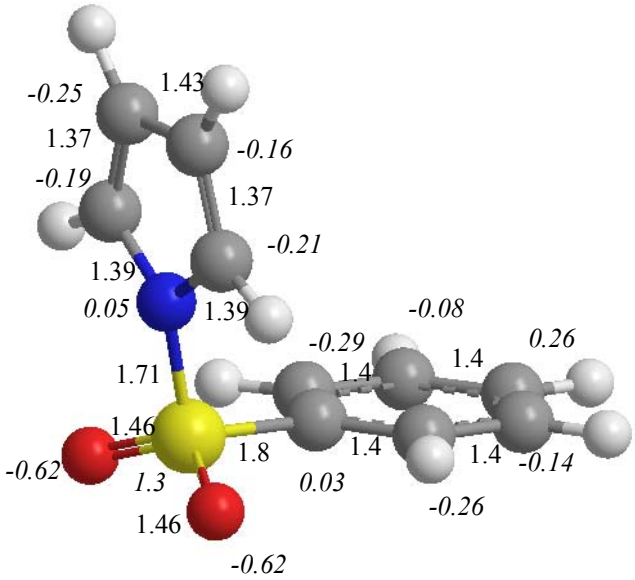

Figure 4.20 The bond length and ESP charges of the global minimum of 1-(Phenylsulfonyl)pyrrole **(M8)**

M9 (1-(2-Cyanoethyl)pyrrole)

In this monomer, pyrrole ring has a planar structure. Similar to **M7** and **M8** monomers the N-C_1-C_2-C_3 dihedral is 180˚. C_α-N-C_1-C_2 dihedral between cyano ethyl and pyrrole ring is 86.6˚. The shortening of N-C_α distance (1.381 Å) supports the delocalization.

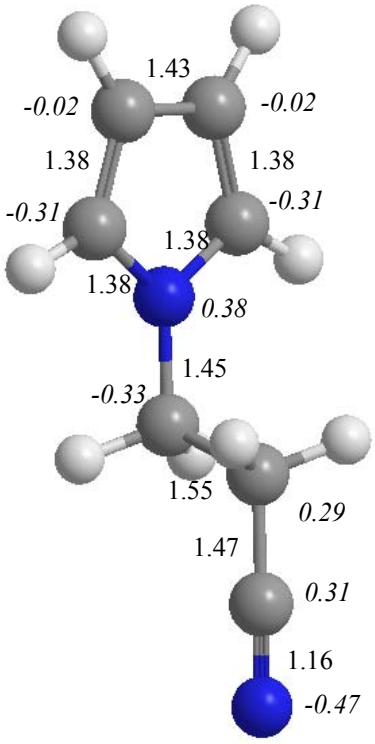

Figure 4.21 The bond length and ESP charges of the global minimum of 1-(2-Cyanoethyl)pyrrole **(M9)**

M10 (N-carbo-t-butoxypyrrole)

This monomer has the –COO group coplanar with the pyrrole ring, which allows delocalization on pyrrole to extend on to the C-O bonds. The bond linking the N-substituent to the pyrrole ring is 1.404 Å which is higher than that of **M1**. **M10** lacks the extended delocalization that is present in some other monomers that is studied. Then, N-C_1 bond length is at an intermediate value.

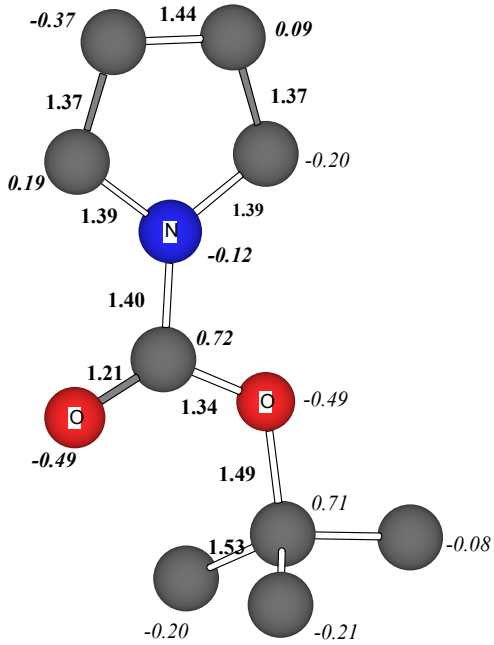

Figure 4.22 The bond length and ESP charges of the global minimum of N-carbo-t-butoxypyrrole **(M10)**

M11 (1-(Dimethylamino)pyrrole)

The pyrrole ring with N-$(CH_3)_2$ substituton is shown in Figure 4.23 The lone pair on substituent N is eclipsed with the pyrrole ring. Gauche orientation of N's lone-pair could not be obtained as a stationary point. In the gauche orientation, the lone pair is in a better orientation for N substituent to contribute to delocalization but the H's on α-C's and methyl group causes unfavorable steric interaction.

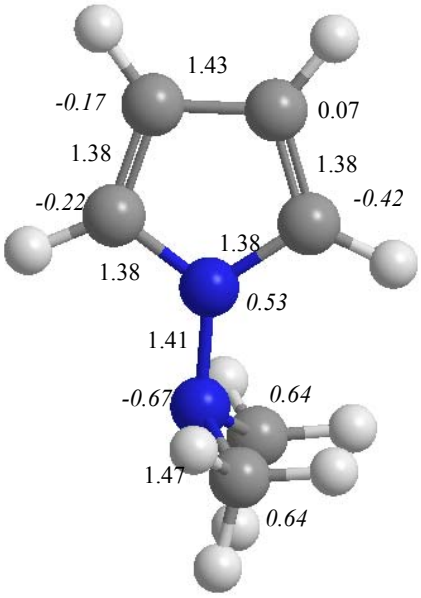

Figure 4.23 The bond length and ESP charges of the global minimum of 1-(Dimethylamino)pyrrole **(M11)**

4.2.2 The Effect of Chain Length

To see the effect of the number of monomers in calculated properties, 3-dimensional geometries of oligomers of a representative of the set of monomers discussed in this text, namely **M1**, have been investigated. The number of monomer units are increased in order to account on the 3-dimensional geometry of oligomers. For that purpose, the geometry of oligomers up to n=7 have been optimized with the DFT theory B3LYP/6-31G*. It is obvious that the optimizations become more complex as the number of monomers increase due to increasing number of rotatable single bonds. In monomer calculations, it is seen that the pyrrole and the phenyl rings are not coplanar.

The pyrrole rings will be referred to as "*cis*" or "*trans*" depending on their orientation with respect to each other. However, these *cis* and *trans* isomers will deviate from their ideal N-C_α-C_α-N dihedral angles, which are 0˚ and 180˚, respectively. In the ideal *cis* orientation, the H's of C_α will have steric interaction and this dihedral (N-C_α-C_α-N) was obtained as 60˚ in the dimer (*cis* dihedral). Thus, in forming input structures for oligomers, this dihedral was the starting geometry for *cis* isomers. In ideal *trans* geometry (where N-C_α-C_α-N dihedral is 180˚), the H's on β-carbons and the phenyl ring have unfavorable steric interactions. Thus, the pyrrole rings destruct their coplanarity slightly (N-C_α-C_α-N=141˚) in order to relieve the

steric crawding in favor of losing extended delocalization. Likewise, this 141˚ was considered as the starting geometry for *trans* oligomers. In calculations, rather than spanning all rotations, these two isomeric structures were considered as starting geometries. In the monomer the phenyl ring was tilted 38˚ out of the plane of pyrrole. In the dimer, these C_{α}-N-C_1-C_2 dihedral angles are reduced to approximately 34˚ and 20˚ due to the presence of a neighboring monomer, in both the cis and trans structures.

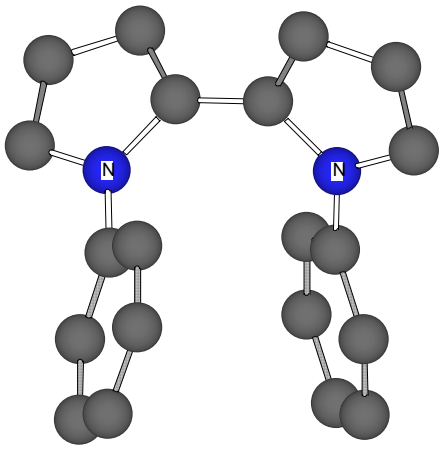

Figure 4.24 The most stable geometry of cis dimer for **M1**

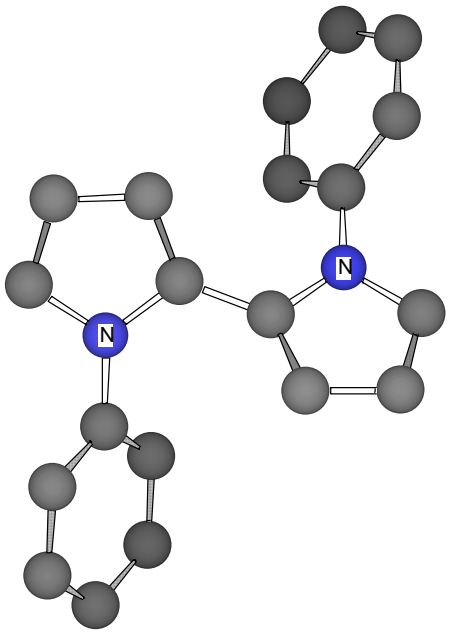

Figure 4.25 The most stable geometry of transdimer for **M1**

When the number of monomer units are increased, the general trend that has been observed is that the phenyl ring is oriented such that it has C_{α}-N-C_1-C_2 dihedral angle

as 60˚ or 120˚. Thus, the phenyl rings are not completely perpendicular to the pyrrole ring and bends slightly on either side.

In this chain, it is possible that there may be many combinations of cis and trans linkages for pyrrole ring and all possible linkages have not been calculated. However, in all calculations if the pyrrole linkage is cis, than N-C_α -C_α-N dihedral is around 60˚ and if it is trans, than N- C_α - C_α -N dihedral is around 140˚. No other value for this dihedral angle is observed on oligomers.

This reveals some general trends about the 3-dimensional geometry of the polymer, however since complete conformational analysis has not not been performed on these oligomers, results should be interpreted carefully. The most stable structures that are observed for n=6 and n=7 oligomers are shown in Figures 4.26 and 4.27 Full conformational search is beyond the scope of this thesis, so this is left as the subject of another study. However, it is still possible to draw some general facts about oligomers.

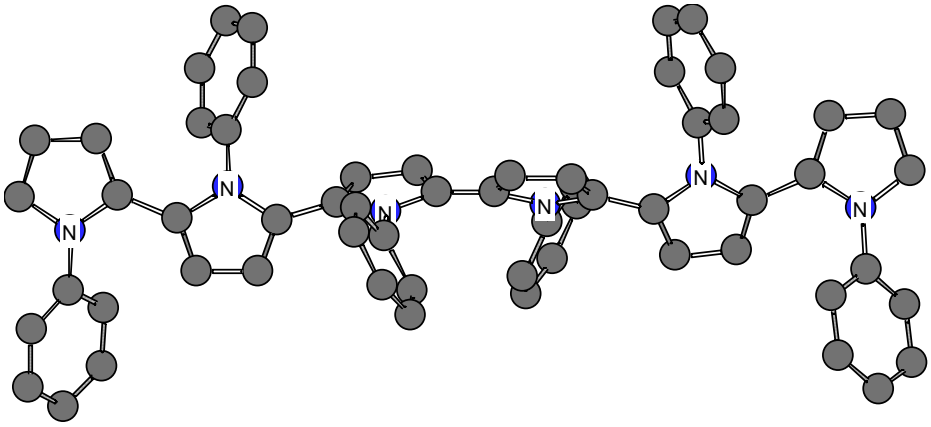

Figure 4.26 The most stable geometry of n=6 for **M1**

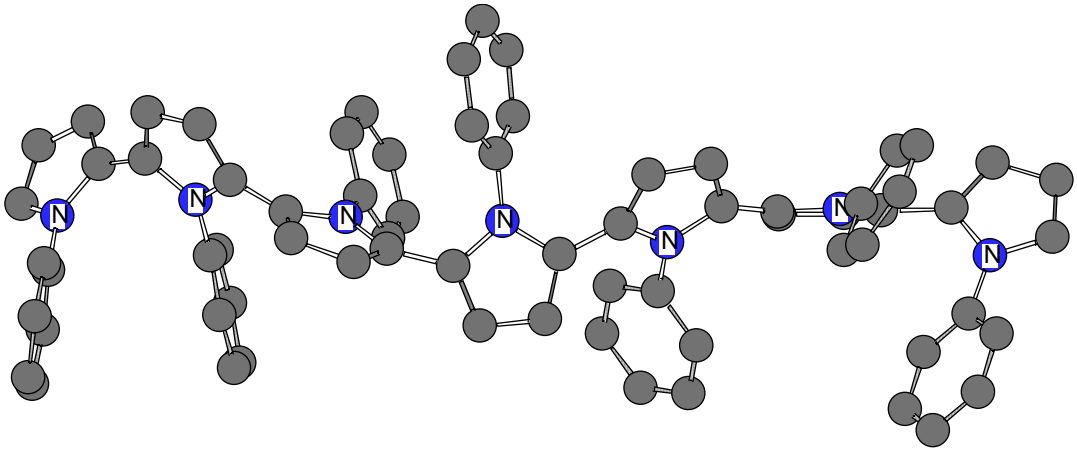

Figure 4.27 The most stable geometry of n=7 for **M1**

Small oligomers of pyrroles have been stated as well-structured molecules, which allow the rationalization of structural effects on electronic properties of their parent polymers. Thus, one can expect to draw direct relationships between oligomer and material properties [18]. Thus, polymer properties can be obtained from oligomer calculations by plotting the results, against inverse chain length and extrapolating to infinity [18, 19]. This approach is well established for band gaps and IPs [2, 25].

Extrapolations based on oligomers provide an alternative way to calculate bandgaps. A combination of semi-empirical geometry optimization followed by a hybrid functional density functional theory (DFT) calculation for the energy levels of molecular oligomers provides a reliable and computationally efficient method for predicting bandgaps of a group of diverse conjugated polymers [18, 19].

In a study, HOMO-LUMO gaps of polyacetylene (PA) oligomers as a function of $1/N$c, where Nc is the number of carbon atoms along the PA chain were examined. Linear regression data of oligomer band gaps as a function of Nc were found. Similar results were obtained for polypyrrole [18, 19].

In another recent study, DFT calculations on pyrrole oligomers have been used to estimate band gaps, ionization potentials, electron affinities, and bandwidths for polypyrrole. Polymer data are obtained from oligomer calculations by plotting the results against inverse chain length and extrapolating to infinity. Also in that study, vertical excitation energies in solution and HOMO-LUMO gaps at the B3P86-30% level is correlated for pyrrole through heptapyrrole. Theoretical and experimental data show that monomers do not lie on the straight lines going through the other points for the larger oligomers. [19].

In this sudy, HOMO-LUMO gaps, HOMO and LUMO energy levels are obtained by DFT method at B3LYP/6-31G* level for N-phenypyrrole (**M1**) through heptaphenylpyrrole (n=7) and these data are shown in Table 4.2.

Table 4.2 The HOMO-LUMO energy differences, HOMO and LUMO energies and their relative energies (in au) for n=1 to n=7 of **M1** by B3LYP/6-31G*. (Numbers in paranthesis are the differences between HOMO and LUMO energies and HOMO energies in ev)

# of Monomers	|HOMO-LUMO| (au)	HOMO (au)	LUMO (au)
n=1	0.19508 (5.31)	-0.20776 (5.65)	-0.01268
n=2	0.17604 (4.79)	-0.18838 (5.13)	-0.01234
n=3	0.17241 (4.69)	-0.18719 (5.09)	-0.01478
n=4	0.14877 (4.05)	-0.16442 (4.47)	-0.01565
n=5	0.14771 (4.02)	-0.16354 (4.45)	-0.01583
n=6	0.13479 (3.67)	-0.15245 (4.15)	-0.01766
n=7	0.13331 (3.63)	-0.15121 (4.11)	-0.0179

It is seen that as the number of monomer units increases, HOMO energies increase and the LUMO energies decrease. HOMO energies, which may be considered as IP analogues are observed to increase as n increases which physically means that the oligomer more easily oxidizes in electrochemical polymerization. The increase in HOMO and the decrease in LUMO causes a net decrease in band gap. Additionally, the decrease in LUMO energy is much less than the increase in HOMO, which implies that LUMO is not effected by extended delocalization occuring by increasing chain length.

To examine the relationship between these calculated values and inverse chain length some correlations are performed on optimized geometries. In reality as the number of monomer units increases, then there is a much more extended delocalization. A correlation is looked for between the HOMO, LUMO, HOMO-LUMO energy levels and the reciprocal of the number of monomer units. In the following figures, the correlation between the inverse chain length (1/n) and the calculated -HOMO, -LUMO and HOMO-LUMO energy levels are plotted. It is seen that there is a linear relationship between these values, with regression values approaching 1. As the number of **n** increases, there is a more linear correlation in both plots, which is in accordance with the literature findings where the linearity between IP and 1/n, EA and 1/n become more obvious as **n** increases [45]. If n=1 data is omitted regression coefficient values increase to 0.92, 0.93, 0.97 from 0.91, 0.91, 0.81 in -HOMO vs

1/n, HOMO-LUMO vs 1/n graphs and -LUMO vs 1/n graphs, respectively. If n=1 and n=2 data are omitted regression coefficient values increase to 0.97 and 0.97 from 0.92 and 0.93 in -HOMO vs 1/n and HOMO-LUMO vs 1/n graphs, respectively but regression coefficient value decrease to 0.92 from 0.97 in -LUMO vs 1/n graph. These graphs are shown in the following figures. Also in 1/n graphs, extrapolating to infinity provide one to calculate bandgaps and IPs [2, 25]. Regarding to this information, IP value for phenylpyrrole is obtained from - HOMO energy vs 1/n graph due to the HOMO energies may be considered as IP analogues. Besides, band gap value is obtained from the difference of HOMO and LUMO energies vs 1/n graph. IP and band gap values for phenylpyrrole are found as 3.35 ev and 2.81 ev, respectively. These values are accordance with the literature findings (IP= 4.47, Band gap= 3.16 for polypyrrole).

It is also expected that there may be a point of convergence where increasing the number of monomer unit does not make a significant change in properties. The calculated band gaps are observed to decrease less as **n** increases. There is a very small decrease in going from n=6 to n=7 which indicates that the band gap may converge around n=7. However, more detailed calculations and n=8 calculations are necessary to draw strong conclusions.

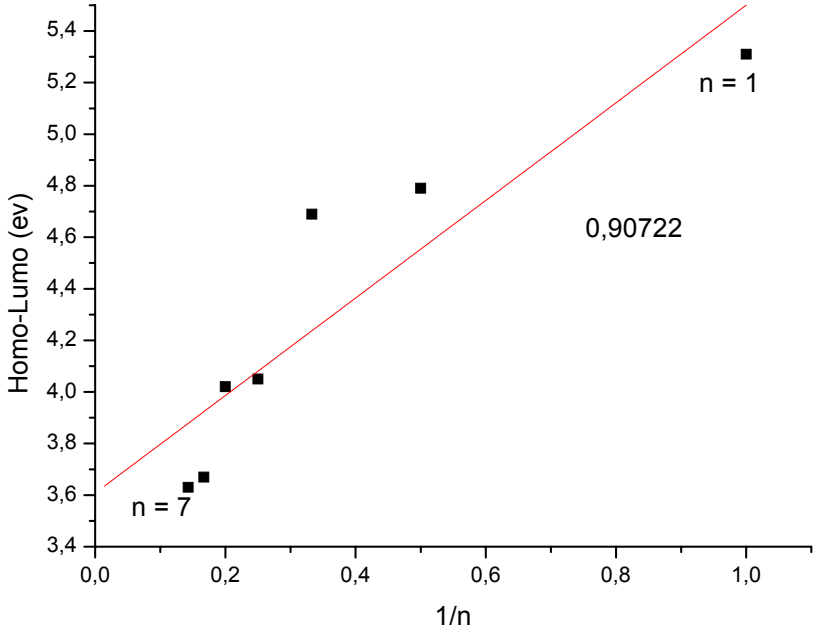

Figure 4.28 Plot of HOMO-LUMO vs 1/n

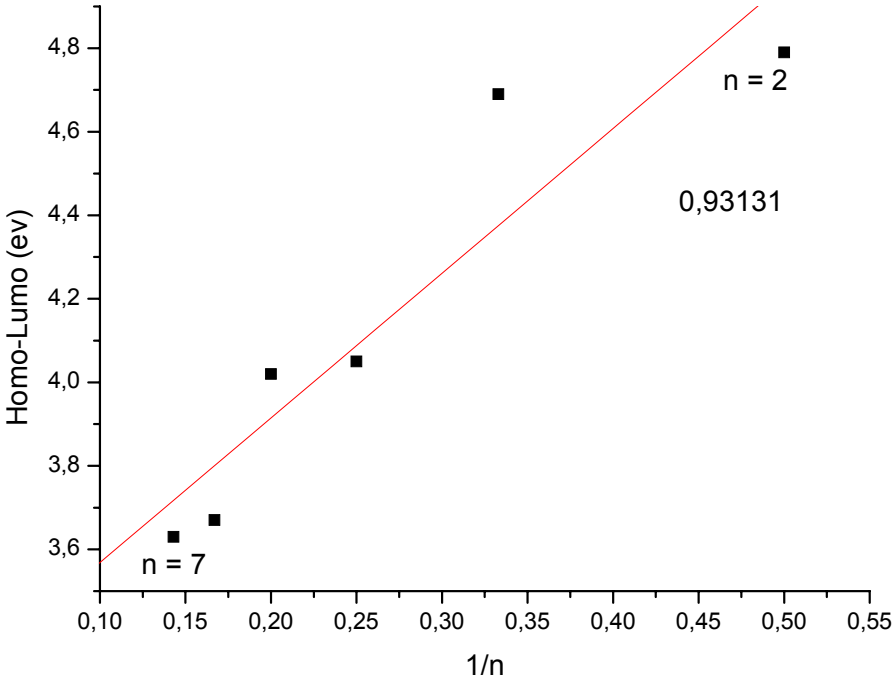

Figure 4.29 Plot of HOMO-LUMO vs 1/n (n=1 data is omitted)

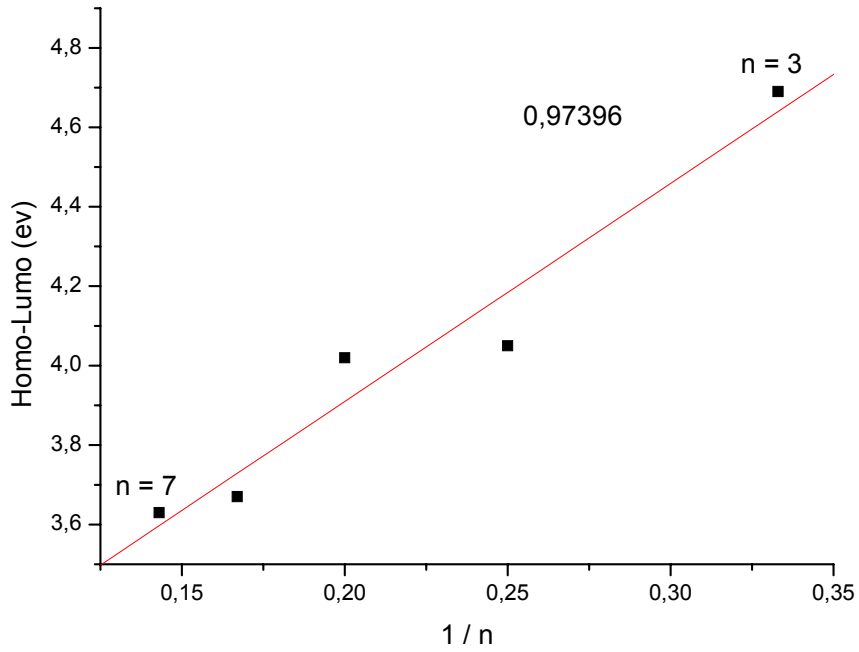

Figure 4.30 Plot of HOMO-LUMO vs 1/n (n=1 and n=2 data are omitted)

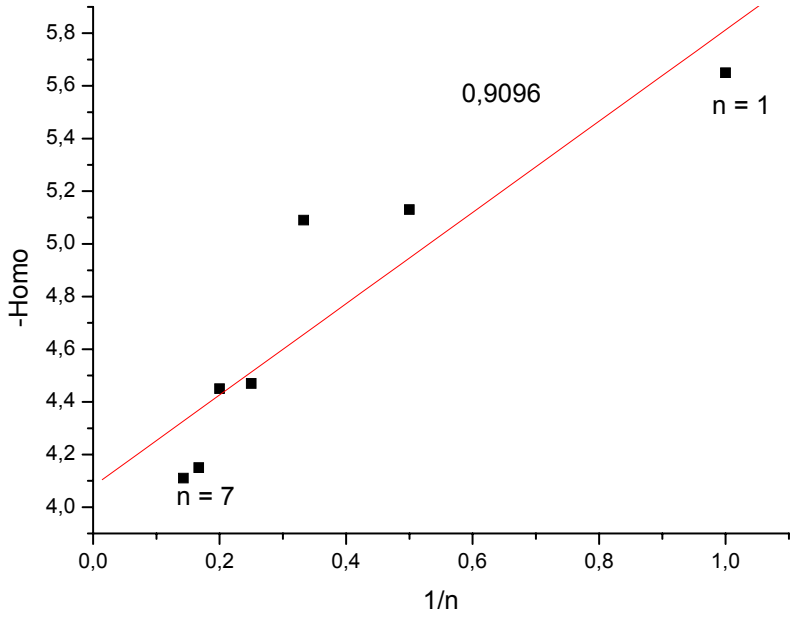

Figure 4.31 Plot of -HOMO vs 1/n

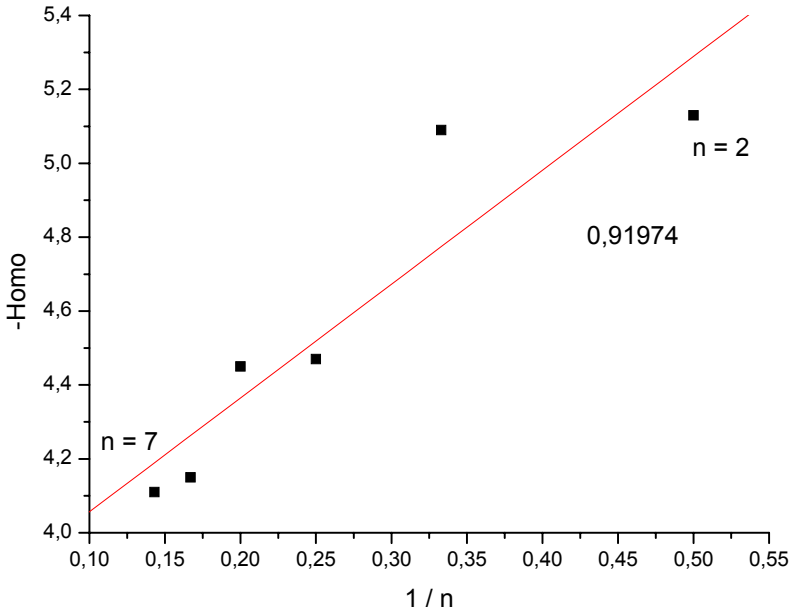

Figure 4.32 Plot of -HOMO vs 1/n (n=1 data is omitted)

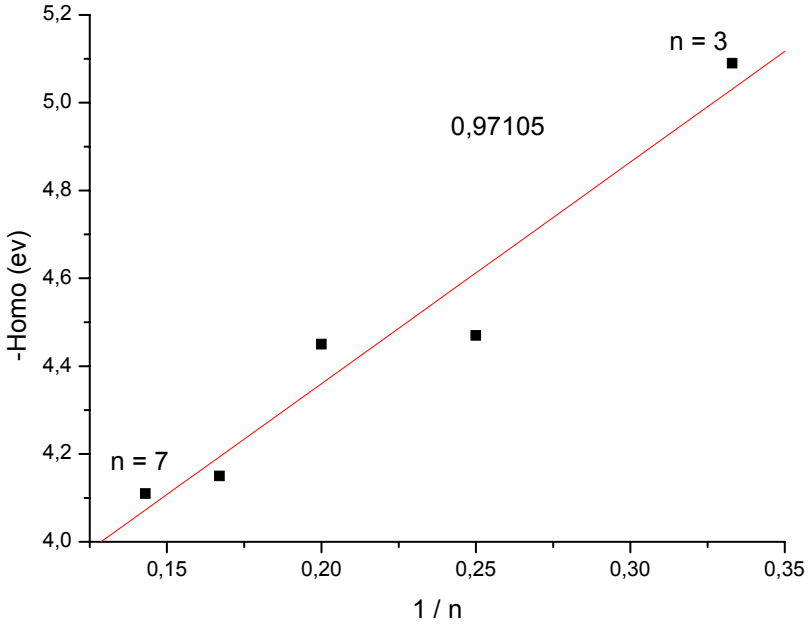

Figure 4.33 Plot of -HOMO vs 1/n (n=1 and n=2 data are omitted)

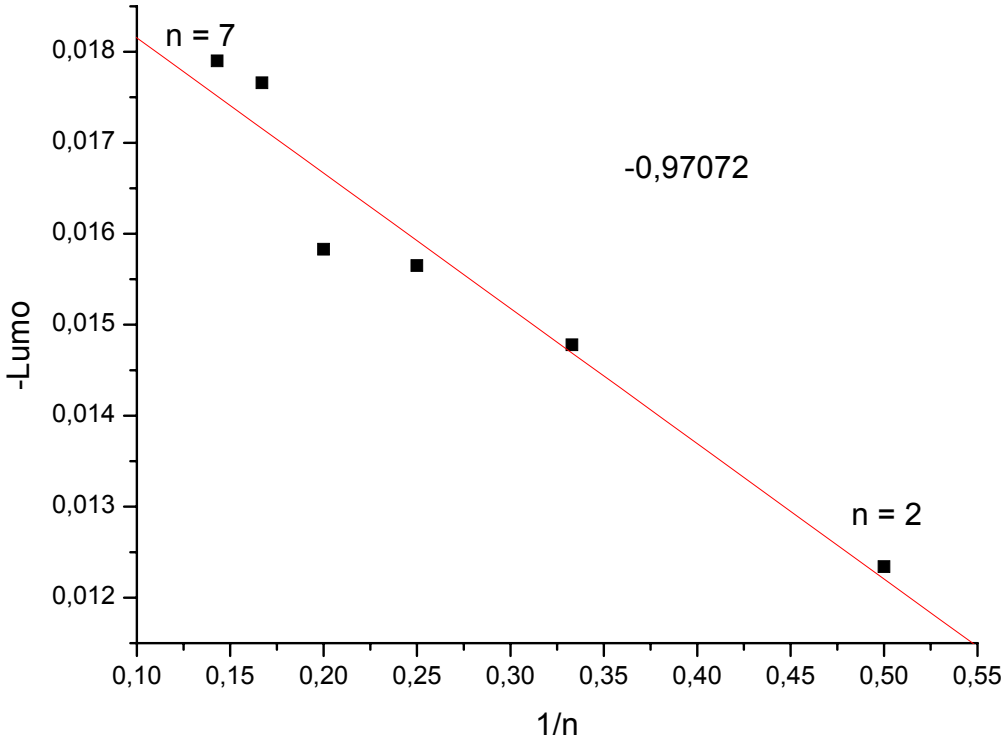

Figure 4.34 Plot of -LUMO vs 1/n (n=1 data is omitted)

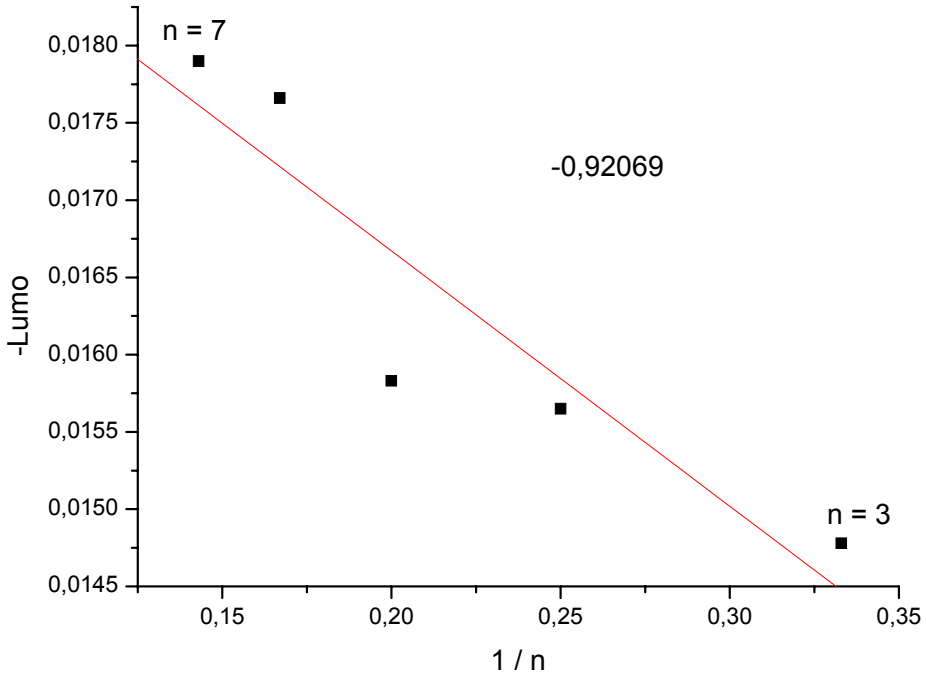

Figure 4.35 Plot of -LUMO vs 1/n (n=1 and n=2 data are omitted)

4.2.3 Spin Density

During oxidation, pyrrole oligomers undergo coupling reactions (oligomerization or poymerization). These processes are very sensitive to the structure of the oligomers such as their substituents and positions. For example, substitution modifies the accessibility of the reactive sites but also can change the electronic density in the cation radical and in the produced diprotonated dimer.

In principle, both linear (α-α' coupling) or branched structures (involving at least one of the β-β' positions) can be expected from early theoretical calculations predicting that the unpaired electron density of the radical intermediate can be almost as high in the β positions as in the α positions. However, until now, only α-α coupling is faster than branched coupling. In conclusion, when the α positions are free, the cation radical undergoes a fast coupling reaction in solution, leading to either a dimer or a polymer involving the coupling between two cation radicals.

There are many studies on spin density calculation [45]. In one of these studies, spin density calculation in cation radicals by DFT method indicated that dimerization through the β or β' does not play a major role, suggesting that the α-α coupling is the

major process even in the substituted compound and that branched coupling are negligible.

In the case of oligothiophenes, this conclusion is also supported by well-known results where the substitution of the two α terminal positions allow a large stabilization (increase of its lifetime) of the corresponding cation radicals. Morover, the formation of branched C-C bonds when they occur during the polymerization creates defects in the conjugation of the parent polymer and a decrease of its conductivity.

Reactivity studies of these oligomers as a function of the substituent position and of its nature permit useful information about the relative kinetic rate constants involving the different reactive positions to be obtained. However, great care should be taken in such investigations, because the substitution of one hydrogen by another chemical group or atom in these conjugated molecules has generally not only steric but also electronic effects [18].

In this study, spin density calculations in cation radicals of all N-pyrrole derivatives have been performed by DFT method. Spin density values for molecules are shown in Table 4.3. The results indicate that the radicalic site is localized in α positions for **M1, M2, M6, M7, M8, M9, M10, M11** and these molecules' cation radicals may prefer to undergo coupling reaction from α position. On the otherhand, **M3**, **M4**, **M5** molecules having electron donating groups have higher spin densities on β-C's which may increase their tendency to undergo β coupling from the β position. The other interesting object is that nitrogen is negatively charged in molecules prefering α-coupling reaction. On the contrary, in molecules prefering β-coupling reaction, charge on nitrogen is slightly positive.

In order to see the effect of basis set in spin density distribution, geometry optimizations with B3LYP/6-311+G** calculations have been performed. These calculations have given 0.55 and 0.06 for α and β spin densities for **M6** and -0.08 and 0.17 for α and β spin densities for **M3**, respectively. The monomers with high α spin densities have much higher values than their β spin densities. However, monomers of high β spin densities do not have that much of difference between their values, in both methods. This suggests that β preference may be slightly enhanced with

monomers of high β spin density. In the other monomers, α-α coupling is much more strongly suggested.

Table 4.3 Spin density values for molecules

Pyrrole Derivatives	C_{α}	$C_{\alpha'}$	C_{β}	$C_{\beta'}$	Average C_{α}	Average C_{β}	N
M1	0.546185	0.546185	0.052352	0.052352	0.546185	0.052352	-0.148597
M2	0.548195	0.548195	0.052647	0.05247	0.548195	0.0525585	-0.149778
M3	-0.090091	-0.095768	0.180263	0.191164	-0.092930	0.1857135	0.261524
M4	-0.082465	-0.064999	0.168187	0.138315	-0.073732	0.153251	0.211485
M5	-0.060348	-0.060348	0.127956	0.127956	-0.060348	0.127956	0.170802
M6	0.551365	0.551333	0.051859	0.051867	0.551349	0.051863	-0.145287
M7	0.522340	0.521840	0.069530	0.070832	0.522090	0.070181	-0.123797
M8	0.521527	0.521770	0.068871	0.068718	0.5216485	0.0687945	-0.121910
M9	0.550282	0.550285	0.046967	0.046960	0.5502835	0.0469635	-0.137203
M10	0.524774	0.522160	0.061861	0.069032	0.523467	0.0654465	-0.104674
M11	0.573504	0.507013	-0.009256	0.120524	0.540285	0.055634	-0.136296

Fukui calculation can be performed on monomers to find the most available site for radical formation. With this purpose, the procedure outlined in section 2.1.3.2 has been applied and the f˚ values (equation 2.1.3.2.9) have been calculated. In Table 4.4, f˚ values, charges on α, α', β and β' for N+1 and N-1 structures where N is the number of electrons in the system calculated by the B3LYP/6-31+G* basis set are shown for **M6** and **M3.**

Different charge methods have been applied, including Mulliken, NBO and Chelp charges. However, in all of the methods, almost all of the f˚ values are negative, which may be considered as an artifact of the methodology. Thus, fukui results were not succesfull in locating the most available site for radical formation.

Table 4.4 f˚ values, charges on α, α', β and β' for N+1 and N-1 structures for **M6** and **M3.**

NO_2 (M6)	**α (N+1)**	**α' (N+1)**	**β (N+1)**	**β' (N+1)**	**α (N-1)**	**α' (N-1)**	**β (N-1)**	**β' (N-1)**	**f° α**	**f° β**
CHELP	-0.018	-0.019	-0.286	-0.286	-0.065	-0.065	-0.078	-0.077	0.024	-0.104
MULLIKEN	0.020	0.020	-0.204	-0.204	0.045	0.045	-0.132	-0.132	-0.013	-0.036
NBO	-0.082	-0.082	-0.338	-0.338	-0.072	-0.072	-0.154	-0.153	-0.005	-0.092
CH_3 (M3)	**α (N+1)**	**α' (N+1)**	**β (N+1)**	**β' (N+1)**	**α (N-1)**	**α' (N-1)**	**β (N-1)**	**β' (N-1)**	**f° α**	**f° β**
CHELP	-0.205	-0.212	-0.228	-0.205	-0.071	-0.171	-0.231	-0.064	-0.044	-0.182
MULLIKEN	0.031	0.031	-0.207	-0.207	0.080	0.074	-0.174	-0.124	-0.023	-0.029
NBO	-0.064	-0.065	-0.347	-0.347	0.041	0.005	-0.302	-0.128	-0.044	-0.066

4.2.4 Hammett

The most important of the linear free enery relationships is the Hammett equation. Its wide application stems from the fact that Hammett correlations can provide important mechanistic information and predict unknown rate and equilibrium constants. Hammett found that the effect of meta and para substituents on the acidity of a family of substituted benzoic acids correlated with their effect on the acidity of other acids [46].

Hammett quantified the effect of substituents on any reaction by defining an empirical electronic substituent parameter σ, which is derived from the acidity constants of substituted benzoic acids. Thus, the electronic substituent parameter σ for any substituent X is defined by $\sigma_x = \log K_x / K_H$, where K_x and K_H are the acidity constants for the substituted benzoic acid and benzoic acid, respectively.

Substituents that increase the acidity of the benzoic acid have positive σ values, while those that decrease the acidity have negative σ values. Each substituent gives rise to σ meta and σ para parameters, corresponding to substitution at the meta or para position of the benzene ring. Ortho substituents do not correlate well due to steric effects. The σ value of a substituent is a measure of the electron withdrawing

or electron releasing abillity of that substituent compared with H. The σ value provides this information because the ionization of benzoic acid involves the deprotonation of a neutral molecule to form a negatively charged ion; deprotonation is facilitated by electron withdrawing substituents that partially disperse the negative charge, but is inhibited by electron releasing substituents that impede the charge dispersal. Thus, substituents that are electron withdrawing have positive σ values, while those that are electron releasing have negative σ values. The larger the absolute value of σ, the larger the electronic effect. Since all substituent effects are obtained by reference to H, the σ value for H is precisely 0. So in establishing the set of σ values, Hammett generated an empirical measure of electronic substituent effects [46].

The relationships between Hammett parameters and theoretically calculated values have been sought in N-pyrrole derivatives. For this purpose, many correlations have been made. (σ+ values used as Hammett parameters for **M1, M2, M3, M4** and **M6** are 0, 0.22, -0.17, -0.28, 0.77, respectively. For this purpose, various graphs are plotted between the Hammett parameters of **M1, M2, M3, M4**, **M6** and HOMO, LUMO energies and HOMO-LUMO differences for neutral and radicalic systems. The linearity of these correlations are investigated in terms of regression coefficient.

Among these graphs in radical cation state, Hammet vs HOMO-LUMO has resulted with no correlations and the correlation between Hammet parameters and HOMO is not strong enough. (coefficient 0.85). But in neutral and singlet states Hammet parameters vs HOMO-LUMO, Hammet parameters vs -HOMO, Hammet parameters vs LUMO, in radical cation state, Hammet parameters vs LUMO have resulted with clear correlations as seen in Figures 4.36, 4.37, 4.38, 4.39 given, respectively. The best correlation has been obtained from Hammett parameter vs. -HOMO energy level. This has revealed that electronic property of substitution is effective on both HOMO and LUMO energy levels of the monomer but the effect on HOMO energy level is the strongest and the electron withdrawing substituents have the biggest effect on HOMO energy level. The mentioned result has been theoretically emphasized by the Hammett correlation.

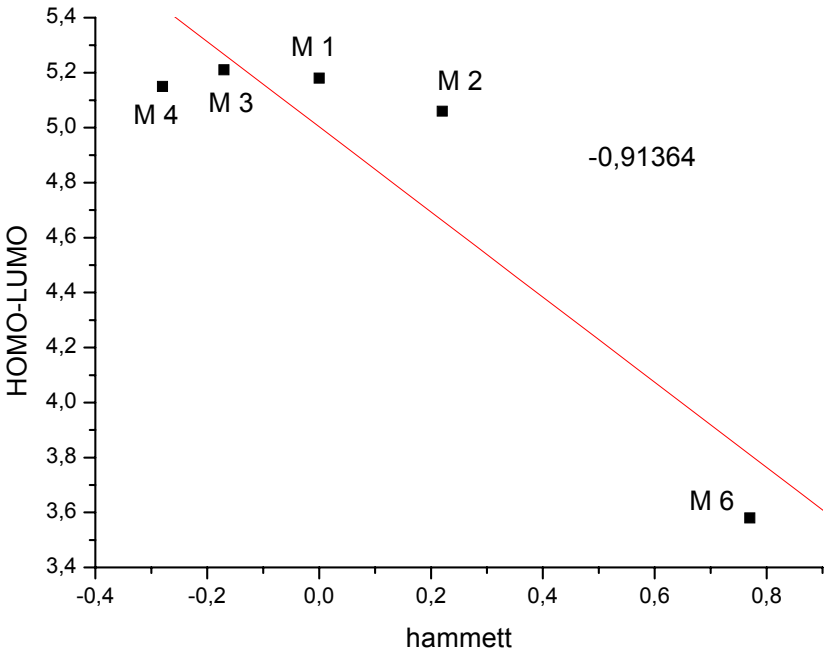

Figure 4.36 Correlation between Hammett parameter (σ) and the HOMO-LUMO energy difference in neutral singlet state

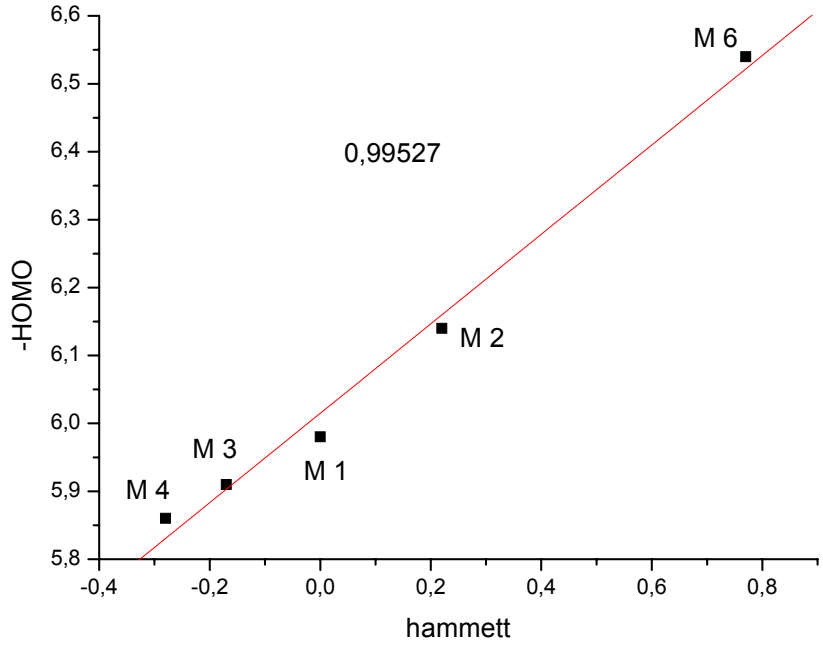

Figure 4.37 Correlation between Hammett parameter (σ) and the -HOMO energy level in neutral singlet state

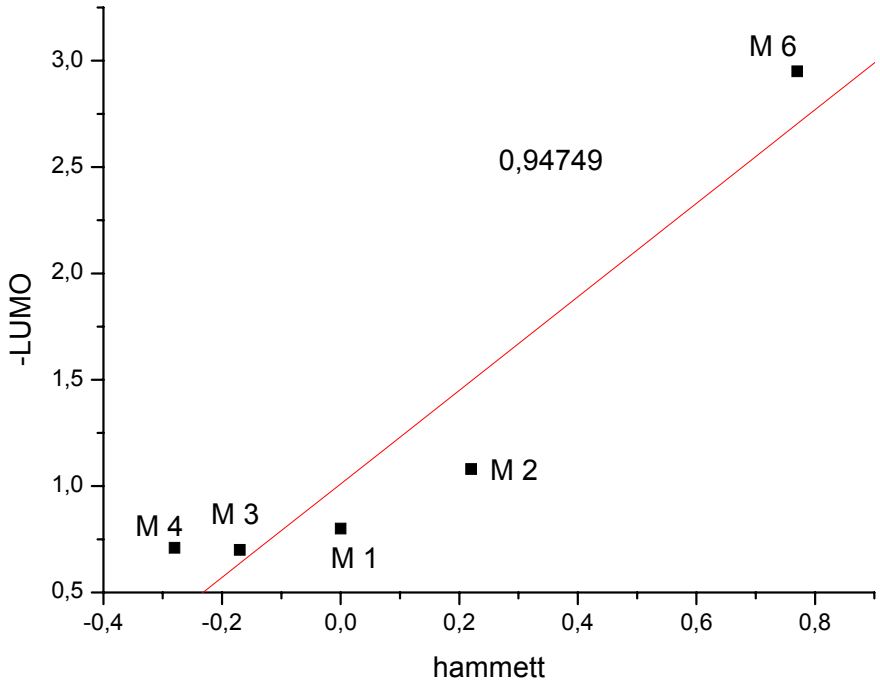

Figure 4.38 Correlation between Hammett parameter (σ) and the -LUMO energy level in neutral singlet state

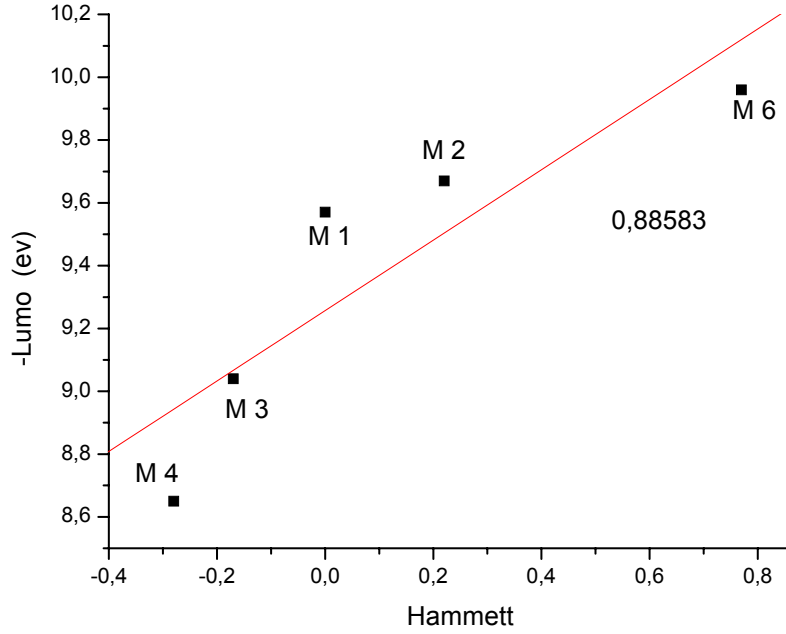

Figure 4.39 Correlation between Hammett parameter (σ) and the -LUMO energy level in radical cation state

4.2.5 The Correlation of Experimental and Calculated Values

For conducting polymers л effects are more important, since band gaps and bandwidths are properties of л system. The л system can be positively or negatively charged depending on the substituent. The effect of substituents on energy gaps, IPs, and EAs is dominated by their relative л -donating and л -accepting power [12].

According to literature, л -acceptor groups withdraw л electrons from the л system and it may reduce л electron density in the molecule. For this reason, lower HOMO and LUMO energy levels are observed [12, 16]. Electron donating groups by raising л –electron density is known to increase the HOMO and LUMO energy level and therefore result in lower IPs and EAs [12, 15]

л -acceptor groups such as cyano groups withdraw л electrons from the л system and reduce л electron density in the molecule. For this reason, lower HOMO and LUMO energy levels and higher IPs and EAs are observed [12, 15]. Methyl groups act as л donors and л acceptors. The л donating ability is slightly stronger than the л accepting capacity. Therefore, a net л donating effect results. The methyl group has little effect on the л electron density. It slightly decreases the positive charge of the л backbone and slightly raises the HOMO and LUMO energy levels [12].

In a recent research, IPs, EAs, band gap, HOMO and LUMO energies of carbazole and its derivatives were calculated by means of DFT B3LYP/6-31G* method [15]. The same results are found for л -donating and л -accepting substituents of carbozole. Also it is indicated that in carbazole with electron withdrawing substituents, LUMO energy decreases much more than that of HOMO. Similar to this, HOMO increases much more than that LUMO in carbazole with electron donating substituent. To conclude this investigation, both electron withdrawing and donating substituents decrease the energy gap between HOMO and LUMO [15].

Also, in another study, the strongest substituent effects are found with pyrroles compared to unsubstituted dimers [14]. Substitution affects HOMO and LUMO energies and energy gap reduction is caused by a stronger decrease of LUMO energies compared to HOMO energies [14].

If substituents can be placed in a position where the HOMO and LUMO are affected differently, then one of the levels can be shifted with respect to the other and band

gaps decrease. If the energy difference between the orbitals decreases, stabilization energies increase and the overlap increases [12].

In an investigation, heterocyclic dimers (compounds l-24) with different substituents were calculated employing density functional theory (DFT), analyzed with the natural bond orbital method (NBO) and established correlations which allow to understand and predict substituent effects on bandgaps [13]. It is found that substitution in 3- and 4-positions leads to parallel shifting of HOMO and LUMO but does not reduce energy gaps. It is demonstrated that alternating donor-acceptor groups do not reduce energy gaps and lead to systems with average HOMO and LUMO levels compared to the parent molecules [13].

However, strong energy lowering effects, as in the case of cyano groups, have the disadvantage that the monomers cannot be electropolymerized due to their large IPs. Substituents such as the cyano group that lower the HOMO level of the monomer, increase the oxidation potential required for electrochemical polymerization [12].

Apart from desirable modification upon substitution, there are also undesirable side effects. Bulky substituents induce deviations from planarity and decrease conjugation [12].

In this study, the effect of substituent has been investigated on HOMO, LUMO, the difference of HOMO and LUMO energies. In Table 4.5, the values extracted from DFT, B3LYP/ 6-31+G* calculations are tabulated. These are HOMO, LUMO energies and the differences between HOMO-LUMO orbitals for neutral monomer. These values are also tabulated for the positively charged radicalic state of the monomer to mimic the p-doped form of the monomer. This is shown by (1,2) designation representing the charge and the multiplicity of the monomer, respectively. The results, found for neutral singlet state monomers, have been discussed in the light of these literature findings and the calculations have shown accordance with them. According to the results, electron withdrawing substituents have a decreasing effect on both HOMO and LUMO energies. This effect causes a decrease in band gap as approximated as HOMO-LUMO difference. Conversely, electron donating substituents create an increasing effect on both HOMO and LUMO energies. This effect is more pronounced with LUMO. The outcome of this effect is the increasing in band gap. The only characteristic in common both electron donating

and electron withdrawing substituents is that the band gap is mostly affected by a stronger decrease or increase of LUMO energies compared to HOMO energies.

The monomers with electron withdrawing groups such as **M2** and **M5,** have a decreasing effect on both HOMO and LUMO energies, thus their band gaps reduce.

The monomers with electron donating groups such as **M3** and **M4**, have higher HOMO and LUMO energies but in these monomers there is a paralel shift, thus, band gap is almost unaffected. Also this situation is in accordance with the literature findings.

The biggest effect is seen with **M6** which has the most electron withdrawing substituent. In this monomer, the band gap is mostly affected by the decrease in LUMO energy. The band gap decrease however results in high IP and high EA, which in turn may decrease their efficiency in electropolymerization.

M7 and **M8** monomers, having electron withdrawing substituents display the same trend with the electron withdrawing N-phenypyrrole monomers.

Table 4.5 Calculated HOMO, LUMO and HOMO-LUMO energy differences (in au) for neutral and the positively charged radicalic state of **M1-M11** by B3LYP/6-31+G*. (The numbers in paranthesis are in ev.)

Pyrrole Derivatives	|HOMO-LUMO| (0/1) (au&ev)	HOMO (0/1) (au)	LUMO (0/1) (au)	SOMO-LUMO (1/2) (au)	SOMO (1/2) (au)	LUMO (1/2) (au)
M1	0.1903 (5.18)	-0.21962	-0.02932	-0.05254	-0.40413	-0.35159
M2	0.18593 (5.06)	-0.22565	-0.03972	-0.0316	-0.38695	-0.35535
M3	0.19151 (5.21)	-0.21720	-0.02569	-0.06216	-0.39451	-0.33235
M4	0.18936 (5.15)	-0.21548	-0.02612	-0.06252	-0.38032	-0.31780
M5	0.18249 (4.87)	-0.22276	-0.04027	-0.05463	-0.36667	-0.31204
M6	0.13174 (3.58)	-0.24027	-0.10853	-0.05006	-0.41595	-0.36589
M7	0.17321 (4.71)	-0.23392	-0.06058	-0.05581	-0.40172	-0.34591
M8	0.17134 (4.66)	-0.23627	-0.06493	-0.06102	-0.41105	-0.35003
M9	0.21491 (5.85)	-0.22842	-0.01351	-0.09014	-0.46257	-0.37243
M10	0.19874 (5.41)	-0.22759	-0.02885	-0.09809	-0.45615	-0.35806
M11	0.21484 (5.85)	-0.21339	0.00145	-0.06202	-0.42003	-0.35801

M9 and **M11** gives interesting results such that the difference of HOMO and LUMO is one of the biggest that is observed for all the other monomers. This is due to a significant increase in LUMO energy as compared to HOMO energy.

For radical cation state of monomers an appropriate relationship could not be found.

One of the main objectives of this study was to find data that can be correlated with the experimentally found properties. This correlation will allow one to understand substituent effects in these monomers and to build up relationships between the nature of substituents and the experimentally observed electrochemical properties. In this section, the experimentally obtained electrochemical data are correlated with the relevant calculated parameters. To avoid effects of experimental variances, a number of monomers are treated at the same experimental conditions (explained at the experimental section). At the specified condition, 4 of monomers which are 1-(4-Methylphenyl)-1H-pyrrole **(M3)**, 1-(4-Methoxyphenyl)-1H-pyrrole **(M4)**, 1-(4-Chlorophenyl)-1H-pyrrole **(M2)**, 1-(2-Cyanoethyl)pyrrole **(M9)** and 1-Phenyl-1H-pyrrole **(M1)** could be polymerized. Experimental data are shown in Table 4.6.

Table 4.6 Experimental data obtained for **M1, M2**, **M3**, **M4**, **M9**

Pyrrole Derivatives	**E_a (V)**	**E_c (V)**	**E_a-E_c (V)**	**$E_{1/2}$ (V)**	**I_a**	**I_c**	**$\|I_a/I_c\|$**	**1-$\|I_a/I_c\|$**
1-phenyl-1H-pyrrole (**M1**)	0.713	0.498	0.215	0.606	1.22 ($*10^{-4}$)	1.45 ($*10^{-4}$)	0.841	0.159
1-(4-Chlorophenyl)-1H-pyrrole (**M2**)	0.842	0.467	0.375	0.655	14.73 ($*10^{-5}$)	-15.46 ($*10^{-5}$)	0.953	0.047
1-(4-Methylphenyl)-1H-pyrrole (**M3**)	0.807	0.497	0.310	0.642	48.28 ($*10^{-6}$)	-51.93 ($*10^{-6}$)	0.930	0.07
1-(4-Methoxyphenyl)-1H-pyrrole (**M4**)	0.850	0.505	0.345	0.678	32.99 ($*10^{-5}$)	-31.08 ($*10^{-5}$)	1.062	0.062
1-(2-Cyanoethyl) pyrrole (**M9**)	0.688	0.614	0.074	0.660	32.62 ($*10^{-6}$)	-44.16 ($*10^{-6}$)	0.739	0.261

The correlations have been performed for both neutral singlet and radical cation states of these N-pyrrole derivatives. For correlations, experimental E_a, E_c, E_a-E_c, $E_{1/2}$, I_a, I_c, $|I_a/I_c|$, 1-$|I_a/I_c|$ values have been plotted versus the calculated HOMO energies, LUMO energies, SOMO energies, HOMO-SOMO differences, HOMO-LUMO differences and the total energy difference between the neutral and the

radical state. Additionally, the calculated values are shown in Table 4.7. Some of these correlations which have regression coefficients less than 0.9 have been excluded in the discussions. The correlations which have regression coefficients bigger than 0.9 are demonstrated in the following figures.

Table 4.7 The HOMO-LUMO energy differences, HOMO and LUMO energies (au) for the neutral and the positively charged radicalic state of **M1, M2**, **M3**, **M4**, **M9** from B3LYP/6-31+G* calculation. (The number in paranthesis are in ev.)

Pyrrole Derivatives	**|HOMO-LUMO| (0/1)**	**HOMO (0/1)**	**LUMO (0/1)**	**|HOMO - LUMO| (1/2)**	**SOMO (1/2)**	**LUMO (1/2)**	**HOMO - SOMO**
1-phenyl-1H-pyrrole (**M1**)	0.1903	-0.21962	-0.02932	-0.05254	-0.40413 (10,99)	-0.35159	0.18451
1-(4-Chlorophenyl) -1H-pyrrole (**M2**)	0.18593	-0.22565	-0.03972	0.0316	-0.38695 (-10,53)	-0.35535	0.1613 (4,39)
1-(4-Methylphenyl) -1H-pyrrole (**M3**)	0.19151	-0.21720	-0.02569	0.06216	-0.39451 (-10,74)	-0.33235	0.17731 (4,82)
1-(4-Methoxyphenyl)-1H-pyrrole (**M4**)	0.18936	-0.21548	-0.02612	0.06252	-0.38032 (-10,35)	-0.31780	0.16484 (4,49)
1-(2-Cyanoethyl) pyrrole (**M9**)	0.21491	-0.22842	-0.01351	0.09014	-0.46257 (-12,59)	-0.37243	0.23415 (6,38)

New energy levels are created when monomer forms cation from neutral state by losing an electron from HOMO energy level. Then, the single electron is located on SOMO energy level. During reduction, incoming electron turns back to its SOMO energy level. According to the correlation seen in Figure 4.40, reduction potential is observed to decrease as the -SOMO energy decreases which is in accordance with the nature of reduction during voltametry. Thus, it becomes easier for cation monomer with low –SOMO energies to get reduced. This result is supported by the energy difference between HOMO and SOMO vs. E_c graph in Figure 4.41. This linearity in Figure 4.41 indicates that as the difference between HOMO and SOMO energies decrease, the reduction potential also decreases. HOMO and SOMO are the molecular orbitals that are affected to a great extent during successive oxidation and

reduction processes. Thus, the energy difference between them may indicate the ease of reduction.

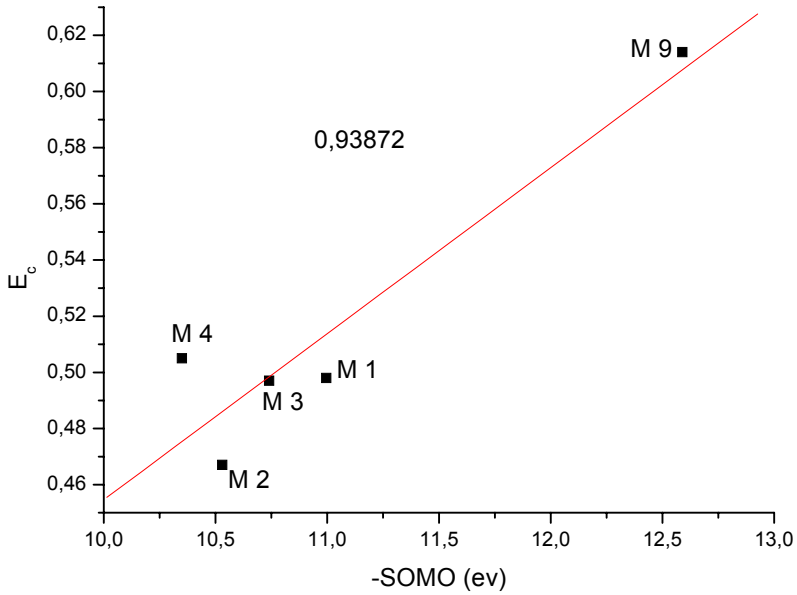

Figure 4.40 Correlation between -SOMO energy and the reduction potentials for monomers **M1**, **M2**, **M3**, **M4** and **M9**

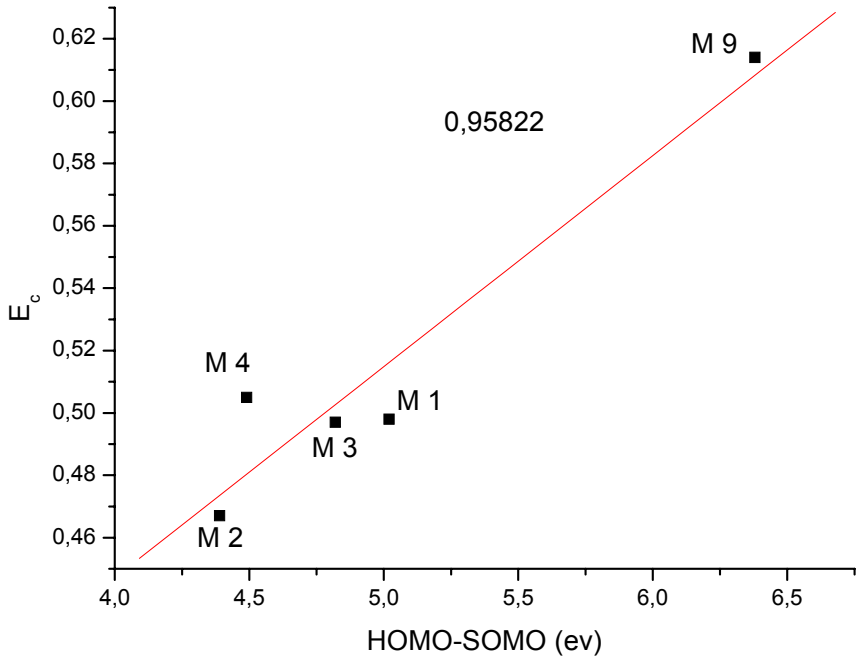

Figure 4.41 Correlation between the HOMO-SOMO energy difference and the reduction potentials for monomers **M1**, **M2**, **M3**, **M4** and **M9**

In CV, successive oxidation and reduction processes take place whose symmetry is an indication of reversibility. Increase in reversibility is proportional to an increase in conductivity. Reversibility is also defined as the ratio of anodic and cathodic currents (I_a/I_c). If this ratio gets closer to 1, the reversibility increases. In this study, in the correlations shown in Figures 4.42, 4.43, 4.44, I_a/I_c values are refined as 1- ($|I_a/I_c|$) and may be expressed as a measure of deviation from reversibility such that the smaller the value, the more reversible is the process. As seen in the Figure 4.42, when the energy difference between the radical cation and the neutral state decreases, the process becomes more reversible. This linearity may be explained in terms of radical cation stability. As a less stable cation forms, it reduces back to its neutral form much easily. The 1- ($|I_a/I_c|$) vs –SOMO graph (Figure 4.43) gives a linear graphic with a high regression coefficient. This graphic suggests that decreasing –SOMO energy of the monomers will be accompanied by an increase in reversibility. The low –SOMO energy is releated to the ease of reduction, which in turn may be correlated with the reversibility. Moreover, although the regression in Figure 4.44 is presumably less than unity, there is an approximate relationship between the difference of total electronic energies between the radical and the neutral state, and the reversibility of process. Thus, with increase in reversibility, oxidation and reduction becomes easier.

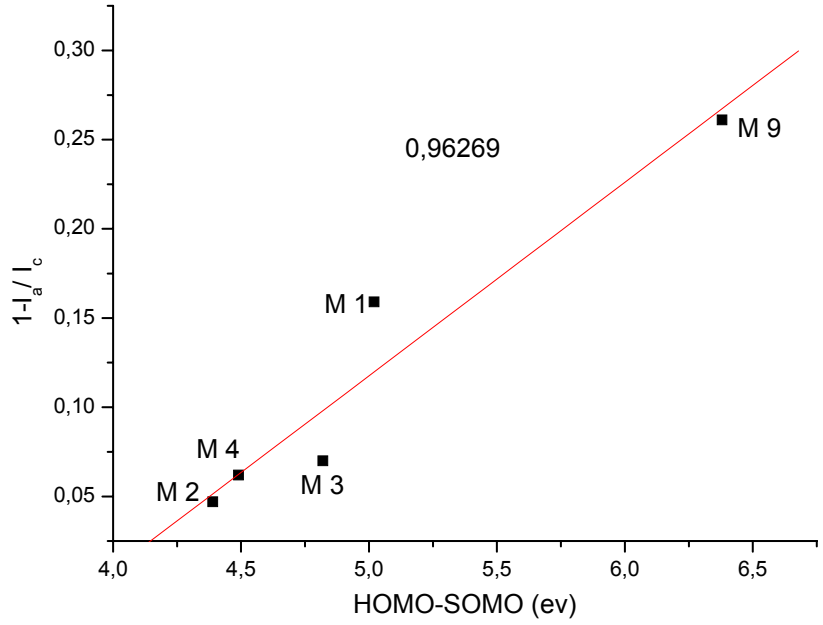

Figure 4.42 Correlation between the HOMO-SOMO energy difference and 1- ($|I_a/I_c|$)

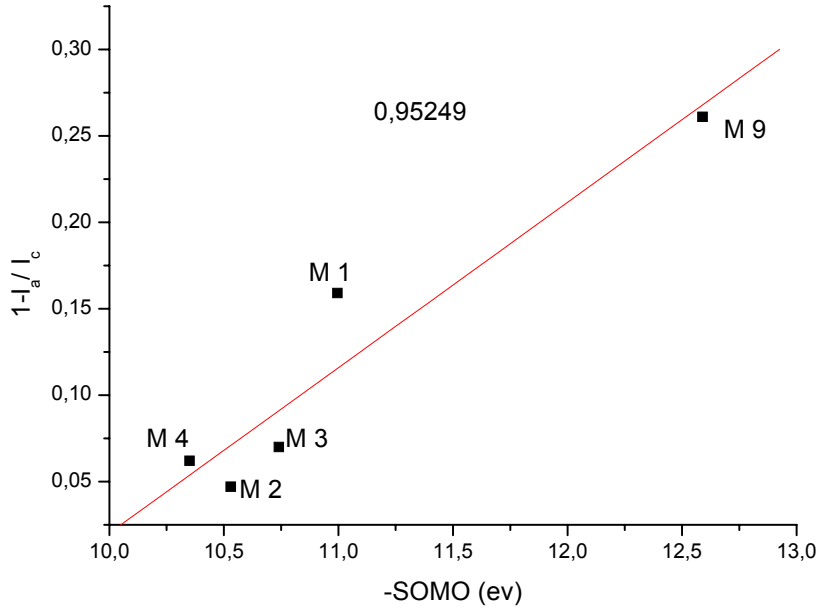

Figure 4.43 Correlation between -SOMO energy and 1- (|Ia/Ic|)

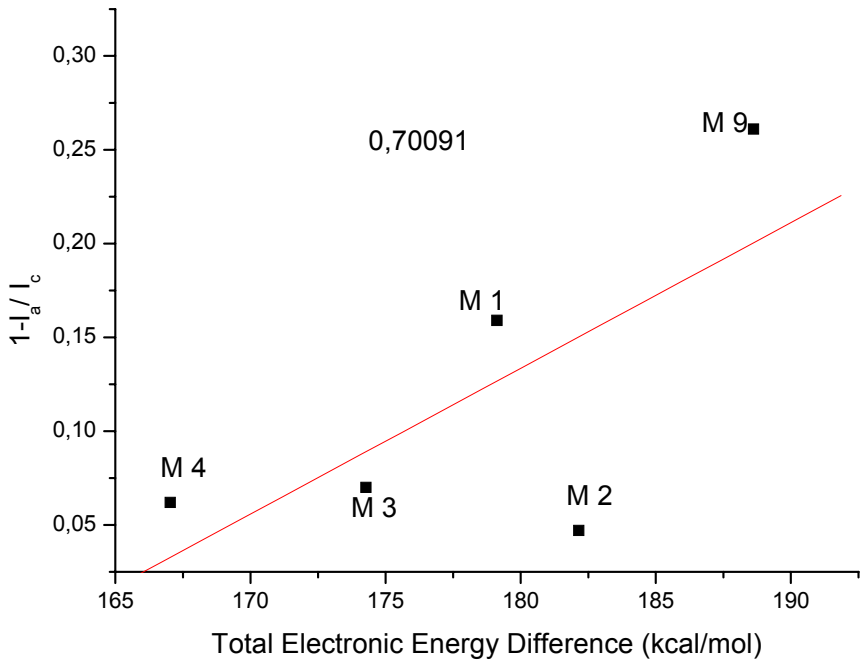

Figure 4.44 The plot of total electronic energy difference between the radical and the neutral state vs 1- ($|I_a/I_c|$)

The correlations for neutral singlet state, HOMO-LUMO vs E_a, E_c, E_a-E_c, I_a/I_c and LUMO versus E_c and the correlations for radical and cation state, HOMO vs E_a, E_c, E_a-E_c, I_a/I_c are well. Although they have perfect correlation as shown in Appendix A,

their physical relationship could not be established. More experiments are needed in order to explain their significance and draw conclusions.

5 CONCLUSION

In this study, experimental electrochemical data of a set of monomers have been produced by enforcing them to electropolymerize exactly at the same conditions. The data that has been extracted have been correlated with calculations from DFT, B3LYP/6-31+G* basis set.

In calculations most stable geometries for monomers are found. In monomers **M1**-**M6** phenyl substituent can not be coplanar with pyrrole due to H-H repulsion. Thus, phenyl is approximately 30˚ tilted out of plane of pyrrole. The dimers and oligomer geometries of **M1** up to n=7 have been obtained. The HOMO-LUMO differences, and HOMO energies are decreased while LUMO energies increased as the number of monomer units increased. The linear relationship between the inverse chain length and HOMO energy allowed us to calculate IP as 3.35 ev. Also the other linear relationship between the inverse chain length and the difference of HOMO and LUMO energy which allowed us to calculate the band gap as 2.81 ev. These results are important in two aspects. First, the results are in accordance with the literature findings on N-substituted pyrrole derivatives. Secondly, polymer properties extracted from monomers can be treated safely in a comparative way since increasing the monomer units have a linear effect on polymers.

The relationships between Hammett parameters and theoretically calculated values have been sought in N-pyrrole derivatives. For this purpose, various graphs are plotted between the Hammett parameters of **M1**, **M2, M3, M4** and **M6** and HOMO, LUMO energies and HOMO-LUMO differences for neutral and radicalic systems. The best correlation has been obtained from Hammett parameter vs. HOMO energy level. This has revealed that electronic property of substitution is effective on HOMO energy level of the monomer.

Spin density calculations in cation radicals of all N-pyrrole derivatives have been performed by DFT method. The results indicate that the radicalic site is localized in α positions for **M1, M2, M6, M7, M8, M9, M10, M11** and these molecules' cation radicals may prefer to undergo coupling reaction from α position. On the otherhand,

M3, M4, M5 molecules having electron donating groups have slightly higher spin densities on β-C's which may increase their tendency to undergo coupling from the β position.

The effect of substituent could be investigated on HOMO-LUMO differences, LUMO and HOMO energies. The calculations have shown that electron withdrawing N-phenyl pyrrole monomers have a decreasing effect on both HOMO and LUMO energies. This effect is more pronounced with LUMO, thus band gap as approximated as HOMO-LUMO difference decreases. Also the other electron withdrawing substituents, bonded from nitrogen of pyrrole ring, display the same trend. Conversely, electron donating substituents, bonded from nitrogen of pyrrole ring, create an increasing effect on both HOMO and LUMO energies. The orbital energy of LUMO increases more than that of HOMO level in electron donating substituents. Thus, HOMO-LUMO difference increases. Among the electron donating substituents, only **M3** and **M4** monomers' band gaps are almost unaffected due to the increase in their HOMO and LUMO energies due to the paralel shifting.

Calculations allow us to understand the effect of the nature of substituent on electrochemical properties. The correlations demonstrated that the calculated molecular orbital energies would be correlated succesfully to experimental data such as Ia/Ic, Ea, Ec. These correlations may in turn guide experimentalists in their design of new monomers. Having results that are in accordance with literature, DFT methodology with B3LYP/6-31+G* basis set can be concluded to be a reliable method to treat systems of this kind.

In future studies, experimental data set may be increased, and chain length effect must be studied in more detail.

REFERENCES

[1] **Shirakawa, H., et al.,** 1977. Synthesis of Electrically Conducting Organic Polymers - Halogen Derivatives of Polyacetylene, (Ch)X, *Journal of the Chemical Society-Chemical Communications*, 578-580.

[2] **Saraç, A.S., Sönmez, G.,** 2002. In Situ Spectroelectrochemistry and Colorimetry of Polypyrrole-acrylamides, *Journal of Materials Science*, 37, 4609-4614.

[3] **Alguno, A. C., Chung, W.C., Bantaculo, R. C., Miyata, H., Ignacio**, E.W., **Bacal, A.M.,** 2001**.** A Density Functional Theory Calculation on Polypyrrole and Polythiophene Energy Band Gaps, *MSU-Iligan Institute of Technology*.

[4] **Saraç, A.S.,** 2004. Electropolymerization, *Polymer Science and Technology Booklet*, 6, 24-28.

[5] **Pratt, C.,** 1996. Conducting Polymers, http://homepage.ntlworld.com/colin.pratt/cpoly.pdf

[6] **Yang, L., Feng, J., Ren, A., Sun, J.,** 2006. The Electronic Structure and Optical Properties of Carbazole-based Conjugated Oligomers and Polymers, *Polymer*, 47, 1397-1404.

[7] **Saraç, A.S., Ustamehmetoğlu, B., Sezer, E., Erbil, C.,** 1996. The Effects of Polyacrylic Acid/Polypyrrole Composite Coating on Photocorrosion and Photoactivity of Pyrite Electrodes, *Journal of Chemistry*, 20, 80-87.

[8] **Rabias, I., Howlin, B.J.,** 2001. A Combined Ab Initio and Semi-Empirical Study on the Theoretical Vibrational Spectra and Physical Properties of Polypyrrole, *Computational and Theoretical Polymer Science*, 11, 241-249.

[9] **Casanovas, J., Cho, L.Y., Ocampo,C., Alem´an, C.,** 2005. A Theoretical Study of The Effects Produced by *N*-Hydroxyalkyl Substitution in Pyrrole Oligomers, *Synthetic Metals*, 151, 239-245.

[10] **Yurtsever, E.,** 2001. A Quantum Mechanical Study of the Electrochemical Polymerization Of Pyrrole, *Synthetic Metals*, 119, 227-228.

[11] **Yurtsever, M., Sönmez, G., Saraç, A.S.,** 2003. Time Dependent Density Functional Theory Calculations for the Electronic Excitations of Pyrrole-Acrylamide Copolymers, *Synthetic Metals*, 135-136, 463-463.

[12] **Salzner, U., Kızıltepe, T.,** 1999. Theoretical Analysis of Substituent Effects on Building Blocks of Conducting Polymers: 3,4'-Substituted Bithiophenes, *Journal of . Org. Chem, 64,* 764-769.

[13] **Salzner, U.,** 1999. Density Functional Theory Investigation of Substituent Effects on Building Blocks of Conducting Polymers, *Synthetic Metals*, 101, 482-483.

[14] **Salzner, U.,** 1999. Theoretical Analysis of Effects of π-Conjugating Substituents on Building Blocks for Conducting Polymers, *Journal of Org Chem,* 64*,* 7419-7425.

[15] **Pan, J. H., Chiu, H., Wang, B.,** 2005. Theoretical Investigation of Carbazole Derivatives as Hole-Transporting Materials in OLEDs, *Journal of Molecular Structure (THEOCHEM),* 725, 89-95.

[16] **Chieh, Y.C., Chen, P.C., Chen, S.C**., 2003. Theoretical Study of the Internal Rotational Barriers in Some N-Substituted Nitropyrroles, *Journal of Molecular Structure (Theochem)*, 636, 115–123.

[17] **Burcl, R., Amos, R., Nicholas, R. D., Handy**, C., 2002. Study of Excited States of Furan and Pyrrole by Time-Dependent Density Functional Theory, *Chemical Physics Letters,* 355, 8–18

[18] **Audebert, P., Catel, M., Coustumer, G., Duchenet, V., Hapiot, P.,** 1998. Electrochemistry and Polymerization Mechanisms of Thiophene-Pyrrole-Thiophene Oligomers and Terthiophenes. Experimental and Theoretical Modeling Studies, *Journal of Phys. Chem., 102,* 8661-8669.

[19] **Salzner, U., Pickup, P.G., Poirier, R. A.,** 1998. Accurate Method for Obtaining Band Gaps in Conducting Polymers Using a DFT/Hybrid Approach**,** *Journal of Phys. Chem.,102,* 2572-2578.

[20] **Yurtsever, M., Yurtsever, E.,** 1999. Structural Studies of Polypyrroles I. An Ab-Initio Evalution of Bonding Through A and B Carbons, *Synthetic Metals,*98, 221-227.

[21] **Casanovas, J., Cho, Ocampo,C., Alem´an, C., Liesa, F.,** 2006. Polymers and Oligomers Derived from Pyrrole and N-hydroxymethylpyrrole: A Theoretical Analysis of the Structural and Electronic Properties, *Polymer*, 47, 3257–3262.

[22] **Salzner, U., Pickup, P.G., Poirier, R. A., Lagowski, J.B.,** 1998. Comparison Of Geometries and Electronic Structures of Polyacetylene, Polyborole, Polycyclopentadiene, Polypyrrole, Polyfuran, Polysilole, Polyphosphole, Polythiophene, Polyselenophene and Polytellurophene, *Synthetic Metals*, 96*,* 177-189.

[23] **Bakhshi, A. K., Ladik, J., Seel, M.,** 1987. Comparative Study of the Electronic Structure and Conduction Properties of Polypyrrole, Polythiophene, and Polyfuran and Their Copolymers, *Physical Review B*, *The American Physical Society,* 35, 704 – 712.

[24] **Park, H., Lee, L.,** 1999. Ab Initio Investigations of the Pyrrole Dimer: A Direct Observation of the Π-Facial Hydrogen Bond, *Chemical Physics Letters*, 301, 487–492.

[25] **Zotti, G., Martina, S., Wegner, G., Schlu¨ter, A.D.,** 2005. Chain-Length Dependence of the Electrochemical Properties of Conjugated Oligofluorenes, *AdV. Mater.*, *26*, 1532-1537.

[26] **Tüzün, N.Ş.,** 2002. Analysis of the Radical Polymerizability of Diallyl Monomers, *PhD Thesis,*Boğaziçi University.

[27] **Shirale, D.J., Gade, V.K., Gaikwad, P.D., Kharat, H.J., Kakde, K.P., Savale, P.A., Hussaini, S.S., Dhumane, N.R., Shirsat, M.D.,** 2006. The Influence of Electrochemical Process Parameters on the Conductivity of Poly(N-Methylpyrrole) Films by Galvanostatic Method, *Materials Letters*, 60, 1407–1411.

[28] **Zheng, J. P., Cygan, P., Jow, T. R.,** 1995. Hydrous Ruthenium Oxide as an Electrode Material for Electrochemical Capacitors, *Journal of Electrochemical Society.,* 142, 2699-2703.

[29] **Saraç, A.S.,** Polymer Science and Technology Booklet, Cyclic Voltammetry.

[30] **Sadki, S., Schottland, P., Brodie, *N.*, Sabouraud, G.,** 2000. The mechanisms of pyrrole electropolymerization, *Chem. Soc. Rev.*, 29, 283–293.

[31] **Pravda, M.,** 2000. Electropolymerization, http*://intel.ucc.ie/sensors/Electropolym.htm*

[32] **Janak, J.F,** 1978. Alternative Density Functional Theory for Atoms and Molecules, *Phys. Rev.* B 18, 7165 – 7168.

[33] **Levy, M., Nagy, A.,** 1999. Variational Density-Functional Theory for an Individual Excited State, *Phys. Rev. Lett.* 83, 4361 – 4364.

[34] **Chen, P.C.,** 1997. Molecular orbital studies of the isomers of 2,4,6-trinitrotoluene and some of its thermal decomposition products, *Journal of Molecular Structure (Theochem),* 397, 21-32.

[35] **Chen, P.C., Tzeng, S.C., Chen, F.M.,** 1999. Molecular Structures of Dinitroanilines and Trinitroanilines, *Computers & Chemistry.*, 23, 503-511.

[36] **Chen, P.C., Tzeng, S.C.,** 1999. Theoretical Study on the Molecular Structures of Dinitrophenols and Trinitrophenols, *Journal of Molecular Structure (Theochem)*, 467, 243-257.

[37] **Frisch, M. J., Trucks, G. W., Schlegel, H. B., Scuseria, G. E., Robb, M. A., Cheeseman, J. R., Montgomery, J. A., Vreven, Jr., T., Kudin, K. N., Burant, J. C., Millam, J. M., Iyengar, S. S., Tomasi, J., Barone, V., Mennucci, B., Cossi, M., Scalmani, G., Rega, N., Petersson, G. A., Nakatsuji, H., Hada, M., Ehara, M., Toyota, K., Fukuda, R., Hasegawa, J., Ishida, M., Nakajima, T., Honda, Y., Kitao, O., Nakai, H., Klene, M., Li, X., Knox, J. E., Hratchian, H. P., Cross, J. B., Adamo, C., Jaramillo, Gomperts, R., Stratmann, R. E., Yazyev, O., Austin, A. J., Cammi, R., Pomelli, C., Ochterski, J. W., Ayala, P. Y, Morokuma, K., Voth, G. A., Salvador, P., Dannenberg, J. J., Zakrzewski, V. G., Dapprich, S., Daniels, A. D., Strain, M. C., Farkas, O., Malick, D. K., Rabuck, A. D., Raghavachari, K., Foresman, J. B., Ortiz, J. V., Cui, Baboul, A. G. , Clifford, S., Cioslowski, J., Stefanov, B. B., Liu, G., Liashenko, A., Piskorz, P., Komaromi, I.,RMartin, . L., Fox, D. J., Keith, T., Al-Laham, M. A., Peng, C. Y., Nanayakkara, A., Challacombe, M.,Gill, P. M. W., Johnson, B., Chen, W.,Wong, M. W., Gonzalez, C. and Pople J. A.,** 2004. Gaussian 03, Revision C.02, *Gaussian, Inc*., Wallingford CT.

[38] **Foster, P., Weinhold, F.,** 1980. Natural Hybrid Orbitals, *J. Am. Chem. Soc*., 102, 7211-7218.

[39] **Reed, A. E., Weinhold, F.,** 1983. Natural Bond Orbital Analysis of Near-Hartree-Fock Water Dimer, *Journal of Chemical Physics*, 78, 4066-4073.

[40] **Reed, A. E., Weihstock, R. B., Weinhold, F.,** 1985. Natural-Population Analysis, *Journal of Chemical Physics,* 83, 735-746.

[41] **Reed, A. E.,Weinhold, F.,** 1985. Natural Localized Molecular-Orbitals, *Journal of Chemical Physics*, 83, 1736-1740.

[42] **Reed, A. E., Curtiss, L. A., Weinhold, F.,** 1988. Intermolecular Interactions from a Natural Bond Orbital, Donor-Acceptor Viewpoint, *Journal of Chem. Rev. (Washington D.C.),* 88, 899-926.

[43] **Chirlian, L. E., Francl, M.M.,** 1987. Atomic Charges Derived from Electrostatic Potentials: A Detailed Study*, J. Comp. Chem*., 8, 894-905.

[44] **Frackowiak, E., Beguin, F.,** 2001. Carbon Materials for the Electrochemical Storage of Energy in Capacitors, *Carbon,* 39, 937 –950.

[45] **Nabais, C., Fartaria, R., Fernandes, F., Abrantes, L.,** 2004. Prediction of Reactive Sites for the Electropolymerization of *p*-Benzenesulfonic Acid Derivatives:Ab Initio and Experimental Study, *International Journal of Quantum Chemistry*, 99, 11-27.

[46] **Pross, A.,** 1995. Theoretical & Physical Principles of Organic Reactivity, John Wiley & Sons, Inc., New York.

APPENDIX

Below are given some other perfect correlations where physical relationship could not be established.

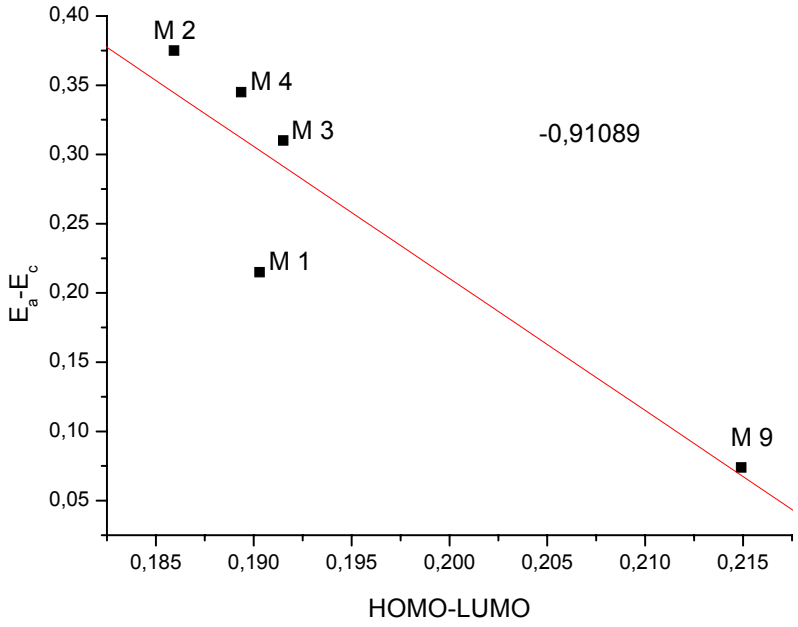

Figure A.1. Correlation between the HOMO-LUMO energy difference in neutral state (au) and potential difference (V)

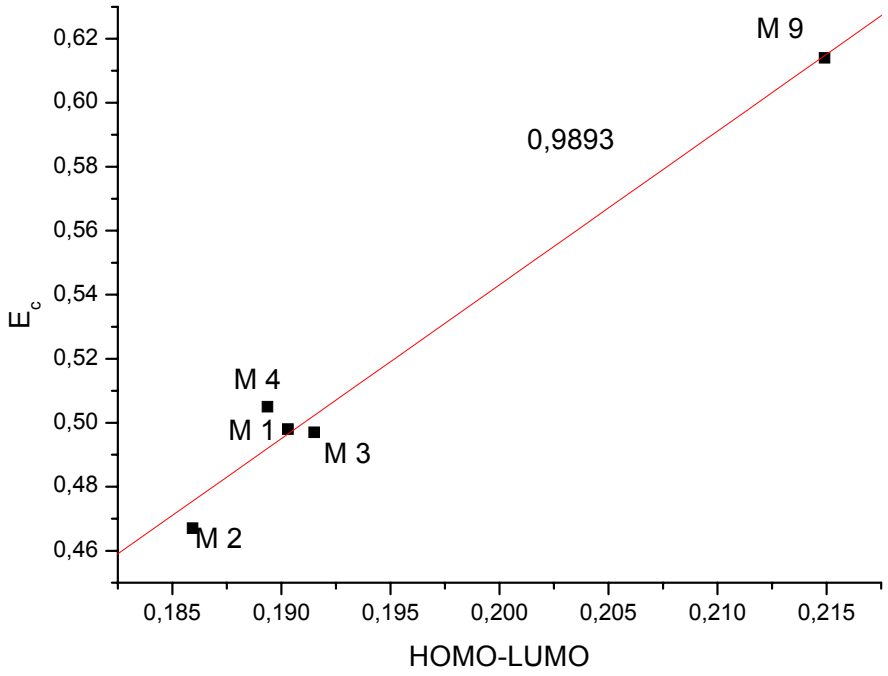

Figure A.2. Correlation between the HOMO-LUMO energy difference in neutral state (au) and reduction potential (V)

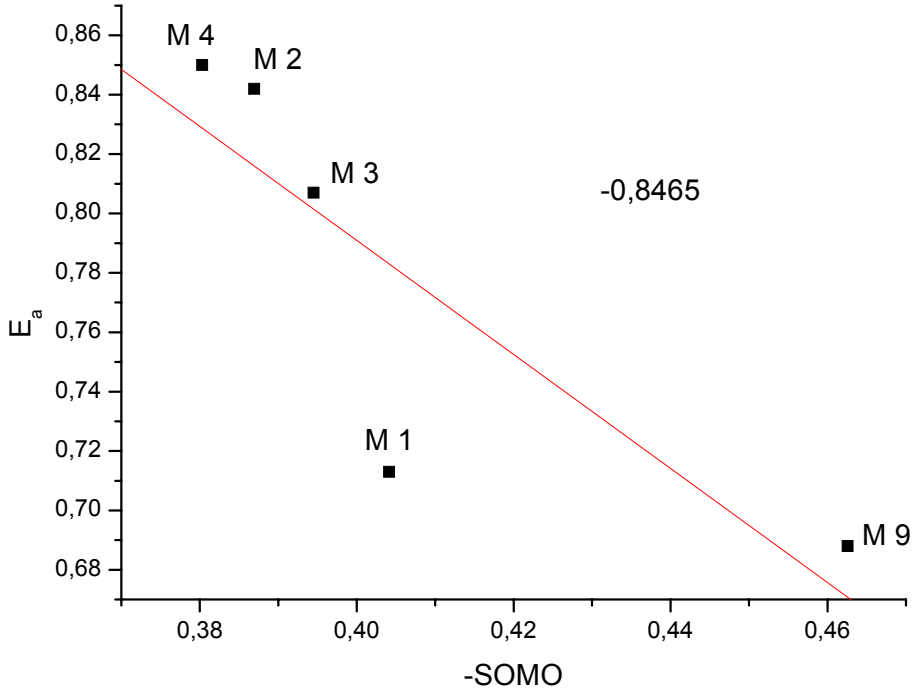

Figure A.3. Correlation between the SOMO energy in radical cation state (au) and the oxidation potential (V)

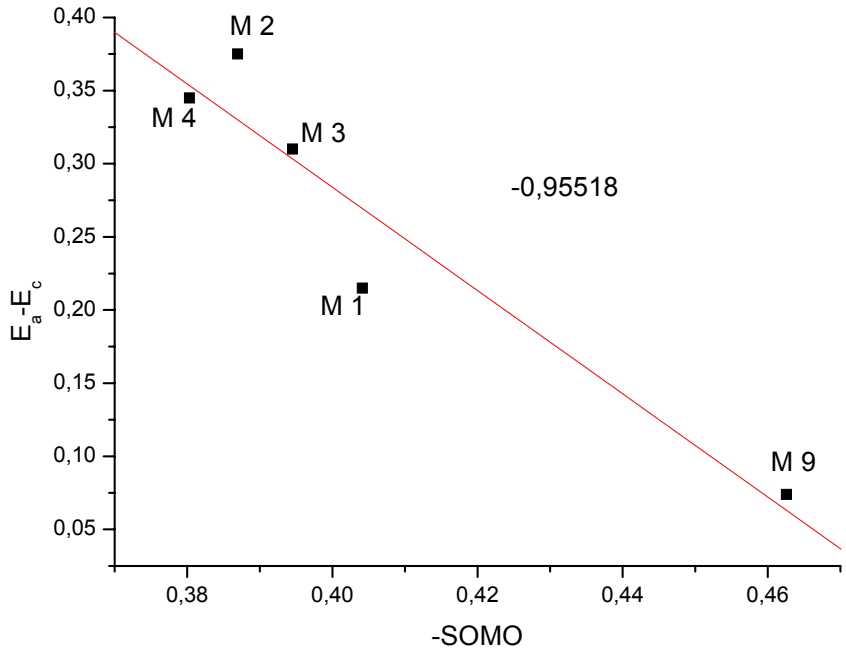

Figure A.4. Correlation between the -SOMO energy in radical cation state (au) and the potential difference (V)

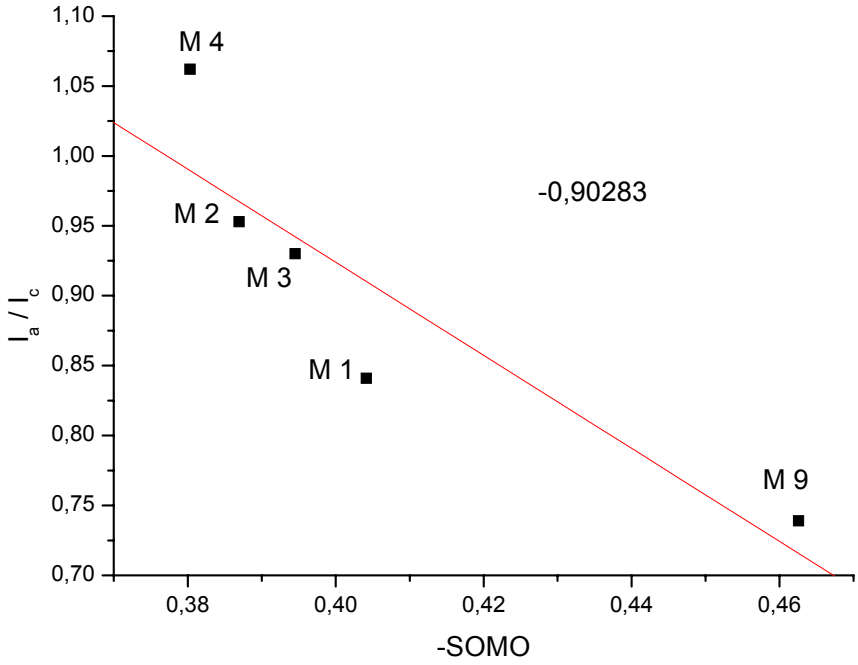

Figure A.5. Correlation between the -SOMO energy in radical cation state (au) and the current ratio

BIOGRAPHY

Fatma BAYATA was born in 1982, Balıkesir. She graduated from Sırrı Yırcalı Anatolian High School - Balıkesir in 2000. She started her undergraduate education in İstanbul Technical University, Chemistry Department, and obtained BSc. Degree at Chemistry Department in January, 2005. Immediately after her graduation, she attended in İstanbul Technical University, Polymer Science and Technology, where she prepared hereby master thesis.